FOXD1^{+} STROMAL CELLS- THE PROGENITORS FOR KIDNEY VASCULAR DEVELOPMENT

Eugene Eng Lin

Houston, Texas

Bachelor of Science, Duke University, 2005

A dissertation presented to the Graduate Faculty

of the University of Virginia in Candidacy for the Degree of

Doctor of Philosophy

Department of Biology

University of Virginia

December, 2015

ABSTRACT

The renal vasculature is crucial for proper kidney function, and defects in the kidney arteries are responsible for many human diseases. However, the molecular mechanisms that underlie the assembly of the renal blood vessels are poorly understood. Using lineage tracing we show that renal stromal cells, characterized by their expression of the transcription factor Forkhead Box D1 (Foxd1), give rise to the entirety of the mural cell layer of the renal arterial tree (including smooth muscle and renin cells) as well as glomerular mesangial cells and interstitial pericytes. The goal of this thesis is to identify the mechanisms that regulate the fate of Foxd1 cells.

We find that Foxd1 itself is necessary for proper kidney development. Deletion of the Foxd1 gene resulted in kidneys that were smaller, fused at the midline, and failed to properly rotate and ascend. Strikingly, the vasculature of Foxd1-null kidneys was completely misoriented, with arteries entering the organ from multiple locations in the kidney periphery in a reversal of the normal arrangement, indicating that Foxd1 plays a crucial role in arterial patterning. We also demonstrate that the Foxd1 cell itself is required for proper differentiation of the mural cells using cell ablation studies. Exposure of Foxd1 cells to diphtheria toxin chain A (Foxd1-DTA) resulted in renal arteries with a disorganized smooth muscle cell layer, delayed arterial formation, and an altered vascular pattern similar to that seen in the Foxd1-null animals. In addition, we observe a potential capability for cells outside the Foxd1 lineage to replace Foxd1-lineage cells in situations of cell injury and death.

Foxd1 cells give rise to another progenitor cell population, the renin precursor cells, which differentiate into arteriolar smooth muscle and glomerular mesangial cells. One

longtime focus of our lab has been identification of molecules that are responsible for the remarkable plasticity of renin cell descendants to reacquire the renin phenotype in response to a homeostatic threat that requires a sustained increase in circulating renin. Using microarray analysis, we find that the protein aldo-keto reductase 1b7 (AKR1B7) is a specific marker for renin cells. This association is maintained throughout development, and in physiological and pathological manipulations that increase or decrease renin levels. Importantly, in renin knockout animals we show that AKR1B7 delineates a population of cells attempting to make renin, and that these cells participate in the resulting vascular pathology. We also demonstrate that AKR1B7, like renin, is regulated by cyclic AMP signaling and RBP-J (Recombination Signal Binding Protein for IG-kJ Region) indicative of a larger, overarching genetic program that regulates the renin cell phenotype.

Finally we investigate the function of RBP-J, the final transcriptional mediator of Notch signaling, in Foxd1 cells ($Foxd1^{RBPJ-/-}$). Conditional deletion of RBP-J resulted in a reduction in the number of renal arteries, a thinner smooth muscle cell layer, and defects in vascular branching. In addition, $Foxd1^{RBPJ-/-}$ displayed a lack of mesangial cells, resulting in glomerular aneurysms. These developmental defects are followed in adult life by prominent vascular fibrosis and glomerulosclerosis. Thus we conclude that RBP-J is necessary for proper differentiation of Foxd1 cells.

In summary, my results illustrate the important role of Foxd1–expressing stromal cells as a precursor for the arterial mural cells and mesangium, and identify three important proteins in their function and differentiation- Foxd1, AKR1B7, and RBP-J. Further study

of Foxd1 cells and the molecules that control their fate will be crucial for understanding the key developmental process of kidney vascular formation.

~~ACKNOWLEDGMENTS~~

REBELS[1]

I would like to start by giving my sincerest thanks to **Dr. R. Ariel Gomez**. Your knowledge about science and writing are absolutely unparalleled. You always seemed to know the best way to motivate and encourage me. And who can forget the bi-monthly installment of “Storytime with Ariel”- science, medicine and career advice rolled into one. Thanks for your mentorship, and for giving me the freedom to pursue my own crazy ideas, even if it probably added a year to my graduation time. Do you remember the day you visited my old lab at Duke- who knew such a fruitful (for me at least, I won’t dare to speak for you) collaboration would come from a chance meeting?

And also to his lovely wife **Dr. Maria Luisa S. Sequeira-Lopez**, who is a mighty scientist in her own right. Your input and enthusiasm will be missed dearly. Thanks for being so available, for always thinking big picture, and apologies for all the times I doubtless did not credit your name correctly in my acknowledgments sections. Hopefully this time I got it right.

To **Dr. Brian Belyea**, who has one of the kindest and most generous hearts I have ever met: thanks for being the point man for anything I was too nervous to send directly to Ariel. And thanks also for all the times we talked about anything BUT science. I pray your scientific career will be as successful as the opposite of the current fortunes of your beloved Redskins; you deserve it.

Abundant thanks to **Dr. Ellen Pentz**. By virtue of your proximal location to my bench and desk you suffered through some of the most inane and stupid questions (and occasional unsafe lab practice) with admirable patience, wisdom and grace. Thank you for your steady guidance, teaching heart, and vegetables from your garden. Enjoy a hard-earned retirement away from the prying inquiries of annoying students.

Thanks also to **Dr. Silvia Medrano**, hands down one of the nicest people ever with an incredibly infectious laugh. You always made yourself available to help, and your genuine scientific curiosity is something I will try to emulate.

My mast cells offer mast-ive (get it?) thanks to **Dani Stumbo**, who saved me hours of sniffling and sneezing. Your work ethic and can-do spirit is truly admirable. When I'm setting up my first lab it's my fullest intention to poach you at the earliest possible timepoint. Don't tell Ariel; hopefully he's stopped reading before this point. If not, oops.

Thanks to **Ted Mehalic** for being the bro-iest bro that ever broing bro’d. Bro.

[1] In honor of one of the funnier UVA traditions by the Sons and Daughters of Liberty (with whom I claim no association)

Apologies to **Dr. Rajwinderjit Kaur**, whose lab space I invaded. It's all yours again. Thanks for being a great roommate.

Thanks to the rest of the **Gomez lab** members for assistance, discussions, and humor.

Thanks to **Dr. Tom Coffman** and the other members of his lab, particularly **Dr. Steve Crowley**, for kick-starting my research career and being the first to believe in my potential as a scientist; I hope you're not too disappointed.

Thanks to the wonderful members of my thesis committee, **Drs. Chris Deppmann, Barry Condron, Ray Keller,** and **Jing Yu**. How could I possibly fail with such highly-regarded scientific minds behind me? My regard is only slightly tainted towards the first two for prompting my switch from the Master's program to PhD.

Abundant thanks to **Dr. Mike Wormington**, for teaching me about… teaching. I enjoyed being Robin to your Batman, and I like to think that ultimately it was the students that won from our partnership, friendly rivalry, and shared dislike of Roy Williams.

Speaking of which, shout-out **to Duke Basketball**, for winning National Championships the years before and after I left Durham. As always, GTHC.

Thanks also to **the UVA football team**, for being the only team that Duke could beat in the ACC for several years. Okay, that's mean. Too bad, it's staying.

Thanks to the **UVA Hospital Cafeteria** for feeding me for the past 6 years. Shout out to **Tawanda, Chris, Greg, Mario, Pauline,** and **Louis** for being friendly and giving me extra food. I know I'm stretching the limits here, but it's my thesis and I'll thank who I want to thank.

Thank you to **Dr. Mordin Solus** for being the very model of a scientist Salarian.

To **my fellow graduate students**, thanks for all your help and support. May you succeed in all your scientific endeavors, which will cumulatively raise the value of my degree which comes from the same institution. Particular thanks to **Drs. Jianyi Lee** and **Ruth Castellanos-Rivera**, and **future Drs. Yan Hu** and **LaToya Roker**. We did it, or will do so in the near future!

Thanks to **my parents** for being loving, encouraging and letting me find my own path in life. Highest regards to **Eng Hong Lin** for being a model of biblical manhood, and for your prayer and guidance. Thanks to **Shun Chen Lin** for your encouragement, and your personality that I thoroughly inherited. It's still in the air who I inherited my brains from.

A brief nod of acknowledgment to my sister **Chelsey Lin**, who I have no doubt will make a great doctor someday, if she decides she wants it enough.

And finally, ultimate thanks to my lovely wife(-to-be) **Michelle Hoi Ying Ko** for your patience and love. Sorry for keeping you in Charlottesville for so long. On to the next adventure!

In nomine e fili e spiritu sancte

TYRANTS

George R. R. Martin. Finish the book, George.

Arbitrary UVA lingo. CAMPUS, QUAD, FRESHMAN/SOPHMORE/JUNIOR/SENIOR, AULD LANG SYNE. Man that felt good.

MR4. Dilapidated building with underpowered HVAC, power blips, mold, and for some stupid reason the exhaust from the mouse facilities is right over the entrance so you get a nice blast of mouse smell every time you enter and leave. And the smoker's lounge for the entire hospital is right outside. Oh and the building's so old that it has cigarette ashtrays embedded in the walls. Seriously, look at this thing:

Waffles and Drogo, my "beloved" dog and cat, for criminal mischief, petty theft, countless hours of lost sleep and a general refusal to do anything useful.

TABLE OF CONTENTS

I. INTRODUCTION

The adult human kidney receives approximately one-fifth of the total blood pumped from the heart per minute. The disproportionate allotment of blood relative to the kidney's small size is a result of the key roles the kidney must play. The kidney is tasked with filtering out the waste products of metabolism from the bloodstream to prevent their toxic accumulation, while retaining important biomolecules such as proteins and sugars. At the same time, the kidney must regulate the fluid/electrolyte balance of the blood while maintaining blood pressure and blood pH. To begin with, I will introduce the basics of renal anatomy, which is integrally tied to proper kidney function– as the architectural principle says, "form follows function"[2]. I will follow this with a brief overview about the mechanisms responsible for building the kidney. Finally, I will discuss the crucial "plumbing" system of the kidney, which is my area of focus- the renal vasculature, and what we know and don't know about its development.

Kidney anatomy- the nephron and the renal vasculature

The kidney can be broadly divided into two regions, the outer layer called the cortex, and the inner layer called the medulla. Both of these regions are spanned by the fundamental filtering unit of the kidney, the nephron (Figure 1.1). Blood enters the nephron at the glomerulus, a spherical body present

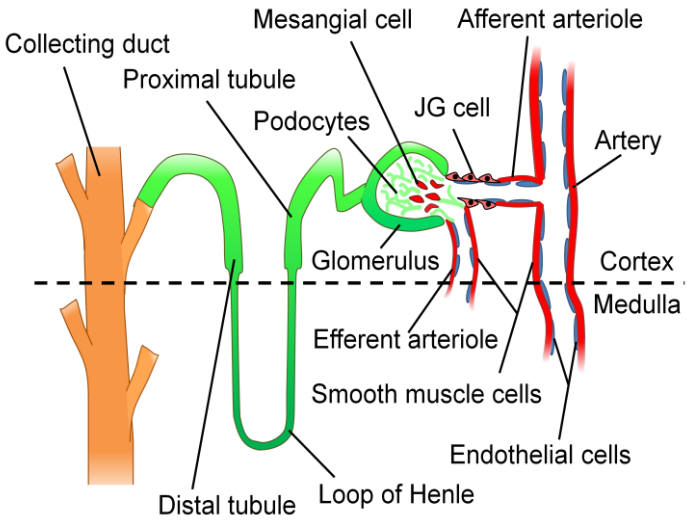

Fig. 1.1 The structures of the adult nephron

[2] My father was an architect, and was fairly strident about me not following in his footsteps.

in the cortex which is the primary site of filtration. In humans there are approximately 1 million glomeruli per kidney[3], although there is significant variation in that number. Inside, the blood enters a network of glomerular capillaries where fluid and electrolyte exchange can occur. Surrounding the glomerular capillaries are two cell types, podocytes and mesangial cells, which control the filtration characteristics of the glomerulus. The filtrate leaves the glomerulus and passes into the renal tubule, which consists (sequentially) of the proximal tubule, loop of Henle, and distal tubule. Here, urine is concentrated as the osmolarity and tonicity of the filtrate is carefully adjusted, and solutes and ions are reabsorbed or secreted into the bloodstream. Finally, the filtrate enters the collecting duct system where it will eventually leave the kidney through the ureter as urine.

Distribution of blood to the nephrons necessitates passing the blood through an extremely complex system of branching blood vessels (Figure 1.2). Blood enters the kidney through the renal artery and flows through a series of successively narrowing arteries (interlobar, arcuate, interlobular) before reaching the end-branch afferent arterioles. The afferent arteriole connects to the glomerulus and passes blood into the glomerular capillary loops- the end tip of each of the blood vessels seen in Figure 1.2 corresponds to a single joining of the vascular network to a glomerulus. Uniquely to the glomerulus,

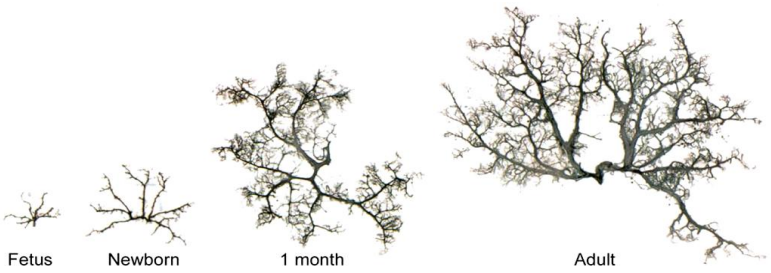

Fig. 1.2 Development of the renal vascular tree. Entire vascular trees were dissected from fetus, newborn, one month old and adult rat kidneys. All views are the same magnification. Taken from (29)

[3] An investigator down the hall, Dr. Jennifer Charlton, is particularly interested in this question. Apparently "How many glomeruli do humans have?" is not nearly as straightforward a question as one would think.

the blood exits the glomerular capillaries not through a vein but rather into an efferent, muscularized arteriole. The efferent arteriole then branches into another network of capillaries, the *vasa recta*, which surrounds the loop of Henle to allow ion and water reabsorption back into the bloodstream. Finally the blood enters the venous system of the kidney and exits the kidney through the renal vein.

Early kidney development and nephrogenesis.

The development of the definitive adult kidney begins in embryonic life with reciprocal signaling between the cells of the branching ureteric bud (Figure 1.3, orange) extending off the Wolffian duct, and the surrounding cells of the metanephric mesenchyme (or metanephric blastema), which includes the inner layers which will form the cap mesenchyme (green) and stroma (red). The ureteric bud and the cap mesenchyme, marked by their expression of Hoxb7 and Six2/Cited1 respectively, will form the

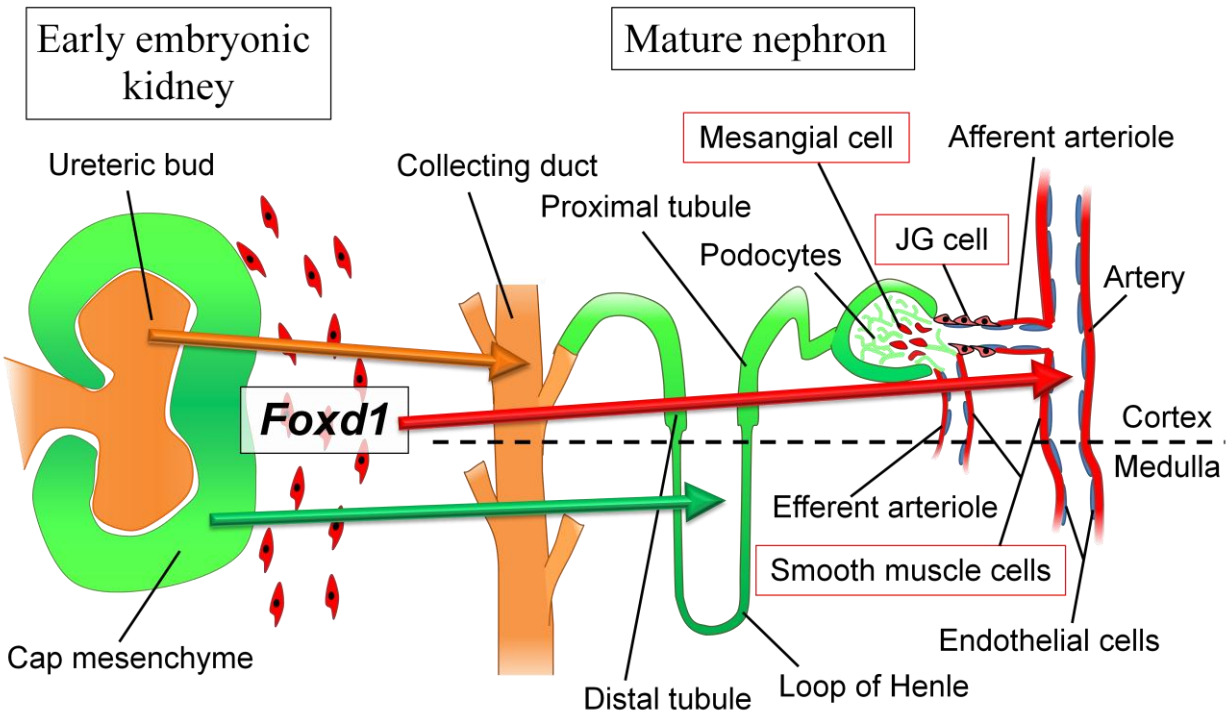

Fig. 1.3 Lineage relationships of the developing kidney. Proposed derivatives of Foxd1 cells are highlighted red.

epithelial components of the nephron through a process called nephrogenesis- the ureteric bud is induced to form the renal urinary collecting duct system(1-3), while the metanephric mesenchyme differentiates into the epithelial component of the nephron (green): the proximal and distal tubules, loop of Henle, and the capsule of the glomerulus (4, 5). As the epithelial nephron differentiates, the metanephric mesenchyme forms a stereotypical series of structures- first the spherical-shaped renal vesicle, then the comma-shaped body, and then the s-shaped body, which will eventually culminate in the formation of a mature nephron (Figure 1.3). In humans, nephrogenesis is completed by about 34-35 weeks of gestation. In mice however, nephrogenesis continues after birth for about 3-5 days.

Another key morphogenetic event in renal development is the proper assembly of the vascular network to distribute blood to the nephrons. The gross morphology of the renal arterial tree is well characterized, and assembly of the arteries occurs rapidly during kidney development in a highly stereotyped fashion (Figure 1.2). At the time of the first division of the ureteric bud, embryonic day 12 in mice, the embryonic kidneys do not have arteriolar vessels. In mice, the first arterioles are seen around 14-15 days of gestation, and by 18-19 days of gestation the basic blueprint of the renal arterial tree has been established (6). This is followed by a burst of fractal branching and elongation of new arteries and arterioles that repeat the basic pattern for about 10 days after birth, resulting in a remarkable increase in the complexity and surface area of the vasculature (Figure 1.2). This choreographed series of events requires that progenitor cells differentiate into the correct cell types, acquire positional information, assemble in the right location within the vessel, and branch in the correct directions. Failure to correctly form the renal

vascular tree is associated with many forms of renal disease, as exemplified by the serious developmental defects in mice where arterial assembly is perturbed (6-9), particularly when the insult occurs in the newborn period when branching is at its peak. In these models, altered vascular patterning is quickly followed by deteriorating renal structure and impaired kidney function. However, comparatively little is known about the assembly of the kidney arteries versus the epithelial components of the nephron. Firstly, the origin of the renal vessels has been long debated. While *in vitro* kidney culture as far back as the first half of the 20th century allowed identification of the progenitors for the epithelial nephron, the progenitor cell or cells that give rise to the renal arteries was unknown, as the renal vasculature does not develop *in vitro*. Further, appropriate differentiation of the mural cells (which are the cells that line the renal arteries including pericytes, smooth muscle cells (SMCs), fibroblasts, but excluding endothelial cells) is important for maintaining vascular integrity and control of vascular tone (10, 11). However, the biomolecules and signaling pathways which underlie the establishment, differentiation and maintenance of the mural cell layer of the renal arteries, are also unknown.

One crucial cell type not yet discussed is the endocrine cells of the juxtaglomerular (JG) apparatus, which are essential for homeostatic regulation, and can be found, like their name implies, adjacent to the glomerulus, lining the afferent and sometimes efferent arterioles (Figure 1.3). These cells are also known as renin cells for their synthesis of the enzyme and hormone renin. Secretion of renin from JG cells results in a physiological cascade, collectively known as the renin-angiotensin-aldosterone system (RAAS), that causes an elevation in blood pressure accompanied mainly by increased reabsorption of

sodium chloride and water with the attendant maintenance of extracellular fluid volume and composition. Control of renin levels in the bloodstream from renin cells in the kidney is one of the primary effectors the body possesses to regulate fluid and electrolyte homeostasis. In addition to homeostatic regulation, renin cells are also associated with branching of the renal blood vessels (12). The factor or factors which control the differentiation of renin cells in particular have long been an area of focus for the Gomez lab and are also investigated in this dissertation.

Renal progenitors of the kidney vasculature

Identifying the progenitor cell population(s) which give rise to the renal vasculature is key to exploring the mechanisms responsible for vascular patterning and development. There were initially questions as to where those precursors were found, as extra-renal origins have been previously suggested for the renal vasculature. However, cross-transplantation studies demonstrated that the progenitors of the renal vasculature are present within the kidney itself (13, 14).

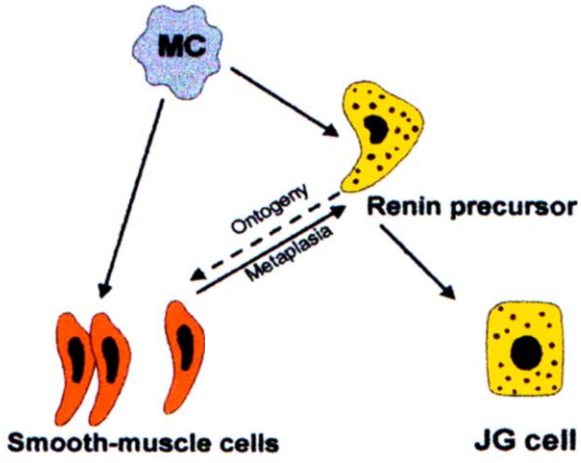

Fig. 1.4 The lineage relationships of the renin cell. Renin precursor cells are derived from metanephric mesenchymal cells (MC). Renin precursor cells differentiate into a subset of the renal arterial smooth muscle cells. These cells retain the ability to re-express renin in response to homeostatic challenge. Figure adapted from (13)

Work done previously in our lab identified the precursors for the JG cells and a subset of the arterial smooth muscle cells and mesangium. Examination of embryonic kidneys at different ages shows that renin expression varies dynamically through development. Early in kidney development renin is expressed in cells lining the large arteries of the kidney vasculature. As the organ

matures renin expression is progressively segregated up the developing arteries until it is restricted to the classical adult juxtaglomerular location described earlier (15). Renin precursor cells give rise not only to mature JG cells that maintain expression of renin but also to other cell types that will not express renin, such as a subset of vascular smooth muscle cells lining the renal arteries and cells of the glomerular mesangium (16). Interestingly, those cells retain the ability to re-express renin in response to stimuli that challenges homeostasis (16). Thus, a need for a sustained increase in systemic renin production is met not only through a significant increase in renin production and release by the JG cells, but instead through an increase in renin cell number, as cells which previously in ontogeny had expressed renin reacquire the ability to synthesize and secrete renin (16, 17). These lineage relationships are depicted in Figure 1.4. It must be emphasized that this increase in cells that secrete renin does *not* involve proliferation of migration of cells, or *de novo* expression by cells previously incapable of synthesizing the hormone. Instead, it occurs through reactivation of a conserved developmental program geared to renin synthesis when homeostasis is threatened (18).

However, it was still unknown whether there existed a single progenitor cell for the entirety of the kidney vasculature, or whether the vasculature arose from multiple cell populations (including renin precursor cells). In this thesis I examine the hypothesis that the progenitors are located in the renal stroma, which is composed of a group of loosely associated cells found in the developing kidney surrounding the cap mesenchyme (Figure 1.3). The stromal cells are characterized by their embryonic expression of the protein Forkhead Box D1, or Foxd1.

Forkhead Box D1 (Foxd1)

Foxd1 is a member of the forkhead box winged helix transcription factor family first identified in 1994 in the developing nervous system in the rostral diencephalic neuroepithelium as “Brain Factor 2” (19). Deletion of Foxd1 resulted in a number of birth defects that resulted in death shortly after birth, including markedly abnormal renal formation. The kidneys had gross anatomical defects, including renal hypoplasia, and a failure to properly separate and ascend (20), as would happen during normal renal development. In addition, it was previously noted that Foxd1-null kidneys had disrupted patterning of the tubules and collecting duct system, indicating that Foxd1 plays a role in the differentiation of those structures. However, lineage tracing studies showed that Foxd1 cells did not give rise to those components of the kidney.

Within the kidney, Foxd1 marks a group of loosely associated mesenchymal cells known as stromal cells, which are located surrounding the branching ureteric bud and cap mesenchyme (Figure 1.3). Based on their location, these cells are excellent candidates for precursor cells giving rise to the cells of the renal vasculature; the first chapter of this thesis investigates this hypothesis, and seeks to determine the role of Foxd1 itself in the development of the renal vasculature.

Genes that confer the identity of renin cells

In addition to determining the precursor(s) for the renal vasculature, there is a need to identify the mechanisms that regulate the differentiation of those precursor cells into the renal vasculature. We have previously studied the differentiation of renin precursor cells which, along with their important physiological role (regulation of blood pressure and fluid-electrolyte homeostasis), also have the interesting capability to differentiate to form a subset of the arterial smooth muscle cells, while retaining the ability to re-express

renin. To define which genes establish the identity of renin cells we performed microarray analysis on FACS-purified renin-expressing cells from the kidneys of newborn, adult, and adult mice stimulated with captopril (to induce an increase in renin producing cells) adult kidneys (18). We identified a core of 118 renin cell transcription factors which are present in renin cells and whose binding sites are conserved in the mouse and human renin promoters (Figure 1.5). Importantly, in developing renin cells we noted the expression of "Recombinant signal binding protein for immunoglobulin kappa J region" (RBP-J, circled), the final transcriptional mediator of Notch signaling, in addition to all the Notch receptors and their ligands (18). Interestingly, we also noted that renin cells in newborn mice express a number of angiogenic factors such as Angiopoietin2, VEGF-D, various integrins, ENPP2/5, and RGS genes, raising the possibility that renin cells play a role in vascular growth; in fact, it was previously known that during kidney development renin is associated with branching events in the kidney vasculature (21). In those studies, we also identified one particular enzyme, aldo-keto reductase family 1 subfamily b member 7 (AKR1B7), which is highly expressed specifically in renin cells. Characterization of the expression of that protein forms the middle part of this dissertation.

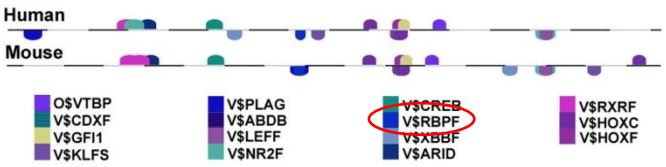

Fig. 1.5 Localization of binding sites for transcription factors enriched in JG cells. Sites conserved in the renin proximal promoter of mice and humans. Red circle, V$RBPF=RBP-J

RBP-J, the Notch signaling pathway, and renin cells

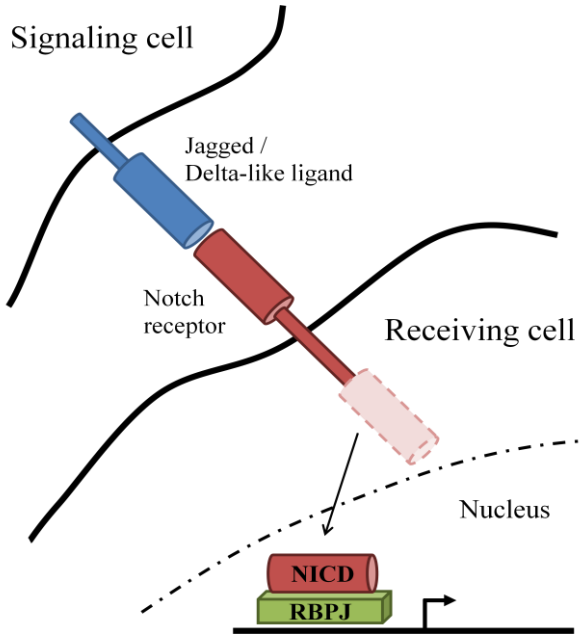

Fig. 1.6 The Notch signaling pathway. Binding of the Notch receptor to the Jagged/Delta-like ligand induces proteolytic cleavage of the Notch intracellular domain (NICD). The NICD translocates to the nucleus where it regulates gene transcription by activating the transcription factor RBPJ .

The Notch signaling pathway is an ancestrally conserved system of direct cell-to-cell communication. Activation of the pathway is mediated by receptor-ligand interactions- in mammals this consists of four Notch receptors (Notch 1-4) and the ligands of the Delta-like (Delta-like 1, 3, and 4) and Jagged (Jagged 1 and 2) families. As shown in Figure 1.6 binding of the receptor to a ligand results in 2 successive proteolytic cleavages of a domain of the Notch receptor- the Notch intracellular domain (NICD) (22). The NICD is trafficked to the nucleus, where it interacts with a transcriptional complex centered on the transcription factor RBP-J (23-25) (CBF1 in humans, also known as CSL, Su(H), and Lag1 in other organisms). RBP-J is the common transcriptional mediator of all the Notch receptors and ligands, and this point of integration is an excellent site to study Notch pathway activation and inactivation.

Canonical Notch cell to cell signaling plays a prominent role during development, imparting cell fate decisions in many tissues and is involved in organogenesis and vasculogenesis in multicellular organisms (26-28). One hypothesis investigated by our lab was that the Notch pathway and RBP-J played a role in the differentiation of the renin cell, which, as mentioned above, is intimately tied to the kidney vasculature.

Utilizing the cre-lox system, our lab deleted RBP-J within renin cells. This resulted in mice with significantly fewer renin-positive JGAs and a total reduction in renin cell number, accompanied by a decrease in circulating renin and hypotension (21). In addition, mice with deletion of RBPJ in renin cells had a significantly blunted ability to re-express renin following a threat to homeostasis (Figure 1.7). It was also found that the renin promoter has an RBP-J site, and that mutation of the site resulted in significantly decreased expression of a reporter gene driven by the renin promoter. Similarly, there are two potential binding sites for RBP-J in the Foxd1 promoter. The final part of my dissertation investigates the hypothesis that RBP-J plays a key role in the differentiation of Foxd1 cells and the development of the kidney vasculature.

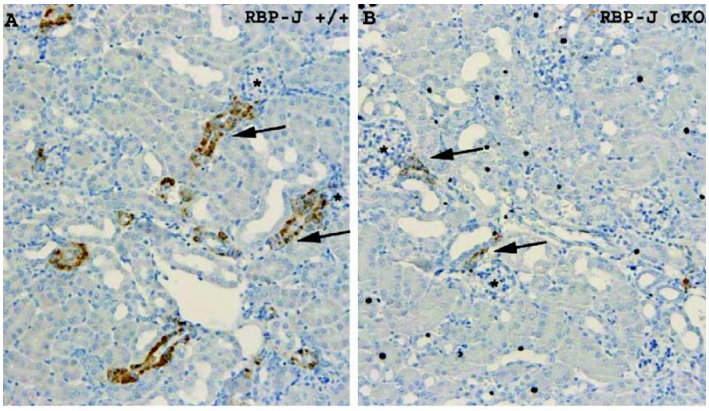

Fig. 1.7 Deletion of RBP-J results in an inability of renin lineage cells to re-acquire the renin phenotype. Staining for renin in wild type animals shows extension of renin staining along the afferent arteriole. Animals with conditional deletion of RBP-J in renin cells fail to re-express renin in those areas. Taken from (21)

Overview

Proper establishment, differentiation, and patterning of the renal arterial tree is essential for the development of a normal functioning kidney. However, the mechanisms and cell populations that are responsible for the formation of the renal vasculature are poorly understood. My thesis examines the role played by Foxd1-positive stromal cells in the formation of the renal vasculature, and identifies key proteins in their differentiation and function.

In Chapter 2, we show that Foxd1 cells are the earliest upstream progenitor for the arterial mural cells, including renin cells, and also glomerular mesangium. We also demonstrate that the transcription factor Foxd1 itself directs the endowment and patterning of the renal vasculature. Finally, we show that the Foxd1 cell itself is required for proper kidney development

In Chapter 3, we investigate the ability of AKR1B7 to serve as a marker for renin cells. We show that AKR1B7 is co-expressed with renin through a variety of manipulations, and that its expression is independent of renin *per se*. We also demonstrate that AKR1B7, similar to renin, is regulated by cAMP signaling.[4]

Chapter 4 looks at the role played by the transcription factor RBP-J in the differentiation of Foxd1 cells. We show that conditional deletion of RBP-J in Foxd1 cells results in a severely stunted renal arterial tree with a thinner layer of smooth muscle cells. In addition, mesangial cells fail to develop properly, and as a result glomeruli are abnormal and have aneurysmatic capillaries. We also show that these effects are exacerbated by aging, followed by a secondary phenotype of prominent vascular and interstitial fibrosis.

Chapter 5 closes my dissertation with a discussion of the implications of my research, and summarizes potential future directions for the work performed here.

[4] This work was originally my Master's thesis, before I switched track to PhD.

II. THE EARLIEST METANEPHRIC ARTERIOLAR PROGENITORS AND THEIR ROLE IN KIDNEY VASCULAR DEVELOPMENT

Formatted as a second-authored manuscript and published as:

The earliest metanephric arteriolar progenitors and their role in kidney vascular development. Sequeira-Lopez ML, Lin EE, Li M, Hu Y, Sigmund CD, Gomez RA. Am J Physiol Regul Integr Comp Physiol. 2015 Jan 15;308(2):R138-49. doi: 10.1152/ajpregu.00428.2014.

Abstract

The development of the kidney arterioles is poorly understood. Mature arterioles contain several functionally and morphologically distinct cell types including smooth muscle, endothelial, and juxtaglomerular cells, and they are surrounded by interconnected pericytes, fibroblasts and other interstitial cells. We have shown that the embryonic kidney possesses all the necessary precursors for the development of the renal arterial tree, and those precursors assemble *in situ* to form the kidney arterioles. However the identity of those precursors was unclear. Within the embryonic kidney, several putative progenitors marked by the expression of either the winged-forkhead transcription factor 1 (Foxd1+ progenitor), the aspartyl-protease renin (Ren+ progenitor), and/or hemangioblasts (Scl+ progenitor) are likely to differentiate and endow most of the cells of the renal arterial tree. However, the lineage relationships and the role of these distinct progenitors in renal vascular morphogenesis have not been delineated. We therefore designed a series of experiments to ascertain the hierarchical lineage relationships between Foxd1+ and Ren+ progenitors and the role of these two precursors in the morphogenesis and patterning of the renal arterial tree. Results show that 1) Foxd1+ cells are the precursors for all the mural cells (renin cells, smooth muscle cells, perivascular fibroblasts and pericytes) of the renal arterial tree and glomerular mesangium and 2) Foxd1 *per se* directs the origin, number, orientation and cellular composition of the renal vessels.

Introduction

The kidney is a highly vascularized organ, which in the adult animal receives approximately twenty percent of the cardiac output (29). Development of a functional kidney requires that each nephron be properly vascularized. Blood enters each glomerulus from an afferent arteriole and leaves it via an efferent arteriole. The spatial arrangement of the pre- and post-glomerular vessels within each nephron is crucial for the regulation of renal blood flow, arterial blood pressure, glomerular filtration rate, urine concentration, acid-base balance, disposal of waste products and other kidney functions that maintain the constancy of our internal milieu and whole body homeostasis. Therefore, proper assembly of the arterioles with their corresponding nephrons is a fundamental morphogenetic event that leads to the formation of a functioning kidney. The mechanisms involved in the development of the kidney vasculature are not well understood but they are intimately linked to nephrogenesis, the formation of the epithelial nephron. Nephrogenesis of the definitive kidney in mammals occurs by the reciprocal inductive interaction of two mesoderm-derived structures: the ureteric bud, an outgrowth of the Wolfian duct, and the metanephric mesenchyme, a condensation of the paraxial, intermediate mesoderm. In mice, nephrogenesis begins around embryonic day (E) 11.5. The ureteric bud undergoes branching morphogenesis and around each ureteric tip it induces mesenchymal cells to arrange themselves in two distinct cell compartments (Figure 1.1): 1) the cap mesenchyme, an inner, condensed cell population, which expresses *Six2* and *Cited1* and is in close contact with the ureteric bud. These cells undergo mesenchymal- to epithelial transformation and generate most of the epithelial nephron including glomerular epithelium, proximal tubules, and loops of

Henle, distal and connecting tubules (whereas the ureteric bud, in turn, differentiates into the collecting ducts and ureter); and 2) an outer layer of loosely arranged mesenchymal cells which express the transcription factor *Foxd1* (stromal cells) (20) or *cKit* (endothelial precursors) (30). Within the loose mesenchyme compartment we have previously identified renin precursors (13). These cells are strategically located to provide the necessary precursors for the formation of the kidney vasculature. However the development of the kidney vasculature is poorly understood. Previous studies from our laboratory using immunostaining, *in situ* hybridization and/or individual cell micro isolation followed by nested RT-PCR indicated that the prevascular embryonic kidney possessed all the necessary precursors (including renin, smooth muscle, and endothelial precursors) for the development of the renal arterial tree, and that those precursors have the capability of assembling *in situ* to form the kidney arterioles (13). We also showed that renin progenitors differentiate to juxtaglomerular cells, a subset of arteriolar smooth muscle and mesangial cells and they are not related to the endothelial lineage (31). Thus, the stromal compartment contains these two progenitor cells (Foxd1+ and Ren1+), which are likely to endow most of the renal arterial tree. However, the lineage relationships, and the role of these two distinct progenitors in renal arteriolar morphogenesis have not been delineated. We designed a series of experiments to define 1) whether Foxd1+ stromal cells are the precursors for the cells that compose the renal arterial tree and 2) whether *Foxd1 per se* regulates kidney vascular morphogenesis and orientation.

Figure 2.1

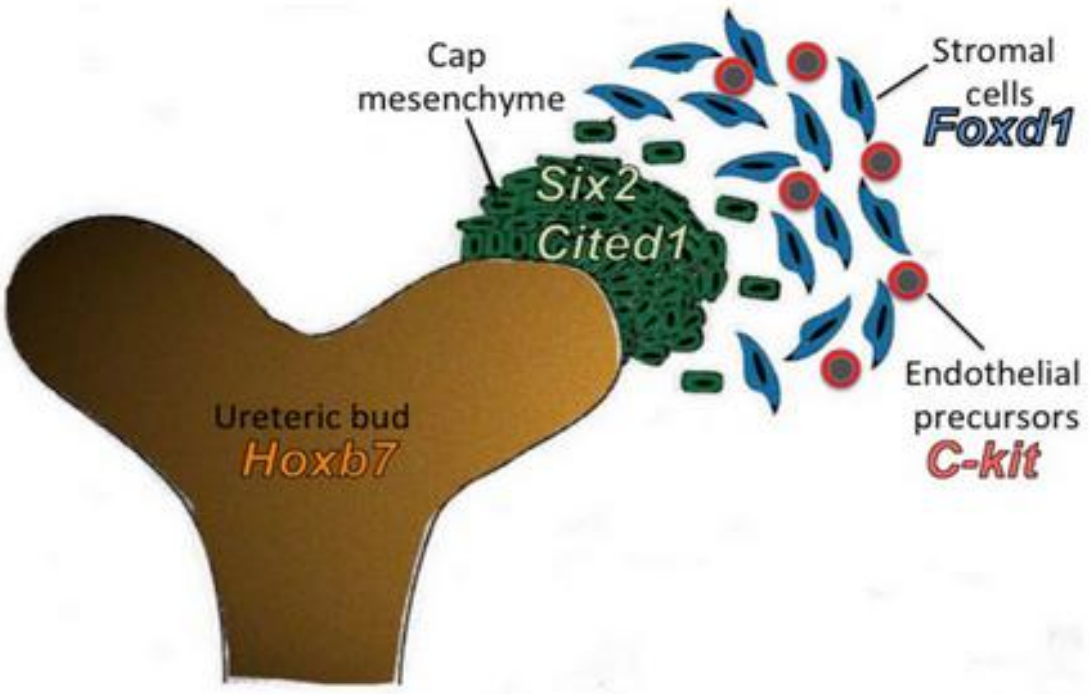

Figure 2.1. Schematic of the early metanephric kidney cells compartments. The Hoxb7-lineage ureteric bud will give rise to the collecting duct system. The cap mesenchyme, which expresses Six2 and Cited1, will give rise to the epithelial components of the tubular nephron. We propose the existence of two other progenitor populations in the nascent kidney: Endothelial precursors, which express C-kit, will differentiate into the vascular endothelium, and Foxd1-expressing stromal cells, which will give rise to the arterial mural cells and mesangium (see Figure 1.3).

Results

Foxd1 cells are an early precursor for mesangial, vascular smooth muscle, renin cells and pericytes

Foxd1 is a marker of stromal cells during kidney development (20). To investigate the fate of Foxd1 cells within the kidney we crossed *Foxd1-Cre* knock-in mice (*FoxD1-GFP-Cre,* referred to as *Foxd1*^{cre} mice) (31) to *R26R* (32) or *mTmG* (33) reporter mice, and followed the distribution of β-galactosidase positive (β-gal+) or green fluorescent protein positive (GFP+) cells within the kidneys during embryonic (E13.5-E17.5) and postnatal life (at 1 day, 1 month and 2 months). As shown in Figure 2A β-gal+ cells were restricted to the undifferentiated stroma at E13.5 with no expression among the developing/branching epithelial cells. By E17.5 there was expression in mesangial cells of the developing glomeruli, afferent and efferent arterioles and within the renal interstitium. In the newborn kidney, the walls of the developing arterioles and arteries were covered by β-gal+ cells. The endothelial cells (ECs), however, were not positive for β-gal. In the adult kidney, when development is completed and therefore mature arterioles and arteries can be easily discerned, β-gal+ cells are present throughout their walls including the adventitia. Again, ECs were not labeled by the blue Xgal reaction product. Within the peritubular interstitium β-gal+ pericytes are present surrounding the ECs that form the peritubular capillaries as previously described (31).

Double labeling studies (X-gal staining and immunostaining for α-smooth muscle actin [α-SMA] and renin) confirmed that Foxd1 derived blue cells correspond to both renin and vascular smooth muscle cells (SMCs) within the developing (Figure 2.2B) and mature vessels (Figure 2.2C).

Isolation of Foxd1-lineage cells from *Foxd1^{cre};mTmG* newborn and 1 month old mice (GFP+) by Fluorescent Activated Cell Sorting followed by RT-PCR for Tie2 (EC marker) and β-globin (EC and blood cell marker) confirmed that cells from the Foxd1 lineage do not differentiate into cells expressing the endothelial marker Tie2 (Figure 2.2D). Immunofluorescence for the endothelial marker Pecam (Figure 2.2E) further shows no coincidence between ECs and cells derived from Foxd1 precursors.

Altogether, these studies suggest that Foxd1+ cells are progenitors for all the mural cells of the arteriole. ECs, however, are not derived from Foxd1+ cells.

Figure 2.2

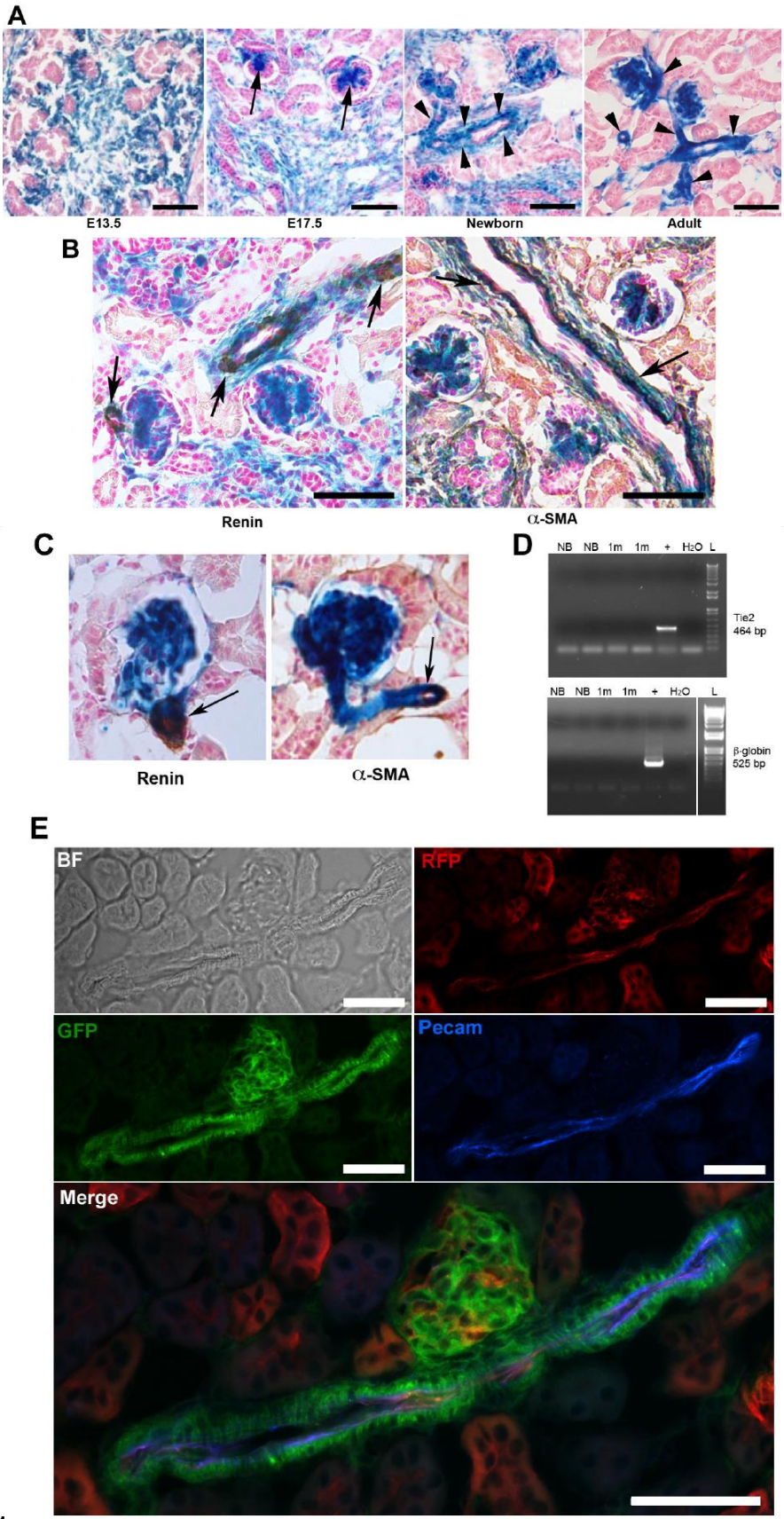
A
E13.5
E17.5
Newborn
Adult
B
Renin
α-SMA
C
Renin
α-SMA
D
NB NB 1m 1m + H2O L
Tie2
464 bp
NB NB 1m 1m + H2O L
β-globin
525 bp
E
BF
RFP
GFP
Pecam
Merge

Figure 2.2. Foxd1+ cells are an early precursor for mesangial, vascular smooth muscle, renin cells and pericytes but not for endothelial cells. A. *Foxd1^{cre};R26R* kidneys sections at different developmental stages showing extensive expression of *β-gal* within the undifferentiated stromal compartment (E13.5), with progressive differentiation into glomerular mesangium (E17.5, arrows), and cells in the wall of the arterial tree (NB and adult, arrowheads). Endothelial cells within the arterioles do not express *β-gal*. B. *Foxd1^{cre};R26R* newborn kidneys sections showing co-expression of β-gal with immunostaining for renin (left, brown) and with α-SMA (right, brown). Endothelial cells do not express β-gal. C. Immunostaining for renin (left) and α-SMA (right) in kidney sections from adult mice show coincidence of the DAB product (brown) with the X-gal staining (blue) (arrows). D. RT-PCR for Tie2 (top) and β-globin (bottom) was positive in samples of whole kidneys (+) and negative in FACS isolated Foxd1-lineage cells from *Foxd1^{cre}*;*mTmG* newborn (NB) and 1 month old (1m) mouse kidneys. L, 1KB ladder; H_2O, negative control. E. Immunofluorescence for Pecam in kidney section from an adult *Foxd1^{cre}*;*mTmG* mouse shows lack of coincidence of the blue fluorescent marker with cells derived from the Foxd1 precursors (GFP). However, ECs identified by Pecam expression are also positive for RFP which marks cells not derived from Foxd1 progenitors. Scale bars, 50 μm. (A performed by MLS, B-C performed by ML, D performed by EEL, E performed by ML)

Embryonic expression of Foxd1 and expression in veins and lymphatic vessels

Our previous work has shown that renal stromal cells, marked by their expression of Foxd1 early in kidney development, differentiate into the entirety of the arterial mural cells (which we define as smooth muscle cells (SMCs), renin cells, and perivascular fibroblasts, but excluding endothelial cells) and glomerular mesangium. In addition, work using an inducible cre system showed that an ever-decreasing portion of mural cells and mesangium is labeled when induction occurs at later embryonic ages, and that Foxd1 promoter activity ceases in the kidney prior to day 10 of post-natal life. In order to understand the precise time course of the expression of Foxd1 within the developing kidney, and to investigate the temporal relation of Foxd1 expression relative to the differentiation of the Foxd1-expressing stromal cell into its downstream derivatives, we generated monoclonal antibodies against several peptide domains in Foxd1, and immunostained for Foxd1 in the developing kidney (Supplementary Figure 2.1). Early in kidney development at embryonic day 13.5, prior to the formation of any renal vasculature, a thin layer of Foxd1-expressing cells stromal cells is found surrounding the condensing mesenchyme. At embryonic day 15.5, when the kidney arteries are established and beginning to become muscularized, Foxd1 staining is found in the abundant stromal cell population surrounding the renal tubules, staining the nucleus and cytoplasm of those cells. By embryonic day 18.5, as the stromal cell population is regressing, Foxd1 expression is now segregated to “islands” of expression throughout the renal parenchyma, in between the renal tubules and along the kidney capsule. Finally, staining kidney tissue from adult mice shows a complete cessation of Foxd1 expression within the kidney. To confirm the specificity of the antibody, we stained Foxd1-null animals. No immunostaining signal was found within the kidney of Foxd1

knockout mice (not shown). Interestingly, we note at all ages that neither the arterial mural cell derivatives of Foxd1 cells nor mesangial cells actively express Foxd1. Thus it appears that once the stromal precursor cells differentiate into those downstream cell types, they cease expressing Foxd1.

However, we note a new population of cells that actively expresses Foxd1 that has not been previously described. During renal development in embryonic life, Foxd1 expression appeared to be detected within the smooth muscle cells of the veins and lymphatic vessels of the kidney. To properly investigate this, we co-stained kidney tissue for Foxd1, as well as markers of veins and lymphatic vessels. LYVE is a marker for lymphatic vessels, while M2a antigen is a marker for both lymphatics and veins. By excluding LYVE-positive vessels from M2a-positive areas, it is thus possible to identify veins. Staining in consecutive kidney sections shows strong, active Foxd1 expression in both veins and lymphatic vessels at embryonic day 18.5 (Supplementary Figure 2.2).

Supplementary Figure 2.1

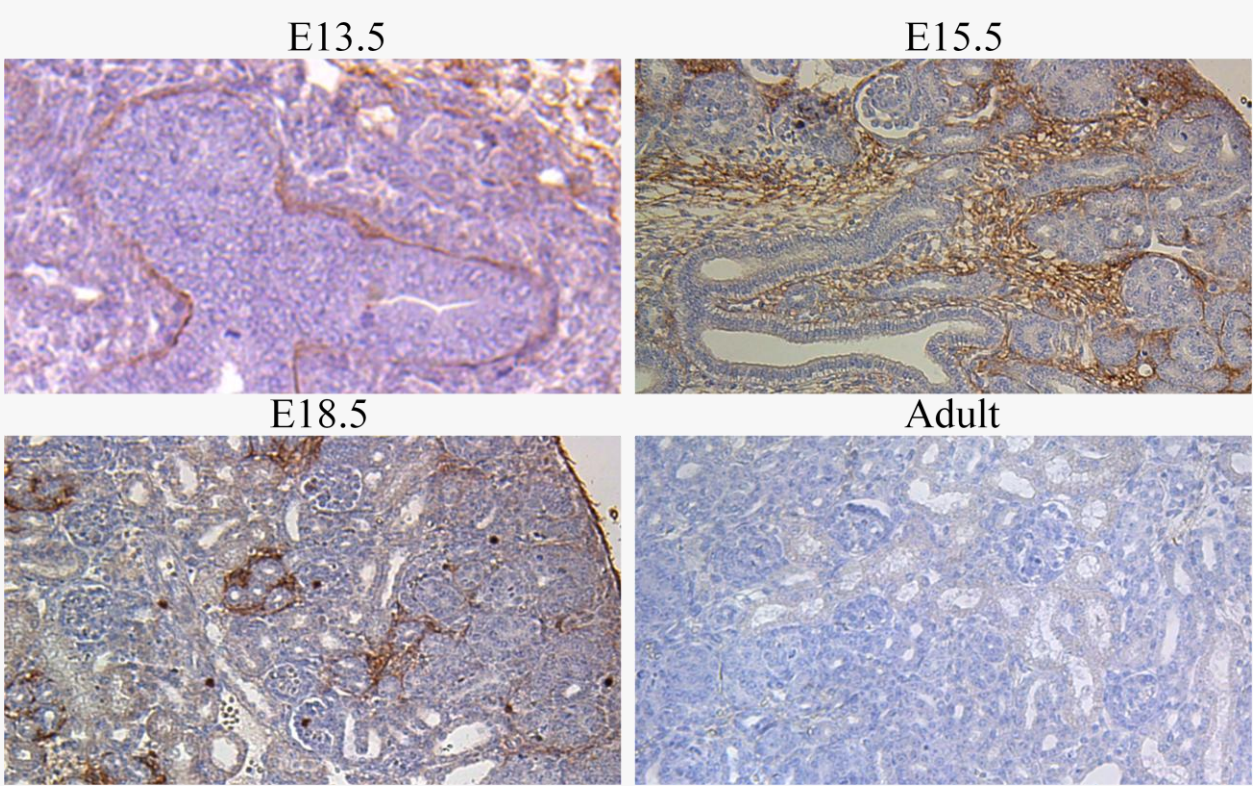

Supplementary figure 2.1: Immunohistochemistry for Foxd1 in the developing kidney. At embryonic day 13.5, Foxd1 is found in the periphery of the condensing mesenchyme. At embryonic day 15.5, Foxd1 is expressed in the loosely associated cells of the stroma, surrounding the developing renal tubules. By embryonic day 18.5 Foxd1 expression is regressing, and is found segregated in focal areas, and along the kidney capsule. By adult life, Foxd1 ceases to be expressed in the kidney. (performed by EEL)

Supplementary Figure 2.2

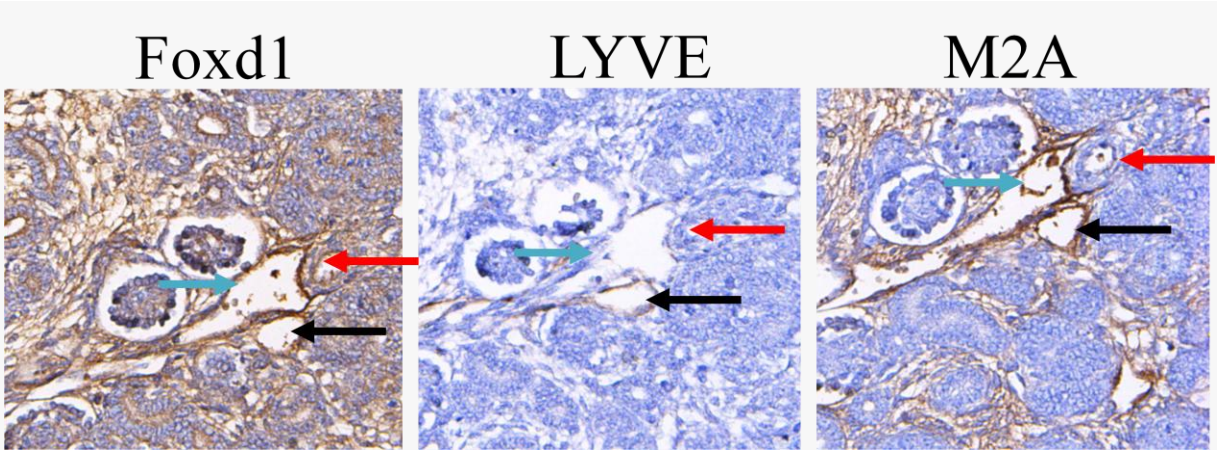

Supplementary Fig. 2.2: Foxd1 is actively expressed in the veins and lymphatic vessels of the developing kidney. Staining with our antibody for Foxd1, and LYVE and M2A in consecutive sections. Lymphatic vessels are marked with LYVE, while veins can be discerned by subtracting the LYVE-positive areas from M2A-positive areas. Foxd1 shows expression within veins (blue arrows) and lymphatic vessels (black arrows). Foxd1 expression is not detected in the arteries (red arrows). (performed by EEL)

Foxd1 is necessary for the proper development of the renal arterial tree.

To address whether Foxd1 is necessary for the development of the kidney vasculature we studied *Foxd1*$^{-/-}$ mice. Mice with deletion of the Foxd1 gene died within the first hours of postnatal life. Shortly after birth they displayed prominent cyanosis, gasping and abdominal distention (their stomachs were filled with ~150mm^3 of air instead of milk) indicating severe respiratory distress (Figure 2.3A). Histological analysis of the lungs showed thickened interstitial mesenchyme with infrequent septation and markedly reduced airway space suggesting that the cause of perinatal death was respiratory failure due to abnormal lung development (Figure 2.3C). Furthermore, the lung weight-body weight ratio was significantly decreased (Figure 2.3B).

In agreement with previous studies (using mice were *Foxd1* was replaced by *lacZ*) (20), the kidneys of *Foxd1*$^{-/-}$ mice were smaller [about 1/3 of the size of the heterozygous or wild type (WT) littermates and with a significantly decreased kidney weight/body weight ratio (Figure 2.3B)], were fused in the midline and to the retroperitoneal wall, failed to ascend and the ureters displayed an abnormal ventral orientation (Figure 2.4A). The renal parenchyma was underdeveloped and instead of the normal centrifugal gradient of nephron differentiation consisted of multiple disorganized lobular areas containing few abnormally distributed subcapsular glomeruli. Furthermore, as shown in Figure 2.5, immunostaining for α-SMA at E17.5 revealed an aberrant distribution of the renal vessels, with subcapsular and capsular arterioles entering the kidney directly from the capsule and connecting to glomeruli in a centripetal rather than in the normal centrifugal fashion. In addition, the nephrogenic zone was disorganized, and replaced in some areas with subcapsular distal tubules in addition to subcapsular mature glomeruli.

Figure 2.3

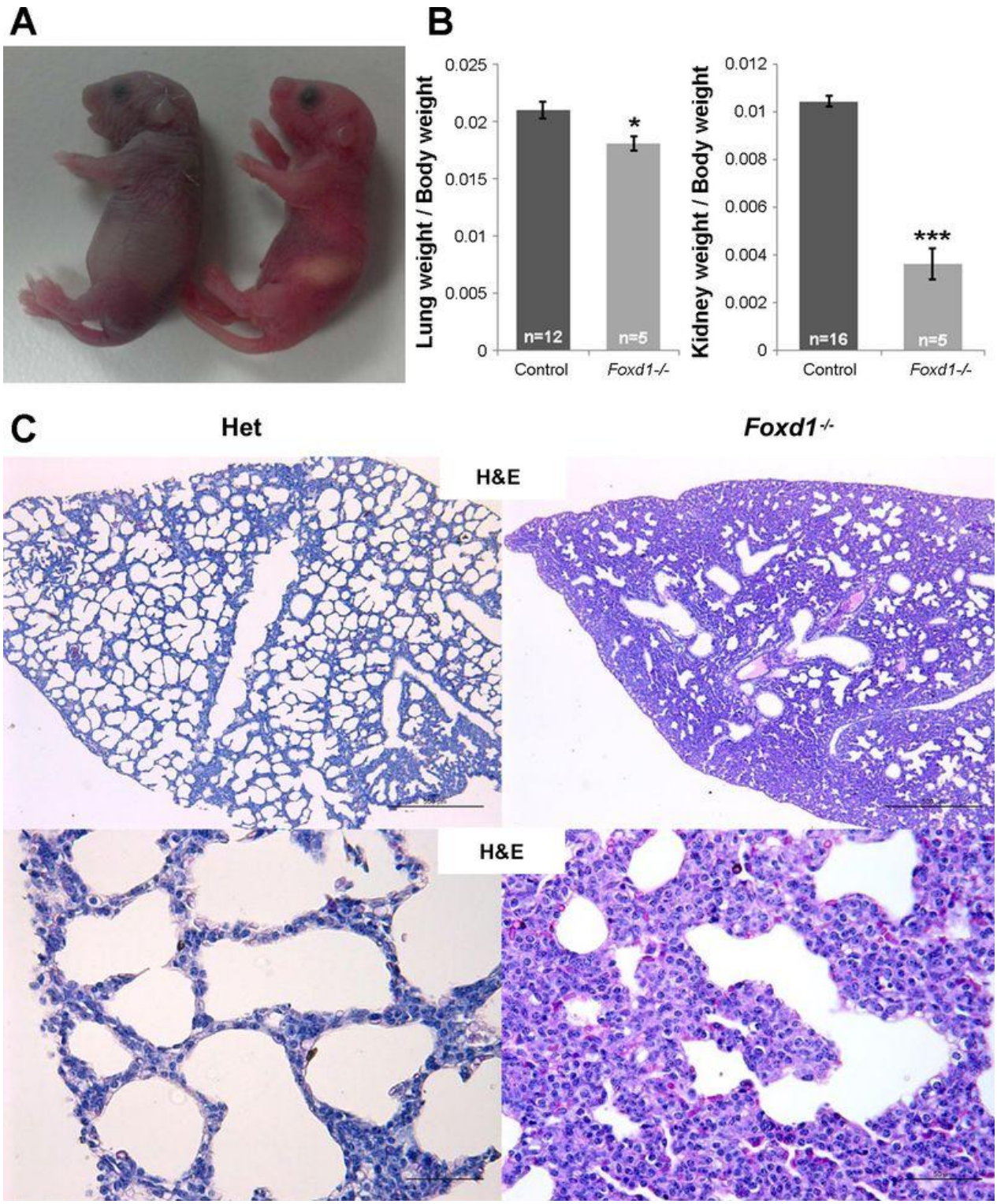
A
B
Lung weight / Body weight
0.025
0.02
0.015
0.01
0.005
0
*
n=12
n=5
Control
Foxd1-/-
Kidney weight / Body weight
0.012
0.01
0.008
0.006
0.004
0.002
0
***
n=16
n=5
Control
Foxd1-/-
C
Het
Foxd1-/-
H&E
H&E

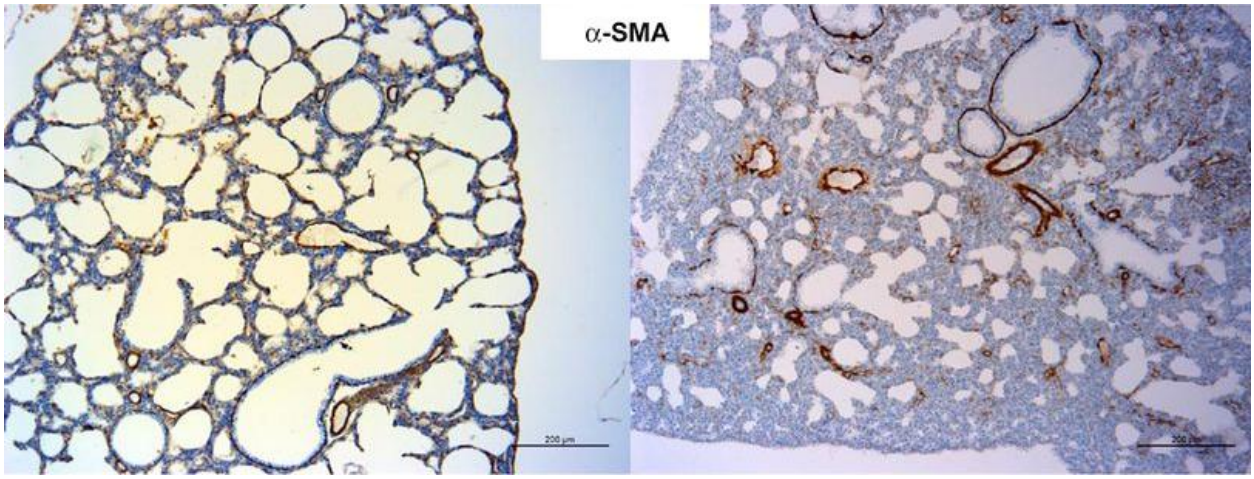

Figure 2.3. *Foxd1* is necessary for normal lung development. A. A newborn *Foxd1*$^{-/-}$ mouse (left) shows cyanosis, abdominal distention, an empty stomach and the mouth wide open indicating respiratory distress; a littermate control (right) shows normal pink skin color and a stomach full of milk. B. Lung weight to body weight and kidney weight to body weight ratios were significantly reduced in *Foxd1*$^{-/-}$ mice (* p<0.05, *** p<0.001). C. Lung sections stained with Hematoxylin and eosin (top and middle panels) and immunostained for α-SMA (bottom panel) show normal lung septation and alveolar development in a *Foxd1* heterozygous mouse and abnormal thickened interstitial mesenchyme with infrequent septation and markedly reduced airway space in a *Foxd1*$^{-/-}$ mouse. Scale bars, 500 µm (top panels), 50 µm (middle panels) and, 200 µm (bottom panels). (Performed by ML)

Figure 2.4

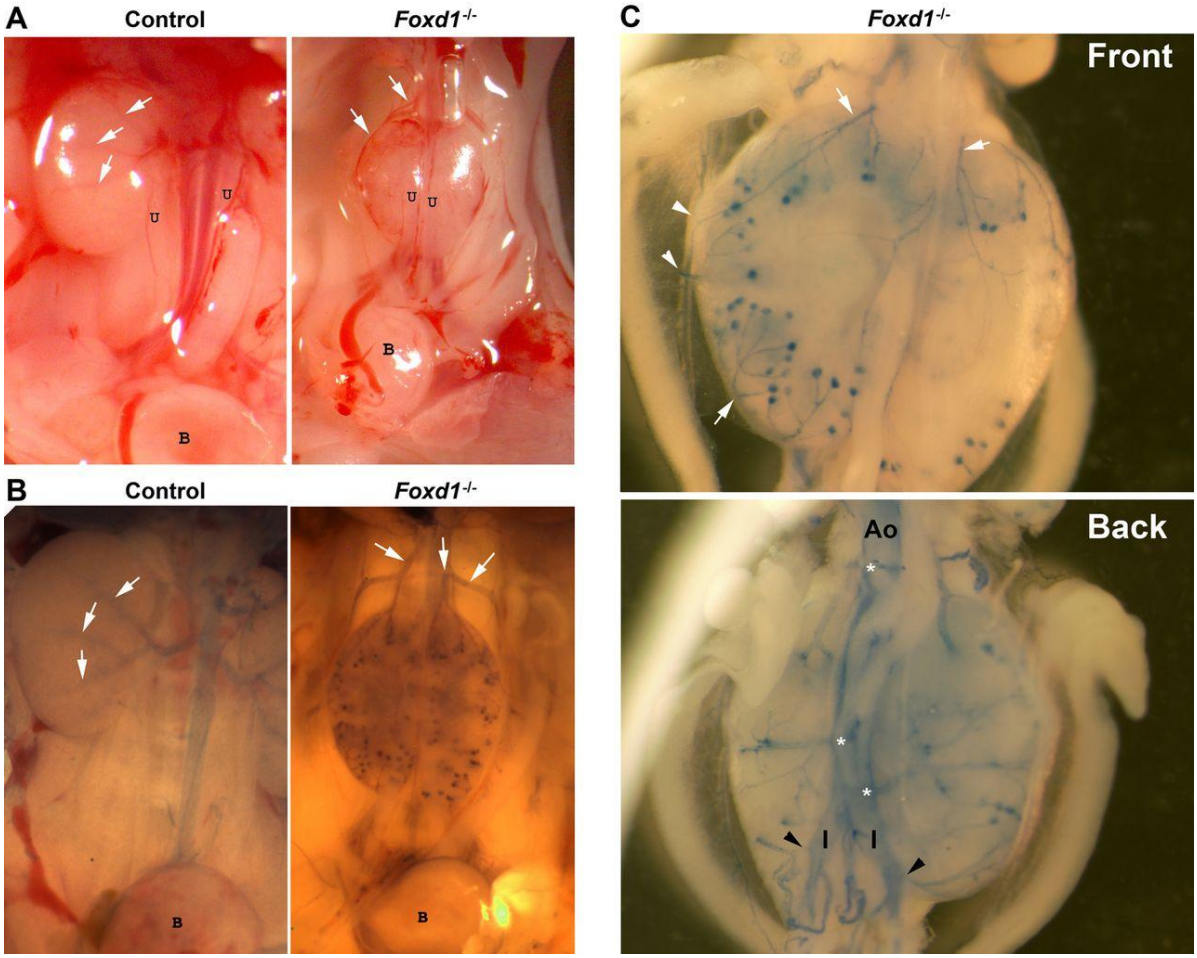

Figure 2.4. Foxd1 is necessary for the proper origin and development of the renal arterial tree. A. Gross morphology of kidneys of control mice show normal intrarenal branches of the renal artery (white arrows) and ureters (u) facing to the midline whereas *Foxd1*$^{-/-}$ mice display capsular arteries (white arrows) originating from the aorta above smaller fused kidneys with ureters oriented ventrally. (B, bladder) B. Evans blue - glycerol labeled perfusion of the aorta and abdominal branches showing the normal arterial branching pattern (white arrows) from a single hiliar renal artery in control mice and aberrant arteries (white arrows) originating from the aorta above the kidneys in *Foxd1*$^{-/-}$ mice. C. Higher magnification of *Foxd1*$^{-/-}$ dissected kidneys area (front and back) attached to the abdominal aorta (Ao) and to the iliac (I) arteries showing in more

detail that there are several subcapsular arteries (white arrows) originating from the aorta at multiple levels (white asterisk) including the iliac arteries (black arrowheads). (Performed by ML)

Figure 2.5

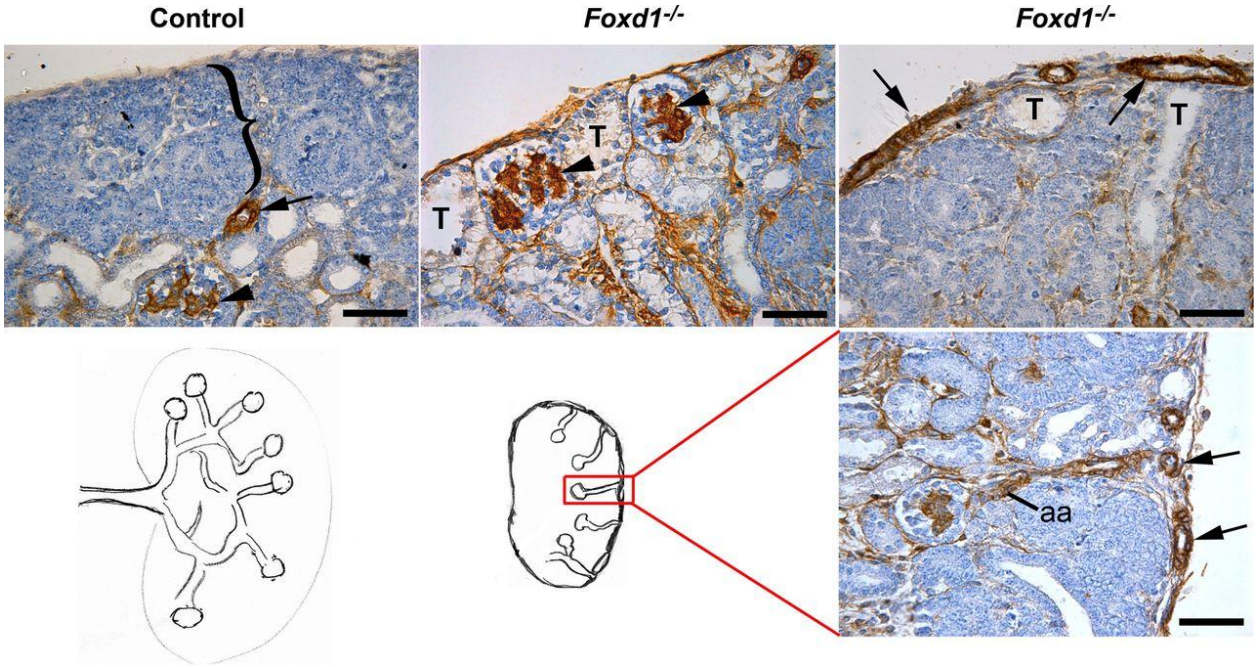

Figure 2.5. *Foxd1*$^{-/-}$ kidneys display abnormal topological orientation of the renal vessels and disorganized renal structure. Immunostaining for α-SMA (brown) of E17.5 kidneys show that control mice present a normal outer undifferentiated nephrogenic zone (bracket) and a further developed inner cortex with arterioles (arrow) and more mature glomeruli expressing α-SMA in the mesangium (arrowhead), whereas *Foxd1*$^{-/-}$ mice present abnormal subcapsular glomeruli (arrowheads) and tubules (T) and capsular arteries (arrows). Lower panel shows a drawing of the vascular pattern in control and *Foxd1*$^{-/-}$ mice as seen in the section stained with α-SMA antibody to highlight the abnormal arteries (arrows) and afferent arterioles (aa). Scale bar, 50 μm. (Performed by ML)

Foxd1 is necessary for the proper orientation and branching of the renal arterial tree.

To define whether Foxd1 is important for the appropriate orientation and branching pattern of the renal arterial tree, we harvested kidneys from newborn mice and manually microdissected the kidney vasculature. The renal arterial tree of WT newborn kidneys displayed normal centrifugal branching of arteries originating from a single renal artery, whereas in *Foxd1*$^{-/-}$ mice, the vasculature consisted of multiple independent arterial and arteriolar branches originating directly from the aorta and not from the renal artery. In turn, those vessels connected with capsular vessels that gave rise to the intrarenal arterioles. Those intrarenal vessels were not properly interconnected with one another. To understand their intrarenal orientation and their connections with their respective nephrons, we performed histological analysis of consecutive sections immunostained for α-SMA to more easily label arterioles (Figure 2.6). Next, we developed a new perfusion technique using 0.5% of Evans blue in glycerol to directly visualize the abnormal preglomerular arterial supply and identify its precise origin. Kidneys from *Foxd1*$^{-/-}$ mice receive their blood supply from anomalous branches originating from the aorta above and below the kidneys (including branches from the iliac arteries) that surround the superior and inferior poles and give rise to sub capsular branches that enter the kidney laterally, often ending as a single afferent arteriole (Figures 2.4-6). Lymphatic vessels in the *Foxd1*$^{-/-}$ kidneys followed the aberrant capsular arteries and veins as evidenced by immunostaining for the specific marker for lymphatic vascular endothelium (LYVE, Figure 2.7). Immunostaining for Neuron-specific class III beta-tubulin (TUJ1) demonstrated that the

capsular vessels were innervated whereas nerve fibers within the kidney were scarce (not shown).

Figure 2.6

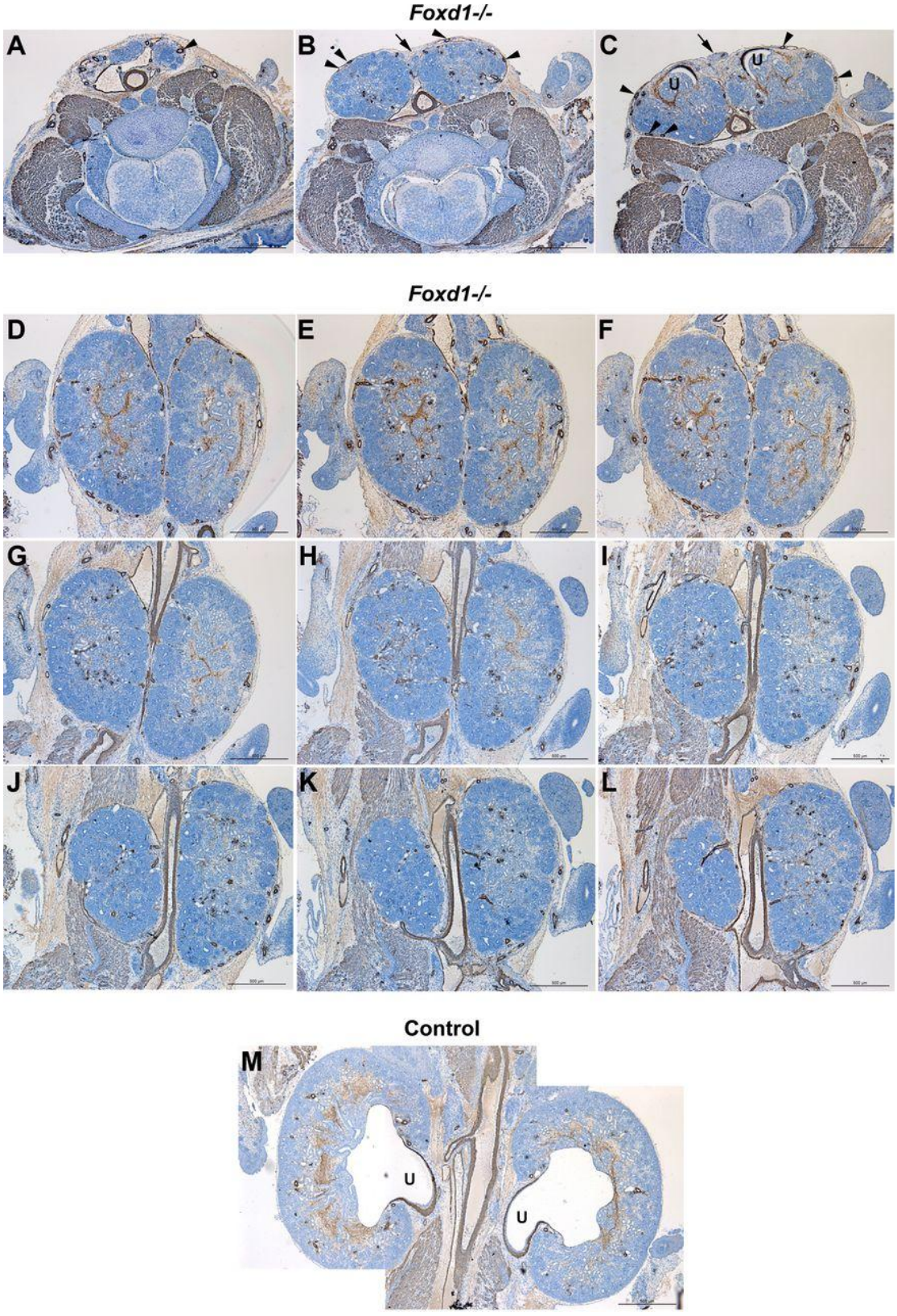

Figure 2.6. *Foxd1*$^{-/-}$ kidneys are irrigated by multiple branches from the aorta instead of a single renal artery. A-C. Transversal sections of E17.5 *Foxd1*$^{-/-}$ kidneys and vertebral area show midline fusion of the kidneys (arrows), ventrally oriented ureters (U, in C) and multiple capsular arteries (arrowheads). D-L Sagittal sections of E17.5 *Foxd1*$^{-/-}$ kidneys show several capsular arteries entering the kidneys and some of them originating from the aorta at different levels. M. Sagittal section of E17.5 littermate control kidneys shows a single renal artery entering the kidney on the left side and normal midline orientation of the ureters (U). Scale bar, 500 µm. (Performed by ML)

Figure 2.7

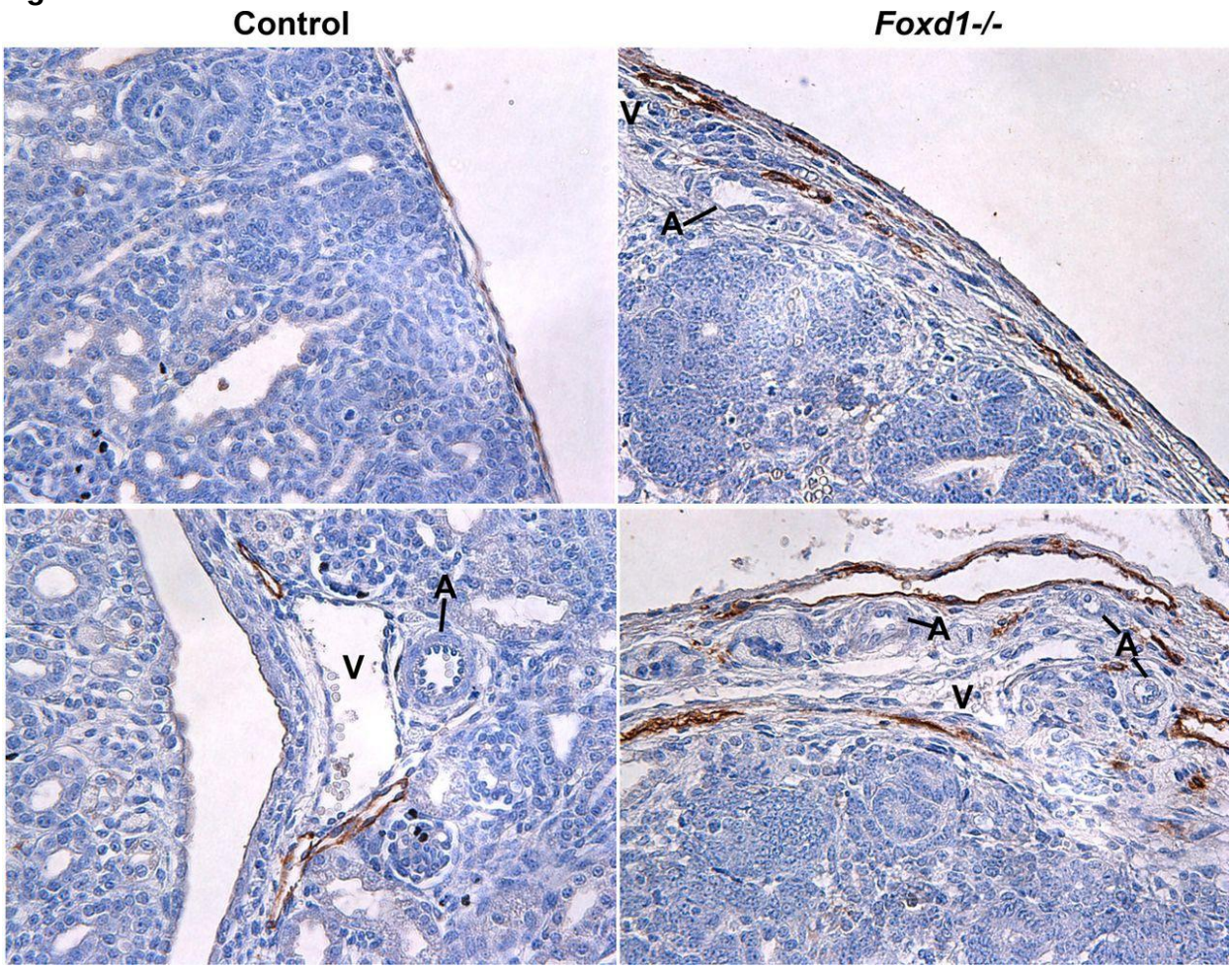

Figure 2.7. *Foxd1*$^{-/-}$ kidneys display abnormal subcapsular lymphatics.

Immunostaining for the specific marker for lymphatic vascular endothelium (LYVE, brown) show in newborn kidneys of control mice (left panels) few lymphatic capillaries within the renal capsule and lymphatic vessels adjacent to a large vein (V) and artery (A), whereas in the *Foxd1*$^{-/-}$ there are multiple large lymphatic vessels adjacent to aberrant capsular arteries and veins. (Performed by ML)

***Mosaic ablation of Foxd1 progenitors phenocopies the Foxd1$^{-/-}$ phenotype*.**

To explore whether deleting or injuring stromal cells would affect the development of the renal vasculature and mesangium, Foxd1 cells were ablated with diphtheria toxin. *Foxd1^{cre}* heterozygous mice were crossed with mice containing the *Rosa-DTA* allele (*R26R^{DTA}*) (34), which expresses diphtheria toxin upon recombination by cre. These mice are referred to as "*Foxd1-DTA*" mice.

At all ages, mice lacking cre recombinase or the *Rosa-DTA* allele were indistinguishable from control animals. *Foxd1-DTA* animals died prior to birth. At E13.5 in control animals the kidneys have normally rotated and separated from each other. However, in *Foxd1-DTA* animals the kidneys were fused at the midline (Figure 2.8A). In addition, the distribution of the arterioles, delineated by smooth muscle staining, was markedly abnormal in mutant mice: whereas in control animals, the arteries and arterioles were located within the developing and still poorly defined corticomedullary junction, in *Foxd1-DTA* animals, they were located at the periphery of the kidney (Figure 2.6B, black arrows).

In addition, in contrast to WT vessels which possess a thick layer of SMCs, the few observable deeper intrarenal vessels found in *Foxd1-DTA* animals had few, small, and poorly defined segments of smooth muscle that did not support a proper vascular lumen (Figure 2.8B, arrowheads). Subsequently, at E17.5, the kidneys had a significant number of smooth muscle coated arteries (arrows) in both controls and *Foxd1-DTA* mice (Figure 2.8C). Interestingly, at this stage, the total number of vessels was not different between WT and mutant kidneys (not shown). However, similar to the phenotype seen in *Foxd1$^{-/-}$* mice, the orientation of vessels in *Foxd1-DTA* kidneys was reversed: the blood vessels laid directly underneath the capsule, turned inward toward the renal parenchyma, and

made connections with glomeruli (Figure 2.8C, dashed arrows). Quantification of this phenotype indicated that two thirds of Foxd1-DTA vessels either rested alongside or originated directly from the kidney capsule (Figure 2.8D). As in the *Foxd1*$^{-/-}$ mice the subcapsular vessels also connect with aberrant and accessory arteries. There was also a significant decrease in the thickness of the vascular smooth muscle layer in *Foxd1-DTA* animals in comparison to controls (Figure 2.8E).

As a lack of developing nephrons at E13.5 implied either delayed or interrupted nephrogenesis and glomerulogenesis in *Foxd1-DTA* animals, we examined *Foxd1-DTA* kidneys at E17.5 to discriminate between these two possibilities. At E17.5, we observed nephrons at all stages of development, including comma-shaped, s-shaped bodies, and mature glomeruli (Figure 2.8C). However, the nephrogenic zone (Figure 2.8C, brackets), an area characterized by rapid cellular proliferation and tissue condensation, was broader in *Foxd1-DTA* animals, an observation consistent with a delay in nephrogenesis. Supporting this hypothesis, the number of comma-shaped and S-shaped bodies, were markedly decreased in mutant animals (Figure 2.8F).

Although diphtheria toxin is purported to be lethal to cells at extremely low concentrations, we noted that some of the cells derived from *Foxd1* cells persisted. To examine the subsequent fate of *Foxd1* cells upon *DTA* expression, the *Rosa-26* reporter allele was bred into *Foxd1-DTA* mice to label Foxd1 cells and their descendants. Whereas in control mice, labeling of mural cells and mesangial cells was uniform, encompassing all the cells descended from the *Foxd1* lineage, labeling in *Foxd1-DTA* animals was patchy. To identify the labeled and unlabeled cells in *Foxd1*-derived structures, we stained for markers of smooth muscle and mesangium. Staining for α-SMA showed mosaic labeling of SMCs:

whereas some cells stained double positive for both α-SMA and the blue lineage marker, other cells positive for α-SMA were negative for β-gal expression (Figure 2.8H). A similar result was found using staining for PDGFR-B (Figure 2.8I), a marker for mesangial and vascular SMCs, showing again the presence of double positive cells as well as cells positive for the mesangial marker but negative for the lineage reporter. These findings indicate that the cell ablation was mosaic: whereas some cells were depleted, others survived and yet others were replaced by adjacent cells. In essence, the *Foxd1-DTA* mice behaved like a *Foxd1* hypomorph, due in great part to the mosaic deletion of cells expressing *Foxd1*. Overall, the findings of *Foxd1-DTA* animal phenocopied those of the *Foxd1*$^{-/-}$ mice underscoring the importance of *Foxd1 per se* in the development of the kidney vasculature.

Figure 2.8

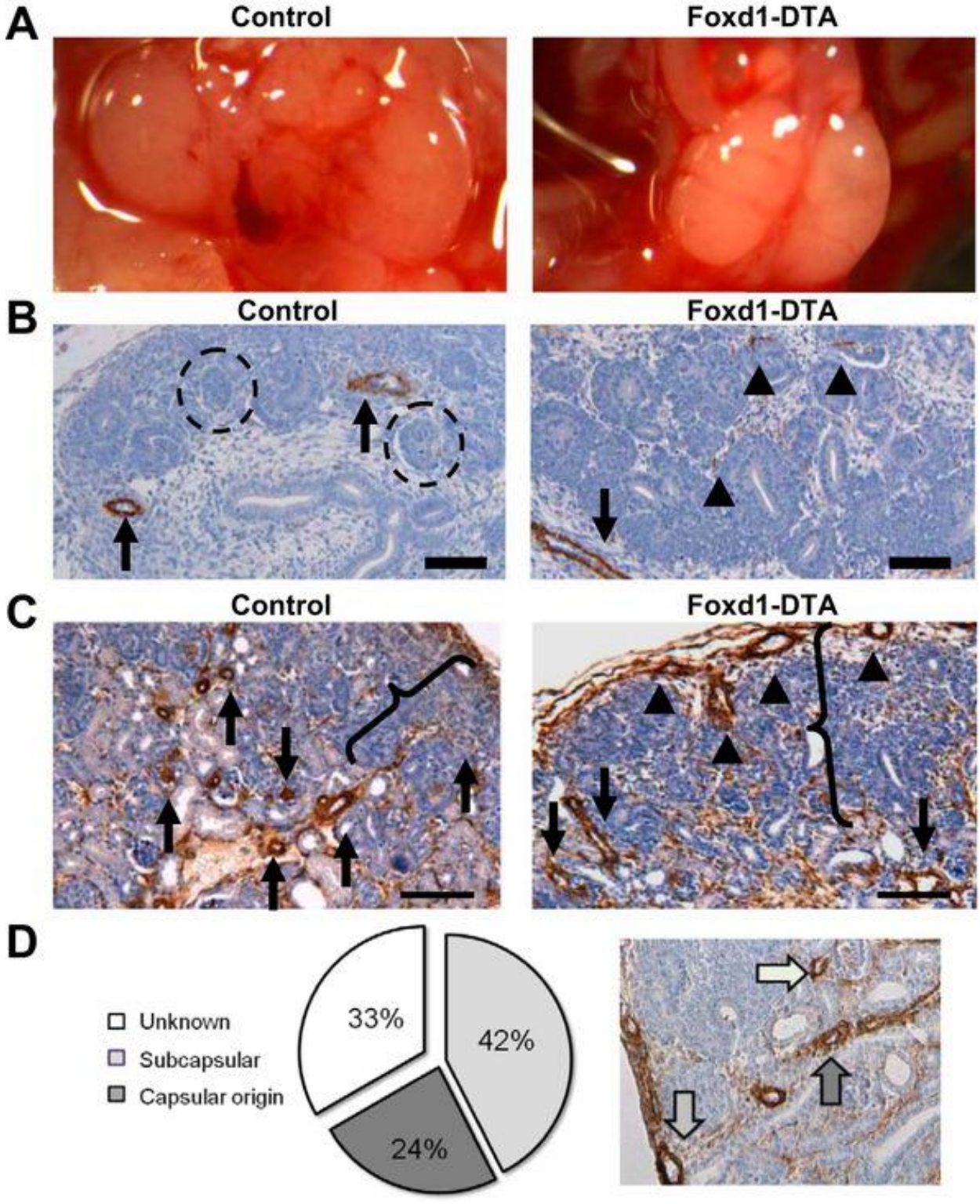
A
Control
Foxd1-DTA
B
Control
Foxd1-DTA
C
Control
Foxd1-DTA
D
Unknown
Subcapsular
Capsular origin
33%
42%
24%

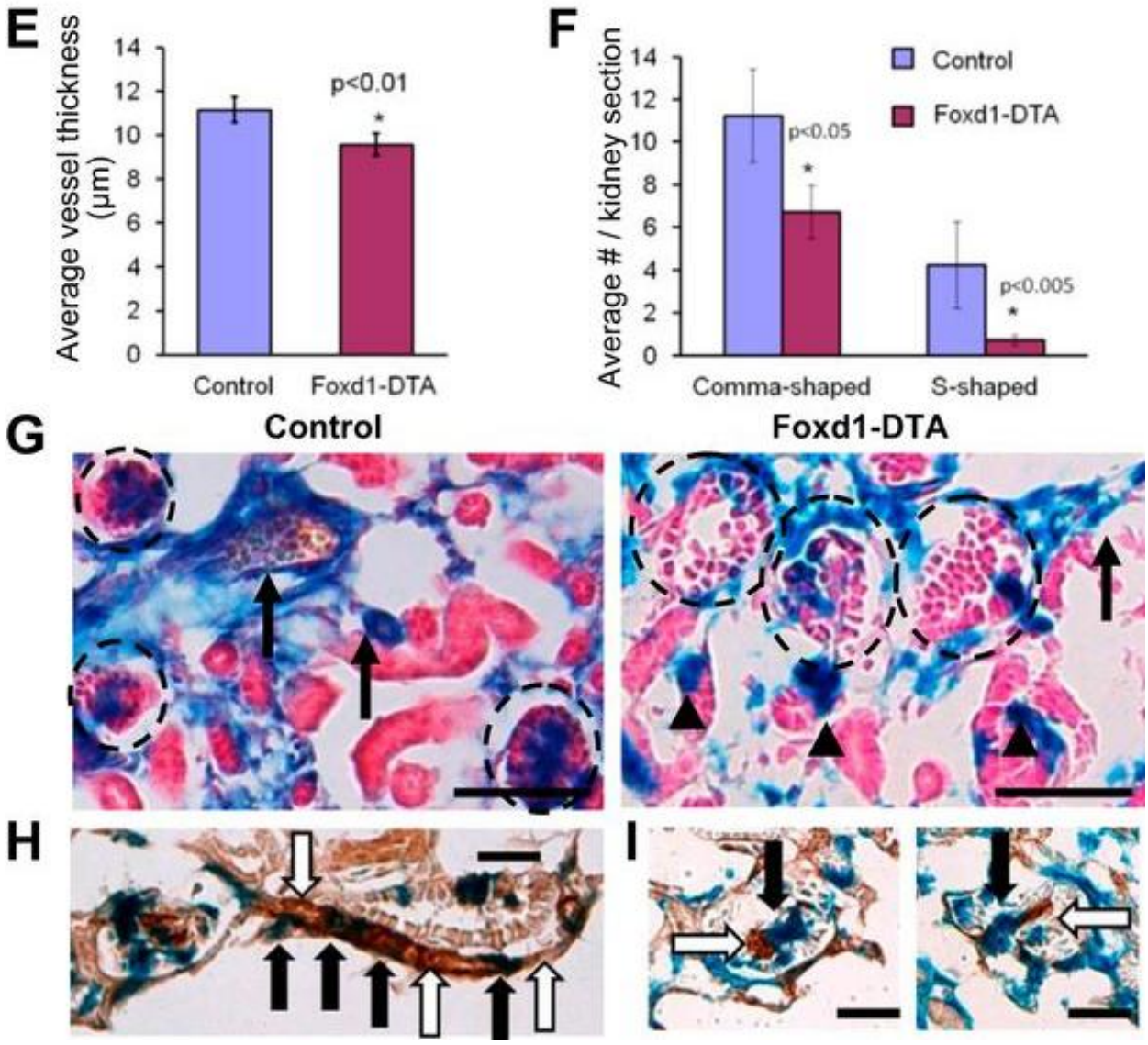

Figure 2.8. Ablation of Foxd1 cells using Diphtheria toxin chain A (DTA) results in significant renal abnormalities. A. Gross morphology of kidneys from mice expressing DTA upon Foxd1-cre-mediated recombination (Foxd1-DTA) reveals midline fusion, a failure to separate from the retroperitoneum, and blood vessels visible on the periphery of the kidney cortex. B-C. Immunohistochemistry for α-SMA (brown) in control and Foxd1-DTA kidneys. B. At E15.5 control kidneys have well-defined SMC layers surrounding major arteries (arrows) in the interior of the kidney. By contrast, Foxd1-DTA

kidneys display areas of diffuse and poorly organized staining within the kidney (arrowheads). However, large, fully coated vessels can be observed along the periphery of the kidney (arrows). At this age, control kidneys also display all the stages of nephrogenesis, up to and including glomeruli (circles). Meanwhile, Foxd1-DTA kidneys lack mature glomeruli or any of the earlier stages of nephrogenesis such as comma-shaped or s-shaped bodies. Scale bar, 100 μm C. At E18.5. control kidneys have multiple actin-positive arterioles (arrows) throughout the kidney cortex. Foxd1-DTA animals meanwhile have comparatively fewer arterioles. In addition, a large subset of arteries appear to originate from the periphery of the kidney (arrowheads). In contrast to E15.5, Foxd1-DTA kidneys now possess all the different stages of nephron development, but we note that the nephrogenic zone (brackets) is broader in Foxd1-DTA animals. Scale bar, 50 μm. D. Quantification of the orientation of arteries seen in E18.5 Foxd1-DTA kidney demonstrates that nearly 2/3rds of vessels observed lay directly underneath or emerge from the capsule. E. The average thickness of the smooth muscle layer of renal arteries and arterioles is reduced in Foxd1-DTA animals at E18.5. F. E18.5 Foxd1-DTA kidneys have relatively fewer comma-shaped and s-shaped bodies. G. Lineage tracing of Foxd1 cells upon ablation. Foxd1-DTA mice were crossed with mice carrying the *R26R* allele, which expresses β-galactosidase upon cre-mediated recombination, labeling Foxd1-expressing cells and their derivatives. In control animals at E18.5, the Foxd1-lineage marker labels arterial SMCs, mesangial and interstitial cells. The same cell types are labeled in Foxd1-DTA animals. However, a decrease in the thickness of the Foxd1-lineage SMC layer (arrows) and a marked decrease in the complement of mesangial cells is observed. We also note increased ectopic expression

of the lineage marker within tubules (arrowheads). Scale bar, 50 μm. H-I. Double staining of Foxd1-DTA kidneys, with LacZ reaction (blue) for Foxd1-lineage cells and immunohistochemistry (brown) for α-SMA. As seen in this afferent arteriole extending from the glomerulus, a subset of arteriolar SMCs are positive for both the lineage marker and α-SMA (arrows), while others are positive only for α-SMA and not the lineage marker (white arrows). I. Some mesangial cells are double positive for both markers (arrows), while others are only positive for α-SMA but negative for the lineage marker (white arrows). Scale bar, 50 μm. (Performed by EEL)

Deletion of Foxd1 resulted in decreased renin expression

To investigate whether deletion of *Foxd1* altered the expression of renin or distribution of renin-expressing cells, we performed renin immunostaining throughout embryonic development. The expression of renin in the kidneys from *Foxd1*$^{-/-}$ mice was markedly diminished at all embryonic developmental points and on the day of birth (Figure 2.9). Because the size of the kidneys from the *Foxd1*$^{-/-}$ mice was smaller than the WTs we corrected the areas of renin expression per total kidney area and per total arterial/arteriolar areas (as elicited by α-SMA staining) and as shown in figure 2.9 expression of renin was still markedly reduced.

Figure 2.9

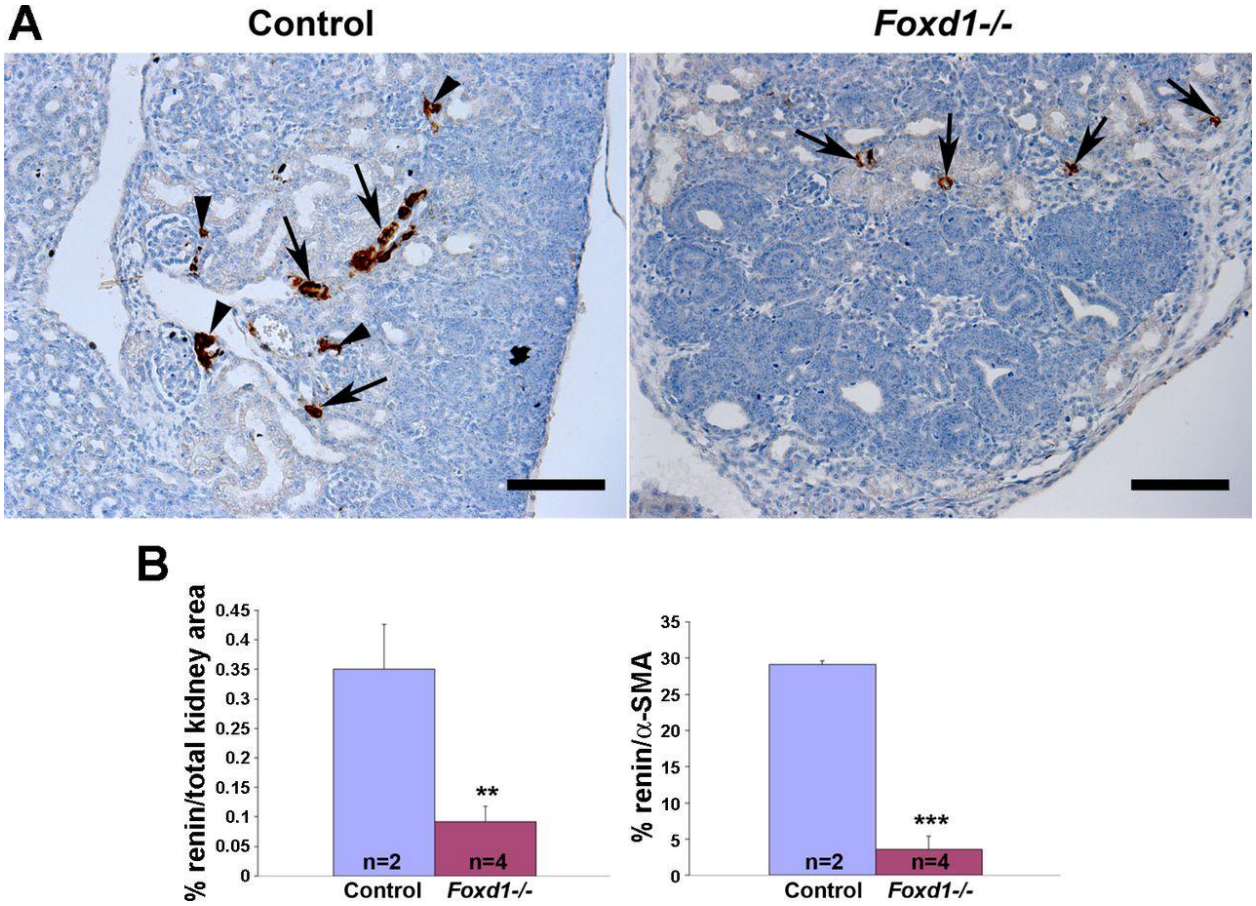

Figure 2.9. Foxd1 is necessary for normal renin expression. A. Immunostaining for renin (brown) of E17.5 kidneys show that control mice present a normal distribution of renin along developing arterioles and arteries (arrows) as well as in JG areas (arrowheads) whereas in *Foxd1*$^{-/-}$ mice there is a marked reduction of renin expression (arrows). Scale bar, 100 µm. B. Quantification of areas immunostained for renin per total kidney area (left) and per total vascular areas positive for α-SMA on a consecutive section (right). (Performed by ML)

Discussion

Results from these studies show that 1) Foxd1+ renal stromal cells are the progenitors for renin cells, arteriolar SMCs, pericytes and mesangial cells, and 2) stromal cells, via their defining transcription factor, *Foxd1*, are essential for proper morphogenesis and orientation of a single renal arterial tree per kidney.

We have previously suggested that early in gestation, the embryonic kidney possesses all the necessary precursors that compose the kidney vasculature well before arteriolar vessels can be discerned (13). We proposed that those as yet unidentified precursors differentiated into all the cell types necessary for the development of the kidney arterioles, including ECs, SMCs and renin cells (13, 35). In fact, cross-transplantation studies of embryonic pre-vascular kidneys under the kidney capsule showed that those precursor cells had the capacity to differentiate, acquire the right positional information and fully assemble to form the kidney arterioles (13). It was not clear, however, whether those various cell types arose from one or multiple progenitors. Work from our laboratory indicated that embryonic renin cells differentiate not only into juxtaglomerular cells but also into a subset of mesangial and arteriolar SMCs (13, 16). Although those studies suggested the hypothesis that a single progenitor may give rise to all of the cells of the kidney vasculature, the fact that renin cells did not differentiate into ECs and only gave rise to a subset of mesangial and SMCs suggested that a much earlier and upstream precursor was indeed the progenitor for all the mural arteriolar cells. Indeed, in a review article and based in our early preliminary work, we suggested that Foxd1+ cells were progenitors for the mural cells of the renal arterioles (29, 36). We show here that Foxd1 cells not only give rise to SMCs, mesangial cells and pericytes but also to the renin progenitor cell. Although

these two progenitors (Foxd1 and Renin progenitor) partially overlap in the generation of descendants, the Foxd1 progenitor is hierarchically upstream of the renin cell: when Foxd1 cells or the Foxd1 gene are deleted, renin cells are frankly diminished. Our results are in agreement with studies demonstrating that Foxd1+ cells differentiate into renal interstitial pericytes, which in pathological circumstances also give rise to myofibroblasts (31).

It has recently been reported that a small subset of ECs located in the renal interstitium may originate from Foxd1 cells (37). However, in our study, we did not find interstitial ECs co-labeled with the lineage tracer or expression of EC markers in sorted cells derived from Foxd1 precursors. Interestingly, and in agreement with the same study we find that ECs from the glomeruli and arteriolar vessels are unrelated to the Foxd1 lineage (37). Thus, arteriolar ECs are likely to originate from a more primitive endothelial precursor. Our results are in agreement with work showing that within the developing renal interstitium, stromal cells expressing Foxd1 and endothelial precursors expressing c-kit constitute two distinct populations originating from different intra embryonic sites (30). A subset of c-kit+ cells also express angioblast markers such as podocalyxin and Flk1 (30), suggesting that at least a subpopulation of c-kit+ cells may be the precursors for the renal ECs. Thus, the available evidence suggests that most if not all of the ECs of the renal interstitium, glomeruli and arterioles originate from a separate precursor unrelated to the stromal Foxd1+ cell. The identity of such precursor as a primitive renal hemangioblast has recently been suggested (29). Further work will be needed to test such hypothesis.

Our results show that Foxd1 cells are necessary for the appropriate morphogenesis, composition and orientation of the kidney vasculature. *Foxd1* $^{-/-}$ mice and *Foxd1-DTA* mice show very similar phenotypes suggesting that most of the effects exerted by Foxd1+ cells

are accomplished via their transcription factor *Foxd1*. The kidneys of *Foxd1*$^{-/-}$ mice displayed numerous developmental defects: they were smaller, they were fused in the midline and failed to ascend and the ureters were ventrally oriented as previously described (20, 38). Multiple accessory and aberrant arteries along the abdominal aorta and the iliac arteries identified in this study are likely the cause that prevents the kidneys to ascend. Whether mutations of the *FOXD1* gene in humans is associated to accessory or aberrant renal arteries remains to be investigated. Given that *Foxd1* is expressed in stromal cells early in development, these findings suggest that Foxd1+ stromal cells affect the development of adjacent nephron precursors in a yet to be defined manner. In agreement with this hypothesis, elegant work from two laboratories began to unravel some the mechanisms involved: first, Das and collaborators have suggested that stromal cells via their production of the cadherin Fat4 inhibits nephron progenitor expansion/renewal and cooperate with Wnt9b produced by the ureteric bud to promote differentiation of progenitors (39) and more recently, Fetting and colleagues suggested the interesting possibility that lack of Foxd1 which under normal circumstances inhibits decorin, may lead to premature differentiation of stromal cells and progenitor retention in the epithelial nephron compartment (40). It is also possible that the alterations in epithelial nephron development are due to the role of Foxd1 cells in vascular development. Given the striking vascular abnormalities seen in Foxd1 null mice and *Foxd1-DTA* animals, inadequate tissue perfusion may have further contributed to impaired development of both compartments. Clearly, the available evidence from those and the current study indicate that the stromal compartment not only regulates vascular-interstitial development but it plays a fundamental role in the development and maintenance of the epithelial nephron as

well (39, 40). In our studies we found occasional labeling of renal tubular structures when crossing *Foxd1*^{cre} mice to either *R26R* or *mT/mG* reporter mice suggesting a residual activity of *Foxd1* in *Six2* nephron precursors after the delimitation of epithelial nephron and interstitial progenitors from a common mesenchymal progenitor (41). This unexpected mosaic labeling of nephrons was recently reported when activating EGFP-L10a expression using *Foxd1*^{cre} mice (41). However, in *Foxd1-DTA* animals we observed increased ectopic renal tubular expression of the lineage marker suggesting either an attempt to increase the expression of *Foxd1* in the common mesenchymal progenitor resulting in further differentiation into more *Six2* lineage cells or a de novo expression of *Foxd1* in an attempt to compensate for the lack of *Foxd1* in stromal derivatives.

To examine the anatomy and distribution of the renal arterial tree we used two different techniques: 1) microdissection under direct stereoscopic visualization and 2) Evans blue - glycerol labeled perfusion. Both techniques as well as immunostaining for markers of the mural cells of the kidney arterioles yielded similar results: *Foxd1* $^{-/-}$ mice display a disrupted origin (multiple) and topological orientation of the renal vessels. Whereas in WT animals the arteries and arterioles arise from the renal artery which enters the kidney through the hilum and divides successively into smaller branches in a centrifugal fashion, in mutant mice, there are multiple accessory and aberrant arteries that originate at various levels from the aorta and iliac arteries that surround the superior and inferior poles within the renal capsule and wherefrom they traverse towards the center of the kidney in a total reversal of the renal circulatory pattern. These results indicate that *Foxd1* is necessary for the proper origin, number and orientation of the renal arterial tree and that *Foxd1* governs a set of guidance cues involved in the appropriate targeting and directionality of the renal

vessels. The results agree with previous work showing that loss of Foxd1 results in defects in ureter branching and equally important, loss of appropriate capsular morphogenesis and cellular composition: in *Foxd1* $^{-/-}$ animals the capsule contains a variety of cell types not normally found in the WT mice (20, 38). The above results also suggest that *Foxd1* is important in the differentiation of progenitor cells in the capsule. Using immunostaining against an endothelial marker (PECAM) a recent study suggested that in *Foxd1-DTA* mice the blood vessels were "thickened" due to an overgrowth of ECs (42). We could not confirm the presence of a thicker endothelium, but verified instead the presence of subcapsular and capsular arterioles and arteries, which normally possess a thick muscle wall composed of SMCs. The presence of capsular vessels in our study indicates that *Foxd1* normally inhibits the ectopic differentiation and assembly of the renal vasculature. The mechanisms and molecules involved are unclear and remain to be defined. Our preliminary unpublished data indicates that *Foxd1* inhibits a genetic program involved in the acquisition of the muscular layers of the renal arterial tree. Further, the results suggest that *Foxd1* participates in the proper orientation of the kidney vasculature. Given that *Foxd1* has been shown to be required for the specification and targeting of ganglion cells in the temporal retina of mammals (43) it is possible that *Foxd1* may exert a similar influence on the orientation and targeting of renal vessels. Whether this is achieved with the participation of axon guiding molecules such as ephrins, semaphorins, plexins, slits and netrins (44) will need to be determined. Further studies will be needed to dissect the mechanism underlying the complex nephron-vascular phenotype ensuing from lack of Foxd1 cells or their transcription factor, *Foxd1*. Furthermore, in this study we also identified that the cause of death of *Foxd1*$^{-/-}$ mice is due to abnormal lung development; whether

Foxd1 is also required for normal branching morphogenesis of the epithelial and vascular compartment of the lung is a possibility that remains to be determined.

Perspectives and Significance

Identification of the Foxd1+ stromal cells as the precursors for the morphogenesis of the renal arterial tree may open new avenues for understanding the mechanisms that govern tissue vascularization and remodeling in normal and disease states. Further, it is becoming evident that the renal vasculature is a major determinant of tissue organization in the developing mammal and appropriate preservation of function and structure in the growing and adult individual.

Acknowledgments

This work was supported by National Institutes of Health grants DK091330 to M.L.S.S.L., DK096373 and HL096735 to R.A.G. and HL048058, HL061446, HL084207 to C.D.S, the American Heart Association 13PRE16920043 to E.E.L. and the University of Virginia Children's Hospital Grant-in Aid to M.L.S.S.L. We greatly thank the technical assistance of Danielle Stumbo for the mouse work.

We thank Akio Kobayashi and Andrew McMahon for providing the *Foxd1*^{cre} mice.

III. ALDO-KETO REDUCTASE 1B7, A NOVEL MARKER FOR RENIN CELLS, IS REGULATED BY CYCLIC AMP SIGNALING

Formatted as a first authored manuscript and accepted for publication as:

Aldo-Keto reductase 1b7, a novel marker for renin cells, is regulated by cyclic AMP signaling. Lin EE, Pentz ES, Sequeira-Lopez ML, Gomez RA. Am J Physiol Regul Integr Comp Physiol. Publication pending.

Abstract

We previously identified aldo-keto reductase 1b7 (AKR1B7) as a marker for juxtaglomerular renin cells in the adult mouse kidney. However, the distribution of renin cells varies dynamically, and it was unknown whether AKR1B7 maintains co-expression with renin in response to different developmental, physiological, and pathological situations, and furthermore, whether certain factor(s) simultaneously regulate both proteins. We show here that throughout kidney development AKR1B7 expression- together with renin- is progressively restricted up the kidney arteries toward the glomerulus. Subsequently, when formerly renin-expressing cells reacquire renin expression, AKR1B7 is re-expressed as well. This pattern of co-expression persists in extreme pathological situations such as deletion of the genes for Aldosterone Synthase or Dicer. However, the two proteins do not co-localize within the same organelles: renin is found in the secretory granules, whereas AKR1B7 localizes to the endoplasmic reticulum. Interestingly, upon deletion of the renin gene, AKR1B7 expression is maintained in a pattern mimicking the embryonic expression of renin, while ablation of renin cells resulted in complete abolition of AKR1B7 expression. Finally, we demonstrate that AKR1B7 transcription is controlled by cyclic adenosine mono-phosphate (cAMP). Cultured cells of the renin lineage reacquire the ability to express both renin and AKR1B7 upon elevation of intracellular cAMP. *In vivo,* deleting elements of the cAMP-response pathway (CBP/P300) results in a stark decrease in AKR1B7- and renin-positive cells. In summary, AKR1B7 is expressed within the renin cell throughout development and perturbations to homeostasis, and AKR1B7 is regulated by cAMP levels within the renin cell.

Introduction

The renin-angiotensin system (RAS) is responsible for maintaining blood pressure and fluid-electrolyte homeostasis. A key point in the regulation of RAS is control of the synthesis and secretion of the hormone renin within highly specialized juxtaglomerular (JG) renin cells in the kidney. Throughout embryonic development and into adult life renin-producing cells show a remarkable plasticity, and their location and number changes in a dynamic but stereotyped manner. Initially, renin cells are found along large arteries of the developing kidney, but as the animal matures, renin expression is progressively restricted downstream toward the glomerulus, until renin is confined to the adult JG location (13, 15). This process does not involve cellular migration or proliferation/apoptosis, but instead differentiation- formerly renin-expressing cells differentiate into a subset of the smooth muscle cells lining the renal arteries (16). A similar phenomenon occurs with the mesangial cells in the glomerulus, with again a subset derived from cells that expressed renin earlier in development (16). Interestingly, these cells retain the capability to re-express renin in response to physiological stress that necessitates an increase in renin production, such as hypotension, blood loss, or sodium depletion (16). This remarkable ability to switch phenotypes has long been an area of interest, as identifying the molecules that establish and regulate the identity of the renin cell may have important implications not only in the study of homeostatic regulation, but also for our understanding of cell memory and/or plasticity.

One barrier to the study of the renin cell has been the lack of a reliable and independent marker for renin cells aside from renin itself, as manipulations which directly affect the expression of renin (and may not otherwise modify the renin cell) will prevent

identification of the cell. Using microarray analysis, we have previously identified one enzyme, aldo-keto reductase family 1, sub-family B member 7 (AKR1B7), which was highly enriched in the adult renin cell of mice (18). AKR1B7 belongs to an enzymatic superfamily of over 100 aldo-keto reductases whose members can be found in many organ systems throughout a multitude of vertebrate and invertebrate animal species. Within the mouse, AKR1B7 expression has previously been described in the vas deferens and the adrenal glands (45, 46). However, little is known about the suitability of AKR1B7 as a marker for renin cells, particularly under developmental, physiological and pathological situations that modify renin expression and renin cell number.

In addition to studying the expression pattern of AKR1B7, we explored whether factor(s) already known to regulate renin expression also regulate AKR1B7, as identification of molecular pathways which co-regulate AKR1B7 and renin could give insight into an overarching program responsible for regulating the phenotype of the renin cell. One potential candidate is cyclic AMP (cAMP). Our laboratory and others have previously shown that cAMP up-regulates renin expression *in vitro* and *in vivo*, and that deletion of elements of the cAMP-response pathway blunts the organism's expression of renin and ability to respond to homeostatic challenge (47-49). Therefore, we hypothesize that cAMP regulates AKR1B7 within the kidney as well.

Results

The ontogeny of AKR1B7 expression

Previous work done in our lab using microarray analysis and immunostaining showed expression of AKR1B7 in the renin cells of adult mice (18). In the present study, we examined the pattern of AKR1B7 expression during kidney maturation, and whether co-expression of AKR1B7 with renin was maintained throughout the dynamic changes to renin cell localization that occur during renal development. Immunostaining for AKR1B7 at various ages showed a pattern of regressing staining along the arterioles that exactly duplicated the well-established developmental distribution of renin. Within the embryonic kidney at embryonic day 15.5 AKR1B7 expression was primarily found along the large arteries of the kidney (Fig. 3.1a). Staining was also seen near mature glomeruli outside the nephrogenic zone, and occasionally in the glomerular mesangium. In the newborn mouse (post-natal day 1), AKR1B7 expression was segregated to developing afferent arterioles and smaller arteries, along with a few JG areas (Fig. 3.1c), while in adulthood AKR1B7 was confined to the few cells adjacent to the mature glomerulus that form the JG apparatus (Fig. 3.1e). We confirmed the co-localization of AKR1B7 and renin using staining in consecutive kidney sections. AKR1B7 staining was always accompanied by renin staining for in the corresponding region (Fig. 3.1b, d, f), demonstrating a consistent association between the expression patterns of the two proteins throughout renal development.

Figure 3.1

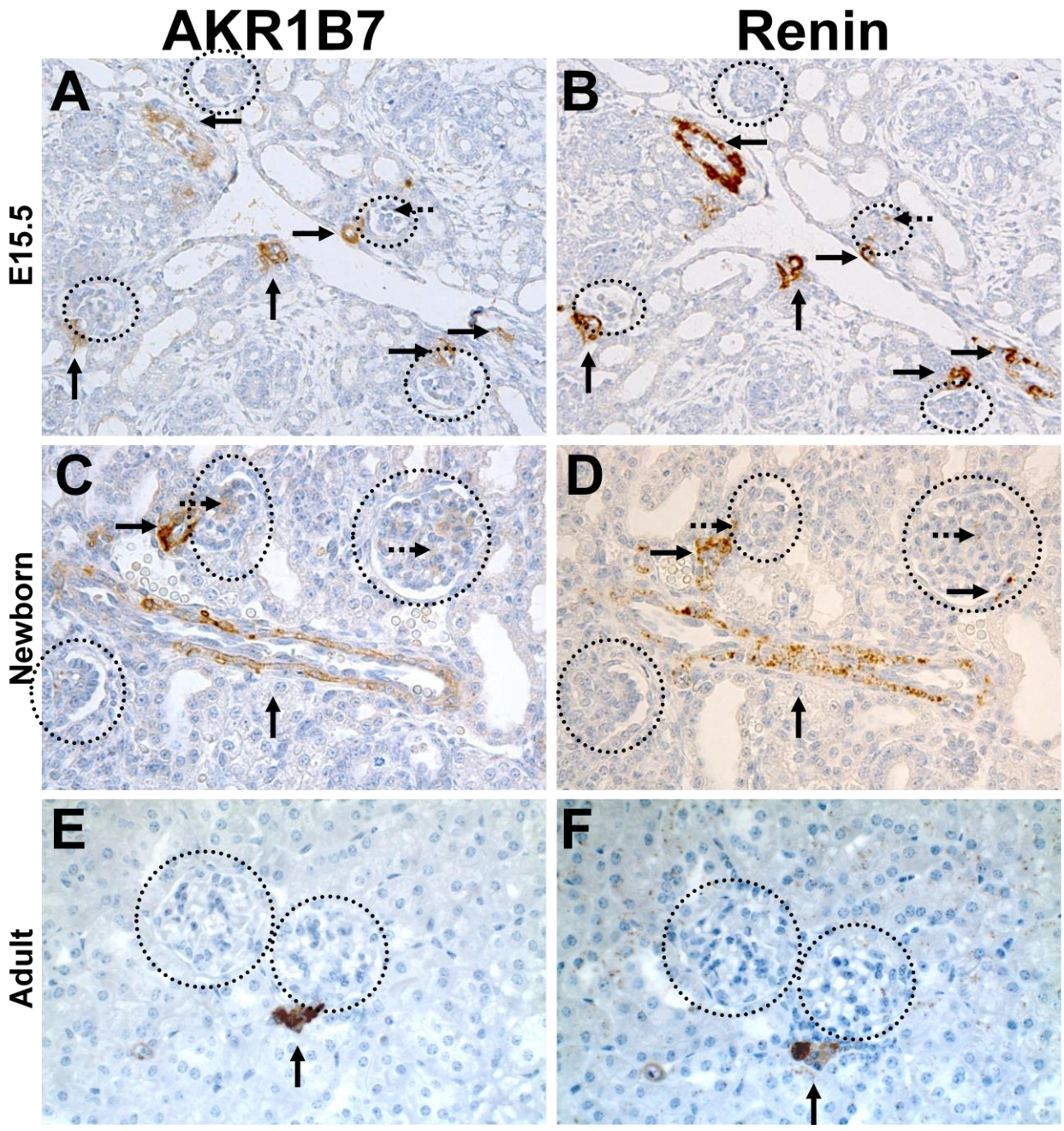

Figure 3.1: Immunostaining for AKR1B7 and renin in consecutive sections at various ages. A, B: AKR1B7 and renin staining in embryonic day 15.5 (E15.5) kidneys. Staining is found along large vessels (arrows) and in the glomerular mesangium (dashed arrows). C, D: AKR1B7 and renin staining in kidneys from newborn animals. Staining is found in arteries (arrows) and JG areas (dashed arrows). E. F: AKR1B7 and

renin staining in adult (post-natal day 45) kidneys. Staining is limited primarily to JG areas (arrow). At all stages, AKR1B7 staining co-localizes to the same areas as renin. Circles indicate glomeruli. (performed by EEL)

Expression of AKR1B7 following pharmacological or genetic manipulation

The co-localization of renin and AKR1B7 throughout kidney development suggests that the two proteins may respond similarly to manipulations known to affect renin synthesis and the distribution of renin cells. We first examined AKR1B7 expression using a well-established method of physiological and pharmacological manipulation that increases renin levels: mice treated with the angiotensin converting enzyme (ACE) inhibitor captopril and fed a low-salt diet show re-expression of renin along the renal arterioles to compensate for diminished blood pressure and electrolyte-fluid depletion (50, 51). Immunostaining for AKR1B7 in treated mice showed a concomitant increase in the number of AKR1B7-positive cells (Fig. 3.2a). Expression of AKR1B7 extended along the afferent arteriole and could be found occasionally within the cells of the glomerular mesangium, in a pattern reminiscent of embryonic life. Staining with renin in consecutive sections showed coincident expression along the renal arterioles and mesangial cells (Fig. 3.2b), confirming that AKR1B7 expresses alongside renin in conditions of homeostatic stress as well as basal state. The reverse result was obtained when examining animals fed a high-salt diet- the decrease in renin-positive cells and fewer renin-positive juxtaglomerular regions was accompanied by a decrease in the number of AKR1B7-positive cells (not shown).

We also investigated the expression of both proteins under pathological conditions previously shown to severely alter renin expression levels. Mice in which the gene for Aldosterone Synthase had been deleted, upon administration of the earlier described sodium depletion and captopril treatment, exhibit a dramatic expansion of renin expression along the kidney arteries (52, 53) to a degree far greater than sodium

depletion and captopril alone. The number of renin positive cells and the amount of renin in each cell increases dramatically, with renin expression extended along almost the entirety of the afferent arteriole and interlobular arteries. Immunostaining in consecutive sections showed that these renin-positive cells also express AKR1B7 (Fig. 3.2c, d), with many AKR1B7-positive cells lining the arteries and arterioles. Although not directly comparable, we note that the increase in the intensity of AKR1B7 staining within each individual cell was not as dramatic as that of renin. The opposite result was found in mice with conditional deletion of the micro-RNA processing enzyme Dicer in renin cells, which have significantly fewer renin-positive JG cells and lower plasma renin levels. The decrease in renin expression is accompanied by a reduction in the domain of AKR1B7 staining, with fewer AKR1B7-positive cells present in the knockout kidneys. However, AKR1B7 still coincides specifically with renin in the few remaining renin-positive JG areas (Fig. 3.2e, f).

Figure 3.2

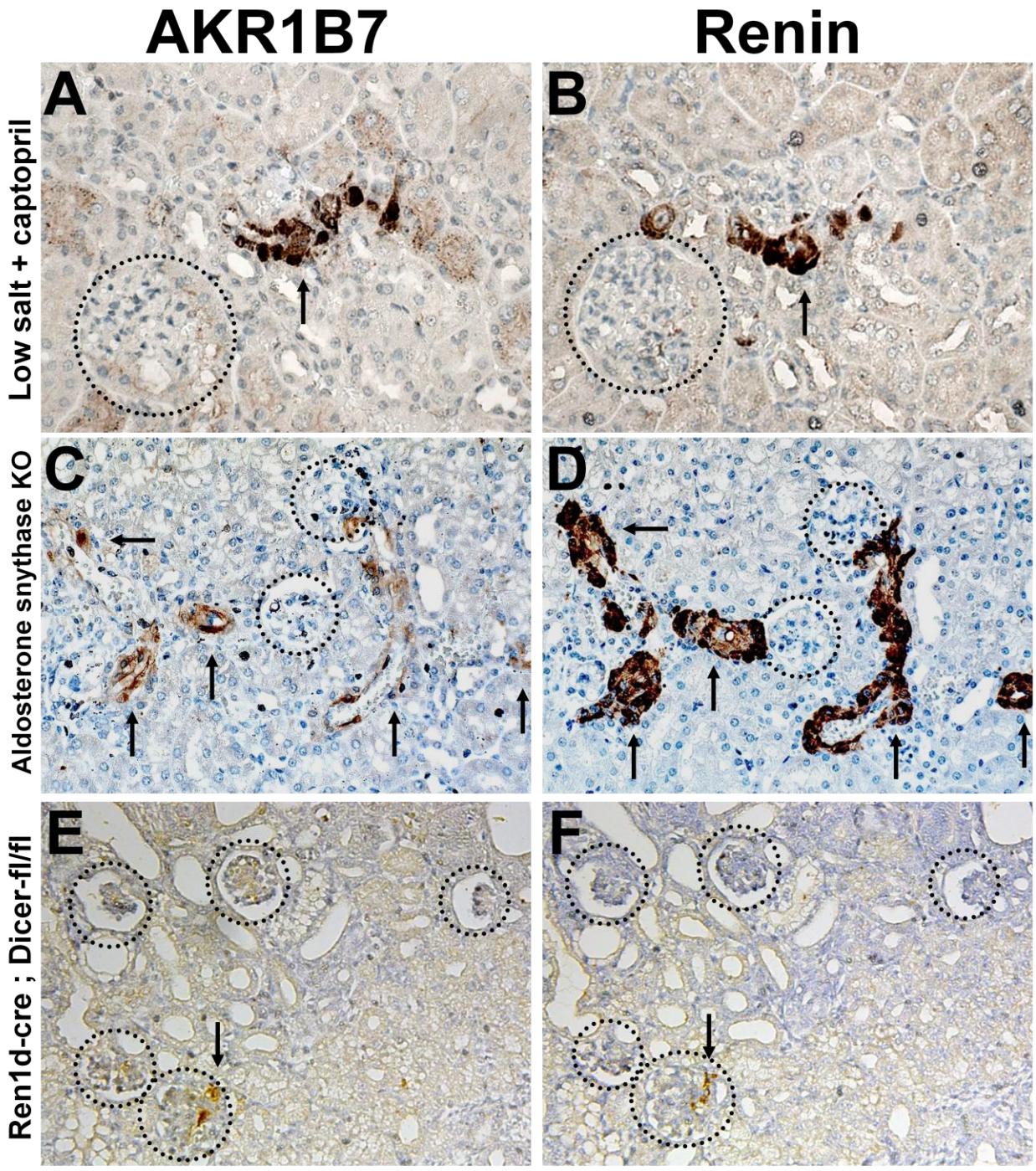

Figure 3.2: Immunohistochemistry for AKR1B7 and renin in consecutive sections under manipulations known to increase renin expression. Circles indicate glomeruli, and arrows indicate staining in arterioles. A, B: The domain of AKR1B7 and renin expression expands in animals treated with captopril and fed low-salt diet, in a

pattern reminiscent of that observed during embryonic development. C, D: AKR1B7 and renin in kidneys from mice homozygous for aldosterone synthase deletion. While the number of labeled cells increases significantly along arteries an arterioles, the increase in intensity of renin expression is not matched by AKR1B7. E, F: AKR1B7 and renin in kidneys from mice with conditional deletion of Dicer in renin cells. The number of renin- and AKR1B7-positive cells is markedly reduced. (performed by EEL)

AKR1B7 localizes primarily to the plasma membrane and endoplasmic reticulum

To confirm co-expression of renin and AKR1B7 in the same cell, and to characterize the sub-cellular localization of AKR1B7, we conducted dual immunofluorescence and confocal microscopy of adult mouse kidney sections. Both proteins were consistently found in the same cells of the juxtaglomerular apparatus (Fig. 3.3a), with renin localized to round bodies in the cytoplasm, corresponding to the secretory granules of JG cells. AKR1B7 however was not associated with the same subcellular structures as renin, as AKR1B7 staining was found in distinct regions within the cytoplasm (Fig. 3.3b), and occasionally near the plasma membrane. The sub-cellular localization of AKR1B7 did not change when examining mice at earlier developmental timepoints (newborn, not shown) or mice treated with captopril and fed a low-sodium diet (not shown).

Interestingly, we frequently observed AKR1B7 in net-like, latticework structures (Fig. 3.3c) suggestive of association with a particular subcellular structure. To investigate AKR1B7 localization to a specific organelle, we conducted co-staining with subcellular markers. JG cells have prominent lysosomes, and it is widely thought that the renin granules derive from lysosomes (54, 55). However, co-staining with LAMP1, a lysosomal membrane protein, showed only occasional co-localization with AKR1B7 (Fig. 3.3d). By contrast, co-staining AKR1B7 with protein disulfide isomerase (PDI), an ER resident protein, demonstrated strong co-localization with AKR1B7 (Fig. 3.3e), with coincident staining in the previously described net-like pattern, indicating that AKR1B7 also localizes to the ER in renin cells.

Figure 3.3

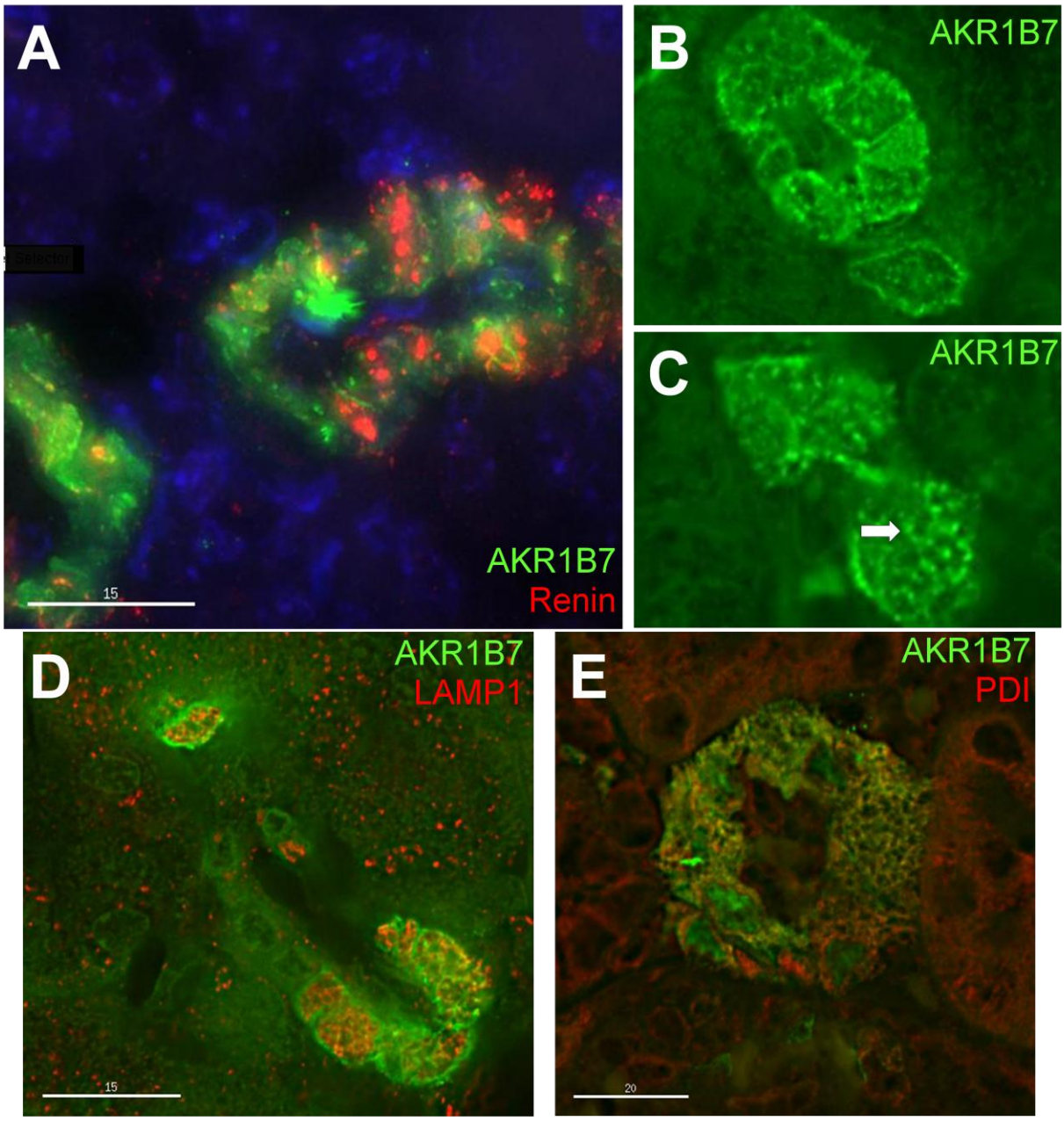

Figure 3.3: AKR1B7 localizes to the plasma membrane and endoplasmic reticulum, and not the renin granules. A: Immunofluorescence for AKR1B7 (green) and renin (red), with counterstaining with DAPI (blue). The two proteins are found in the same cells, but seldom coincide subcellularly (yellow). B, C: Immunofluorescence for AKR1B7 (green). AKR1B7 can be found in or near the plasma membrane (B), and also

in lattice-shaped structures in the cytoplasm (C, arrow). D: Immunostaining for AKR1B7 (green) and LAMP1 (red), a marker for lysosomes. The two only show occasional co-localization. E: AKR1B7 (green) and PDI (red), a marker for endoplasmic reticulum. The two show extensive co-localization (yellow). (performed by EEL)

AKR1B7 is a renin-independent marker for renin cells

As mentioned earlier, studies of renin cells have been complicated by the fact that the only reliable marker for cells of the renin phenotype was renin itself. To test whether AKR1B7 would label cells in the absence of renin expression, we immunostained for AKR1B7 in kidneys from mice with deletion of the renin gene. Global renin knockout mice have kidneys with prominent morphological defects including vascular thickening and a complete absence of renin staining (56). However, AKR1B7 staining is preserved in cells adjacent to the glomerulus (Fig. 3.4a, arrows). In addition, we found significant extension of AKR1B7 expression along afferent arterioles (AA), and occasional staining of the mesangial cells in glomeruli (circles). Interestingly, this pattern is strongly reminiscent of the distribution of renin cells during conditions that acutely or chronically stimulate renin production (see Fig. 3.2a-d). We conclude that the renin cell persists in renin knockout mice and continues to express the marker protein AKR1B7, despite an inability to produce renin.

A contrasting observation was made in mice where renin cells have been ablated using expression of diphtheria toxin chain A (DTA) under control of the renin promoter (Ren1d-DTA, (8)). Kidneys from those animals lack renin cells, leading to a disruption of vascular and tubular patterning that is not seen in renin knockout animals. We detected no AKR1B7 in Ren1d-DTA kidneys (Fig. 3.4b and 3.4c), and AKR1B7 signal was absent from any of the cell types that typically arise from renin cells and might be induced to re-express renin, such as JG areas, arterial smooth muscle cells, or mesangial cells. Thus, while AKR1B7 expression persisted in the absence of the renin gene, deletion of the renin cell itself resulted in the complete abrogation of AKR1B7

expression within the kidney, emphasizing that AKR1B7 marks cells specifically programmed to express renin.

Figure 3.4

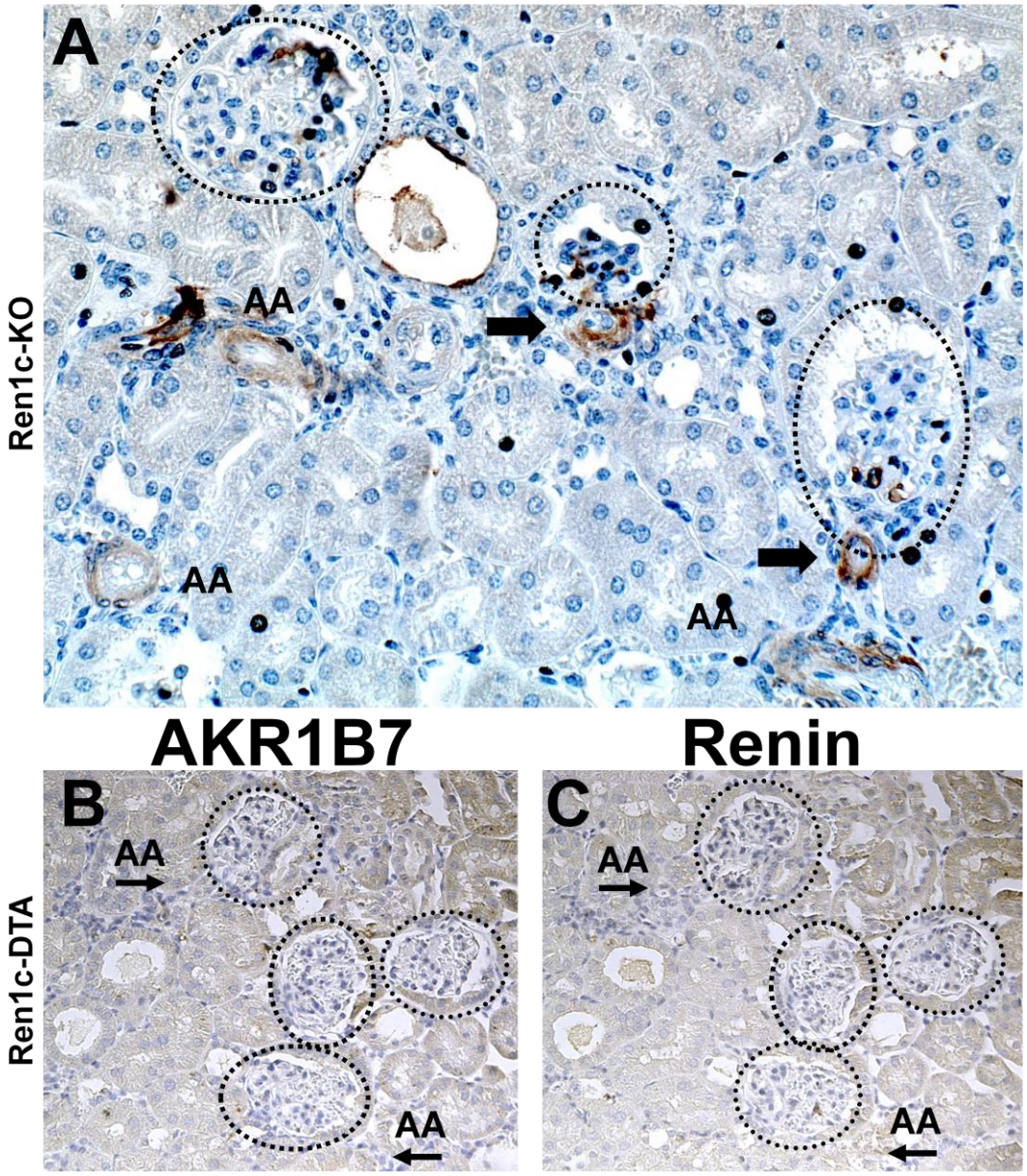

Figure 3.4: AKR1B7 expression is independent of renin, and is only absent upon deletion of renin cells. A: Immunostaining for AKR1B7 in Ren1c KO mice. Mice homozygous for deletion of renin show extensive staining for AKR1B7 in JG cells (arrow), cells in the wall of the afferent arterioles (AA) of the kidney, and in mesangial cells of the glomeruli (circles). B,C: AKR1B7 and renin in kidneys from mice where renin cells have been ablated by the conditional expression of diphtheria toxin A (DTA). No

positive staining can be found near glomeruli (circles) or in afferent arterioles (AA).

(performed by EEL)

cAMP regulates the expression of AKR1B7

We have shown here that AKR1B7 and renin are consistently expressed together, raising the important possibility that the same mechanisms that regulate renin levels also regulate AKR1B7. To examine the regulation of AKR1B7 on a cellular level we utilized our previously described CFP/YFP cell culture system (49). Briefly, CFP/YFP cells are derived from isolated kidney arteriolar smooth muscle cells of the renin lineage that were labeled permanently with CFP using the cre/lox system. When grown in culture these cells do not express renin at basal state, but upon appropriate stimulation re-activate renin expression and report renin promoter activity through YFP expression (Ren1c-YFP, (49)). In this manner, CFP/YFP cells mimic the *in vivo* ability of smooth muscle cells of the renin lineage (CFP^+) to reacquire the ability to express renin (acquiring YFP^+), and are an appropriate platform to study renin regulation.

As we have previously shown that treatments which increase intracellular cAMP, such as incubation with forskolin (57), cause CFP/YFP cells to reacquire renin expression and become YFP-positive (49), we tested whether stimulation of the cAMP pathway would also increase AKR1B7 expression in our cell culture model. Figure 3.5a shows that unstimulated CFP/YFP cells expressed only low amounts of AKR1B7 ("CFP/YFP fsk^-"). However, forskolin-treated CFP/YFP cells, in addition to activating the renin promoter (49), also increased AKR1B7 message levels ("CFP/YFP fsk^+"). As positive controls, we observed that FACS-sorted juxtaglomerular renin cells (isolated from Ren1c-YFP animals), contained significant amounts of AKR1B7 message ("JG"). Interestingly, we find that As4.1 cells ("As4.1"), a kidney tumor cell line that constitutively expresses renin (58), also contained AKR1B7 mRNA. To quantify the

increase in expression we conducted qPCR on RNA isolated from control and forskolin-treated CFP/YFP cells, and found a more than four-fold increase in AKR1B7 message (Fig. 3.5b) after 48 hours of forskolin treatment. This confirmed that in cells of the renin lineage control of AKR1B7 expression, like renin, is cAMP-sensitive.

To investigate this effect *in vivo*, we examined animals that had key elements of the cAMP response pathway knocked out. Animals with conditional deletion (in renin cells) of two important mediators of cAMP response, p300 and CREB-binding protein (CBP) ($CBP^{fl/fl}$ x $P300^{fl/fl}$; $Ren1d^{cre/+}$, (48)), have markedly fewer renin-positive JG cells. Similarly, those animals had significantly fewer AKR1B7-positive cells (Fig. 3.5c), all found within JG areas. Staining in consecutive sections showed that AKR1B7 was still segregated specifically to those cells which still expressed renin (likely due to incomplete deletion) (Fig. 3.5d). Thus the data indicates that the cAMP pathway controls expression of both AKR1B7 and renin *in vivo* and *in vitro*.

Figure 3.5

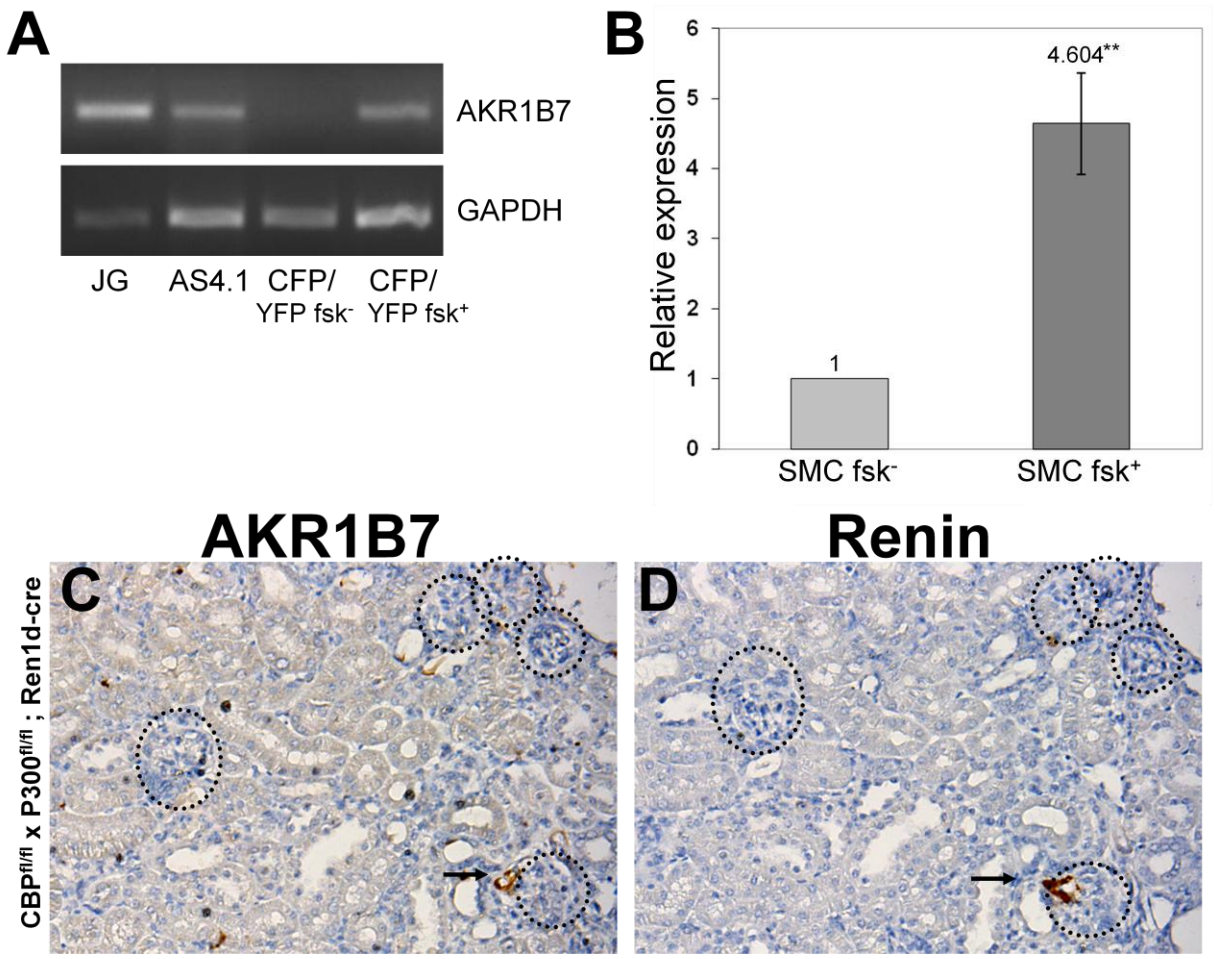

Figure 3.5: AKR1B7 expression is regulated by the cAMP signaling pathway. A: PCR products for AKR1B7 from mRNA isolated from JG cells. We detect AKR1B7 mRNA in JG cells (lane 1) and AS4.1 cells (lane 2), a kidney tumor cell line which expresses renin. AKR1B7 message is nearly absent from unstimulated cells of the renin lineage (lane 3), but appears in cells of the renin lineage stimulated with forskolin (lane 4). B: AKR1B7 mRNA levels as measured with qPCR increase nearly five-fold in cells of the renin lineage after treatment with forskolin when compared to treatment with DMSO vehicle (anchored to a value of one), $p<0.005$. C,D: Significantly fewer AKR1B7- and

renin-positive glomeruli are found in mice where two elements of cAMP-response, the genes CBP and p300, have been deleted. Circles indicate glomeruli, and arrows indicate areas of coincident staining. (performed by EEL)

RBP-J Deletion Affects the Myo-Endocrine Phenotype of Cells of the Renin Lineage[5]

Deletion of the transcription factor RBP-J, the common transcriptional mediator for the Notch signaling pathway, in renin cells results in a drastic reduction in the number of renin-positive cells. We also found that AKR1B7 expression was diminished in mice with conditional deletion of RBP-J in renin cells (Supplementary Figure 3.1A). Quantitation showed significantly fewer AKR1B7-positive JGAs (Supplementary Figure 3.1B), which was accompanied by a reduction in AKR1B7 mRNA in the kidneys, to an extent similar to renin (Supplementary Figure 3.1C). Thus we conclude that RBP-J regulates not only renin production in renin cells, but also other genes that contribute to the overall renin cell phenotype such as AKR1B7.

[5] Data originally published as a third-author manuscript in (59)

Supplementary figure 3.1

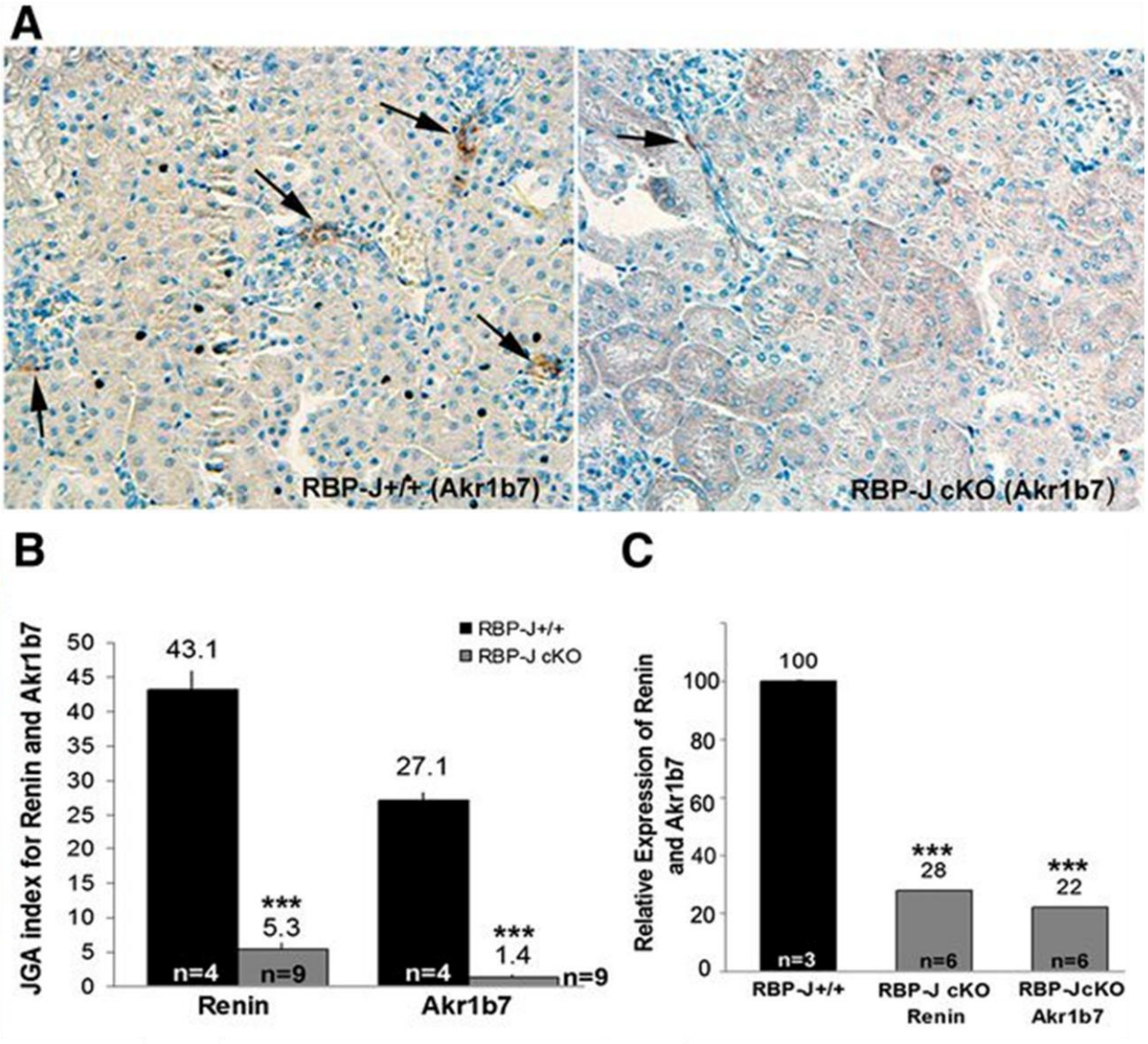

Suppplementary figure 3.1: Deletion of *RBP-J* in renin cells affects expression of genes marking the dual endocrine and SM phenotype of renin cells. (A–C) Expression of *Akr1b7*, an endocrine phenotype marker. (A) Immunostaining for Akr1b7 shows that *RBP-J*$^{+/+}$ mice express Akr1b7 in the JGAs (arrows in left panel).*RBP-J cKO* mice have few or no Akr1b7-positive JGAs (arrow in right panel). (B) In *RBP-J cKO* mice, the JGA indices for both Akr1b7 and renin are significantly reduced. (C) *Akr1b7* and renin mRNA levels in *RBP-J cKO* mice decreased significantly to the

same extent compared with controls. Originally published in (59). (A performed by EEL, B and C by RMC)

Discussion

The present series of experiments demonstrate that AKR1B7 is expressed in the same cells as renin throughout the dynamic changes in renin cell distribution during kidney development, and in response to pharmacological and pathological manipulations that increase or decrease the number of cells expressing renin. Moreover, we show that AKR1B7 is a renin-independent marker for cells attempting to make renin, and that only complete ablation of renin cells using DTA resulted in an absence of AKR1B7 protein. Finally, we demonstrated the key role of the cAMP signaling pathway in regulating the expression of AKR1B7 both *in vitro* and *in vivo.*

AKR1B7 expresses specifically in renin cells throughout a variety of manipulations

We have previously shown that AKR1B7 was highly enriched in renin producing cells of the adult mouse, by means of both microarray study and immunostaining (18). In this manuscript we show using immunostaining that co-expression of renin and AKR1B7 occurs throughout all stages of fetal and postnatal kidney development. Confocal microscopy combined with co-immunofluoresence of AKR1B7 and renin confirmed definitively that the two proteins are co-expressed in the same cell. Thus, AKR1B7 labels renin cells throughout renal development, and can serve as a marker for renin cells when assaying directly for renin is not possible or practical. We also show that the co-expression of AKR1B7 and renin is maintained under physiological and pharmacological manipulations of renin levels. In the same way that smooth muscle cells along the afferent arteriole re-acquire the ability to express renin (16) in response to low salt diet and administration of captopril, they also re-acquire the ability to express

AKR1B7, demonstrating that AKR1B7 is part of a larger genetic program re-activated by former renin-expressing cells in response to a need to increase renin levels. This idea was reinforced by the observation that when the domain of renin cells contracts in response to high-salt diet, AKR1B7 is likewise restricted to the reduced-in-number renin-positive cells. Thus, when cells cease the renin-expressing program, they also stop synthesizing AKR1B7.

We also examine AKR1B7 expression under genetic manipulations which were previously demonstrated to cause widespread pathological alterations of renin expression. Global deletion of the aldosterone synthase gene results in hypotension, abnormal fluid and electrolyte homeostasis, and significantly elevated renin production accompanied by an increase in renin cells. We show that these cells are also positive for AKR1B7, indicating the coordinated response of AKR1B7 to this extreme homeostatic need. By contrast, conditional deletion of the microRNA-processing enzyme Dicer within renin cells results in fewer renin cells and lower plasma renin levels, in addition to lower blood pressure, vascular abnormalities and renal fibrosis. Here we demonstrate that the few remaining renin-positive cells are still positive for AKR1B7. This finding also implicates a possible role for micro-RNAs to regulate AKR1B7, although the identity of the micro-RNAs that regulate renin and AKR1B7 in the renin cell is a matter of ongoing study (60).

Regardless of the manipulation, the result was the same: as the expression domain of renin expands, AKR1B7 is also found in the cells that acquire the ability to express renin. When renin expression decreases and cells cease expressing renin, those cells also stop expressing AKR1B7. Only complete ablation of renin cells using diphtheria

toxin (Ren1c-DTA) results in abolition of AKR1B7 expression within the kidney, emphasizing the specificity of AKR1B7 in the kidney for renin cells.

The specific co-expression of AKR1B7 with renin raises the question of AKR1B7 function in the renin cell. One possibility is that the two proteins exert direct regulatory effects on each other, and are in the same direct molecular pathway upstream or downstream from each other. However, data generated in this study and in other laboratories suggests that this is not the case. Confocal microscopy shows that AKR1B7 and renin are localized to different organelles (the endoplasmic reticulum and lysosomes respectively) and thus are unlikely to directly interact, although this would need to be confirmed using other assays such as co-immunoprecipitation or FRET. We also note that interestingly the amino acid sequence of AKR1B7 lacks the canonical N-terminal ER localization motif lysine-aspartic acid-glutamic acid-leucine (KDEL), and it remains to be determined what mechanism causes the localization of AKR1B7 to the ER. The absence of cross-regulation between AKR1B7 and renin was further supported by our data showing the persistence of AKR1B7 expression after deletion of the renin gene. Conversely, Machura et al. (61) show that systemic deletion of AKR1B7 does not alter the levels of renin transcription and expression. Thus it is likely that AKR1B7 plays a role in parallel to renin as part of a larger genetic program of establishing the renin cell phenotype, but that AKR1B7 does not directly interact with renin.

Other alternatives exist for a role for AKR1B7 in the kidney. Endocrine cells may be particularly vulnerable to oxidative stress due to their increased levels of protein synthesis. Interestingly AKR1B7 has been shown to possess a protective role in adrenal cells by catalyzing the reduction of isocaproaldehyde, a byproduct of hormone

synthesis associated with oxidative stress, into less toxic forms (62). In addition, analysis of adrenal tumors showed that tumoral cells had blunted AKR1B7 expression (63), with oxidative stress being a hallmark of tumorigenesis. It is possible that AKR1B7 functions in a similar role in renin secretory cells to protect against accumulated oxidative stress involved in the renin cell's primary duties of renin synthesis and granulopoeisis. This hypothesis would be supported by AKR1B7s localization to the ER, the primary site of protein synthesis in the cell, although studies of oxidative stress in renin cells are currently sparse.

Alternatively, AKR1B7 could play a role in prostaglandin synthesis; prostaglandins have long been thought to play a role in the regulation of renin (64-66). It was previously found that AKR1B7 was capable of catalyzing the synthesis of prostaglandin F2α, both biochemically (67) and *in vitro* (68). As prostaglandin F2α has also been shown to stimulate renin secretion (69, 70), it is possible that AKR1B7 is responsible regulating renin secretion through prostaglandin F2α synthesis. This hypothesis is supported by the fact that AKR1B7 was described as changing localization to the plasma membrane when synthesizing prostaglandin F2α (68), agreeing with our observation that AKR1B7 localizes to the plasma membrane of the renin cell. However, studies of renin release will need to be performed to answer this question.

AKR1B7 marks cells attempting to synthesize renin, independent of the cell's actual production of renin

Study of renin cells has long been complicated by the fact that the only reliable marker for renin cells was renin itself. In situations where renin expression was blunted or

absent, a separate marker for renin cells would be necessary to identify cells attempting to produce renin. As mentioned earlier we show *in vivo* that AKR1B7 expression persists in the kidney even when the gene for renin is deleted, thus establishing AKR1B7's independence of renin expression. Intriguingly, we also observe that the staining pattern of AKR1B7 in renin knockout mice replicates that of renin cells under conditions that stimulate renin production, such as the earlier-described phenotype following sodium depletion and captopril treatment. This suggests that there is an attempt by cells in the renin knockout kidney to synthesize renin, likely in response to systemic hypotension and sodium depletion, and that AKR1B7 is a marker for those renin-less cells of the renin phenotype. The AKR1B7-marked cells thus represent a system in which the genes for the renin cell phenotype and the renin promoter itself (which is intact in the renin knockout animal used here (56)) would be chronically stimulated, as those cells attempt to compensate for a lack of renin. Isolating these cells could provide an important platform for the study of renin regulation, as studies in renin cell plasticity have been primarily conducted under conditions of acute stimulation.

Mechanisms of AKR1B7 regulation

The degree of co-expression between AKR1B7 and renin, and a lack of evidence that suggests that the two enzymes directly regulate each other, presents the highly interesting possibility that both genes are regulated in a similar manner through an overarching genetic program that controls renin cell fate. Various inputs are incorporated to control the identity and subsequent production and secretion of renin by the renin cell (for a review see (71)), but the exact mechanism(s) which regulates the renin gene is not fully understood. The AKR1B7 gene and its associated promoter could

provide an important tool in that search, as having an additional promoter to look at *in silico*, *in vitro,* and *in vivo* adds a degree of power not previously available. In addition, identifying transcription factors and other regulatory molecules that affect AKR1B7 could provide candidates that potentially regulate renin as well.

One possibility examined here is that cyclic AMP plays an important role in the simultaneous regulation of both proteins. Our lab and others have previously identified the cAMP pathway as an activator of renin expression (48, 72). In addition, there exists a cyclic-AMP response element (CRE) in the AKR1B7 promoter that is key to its regulation, and cAMP has been demonstrated *in vitro* and *in vivo* to play a key role in the control of AKR1B7 transcription in the adrenal glands (46, 63). In this study, we show that cAMP plays a similar role in regulating AKR1B7 in the kidney, using multiple approaches. *In vitro,* increasing intracellular cAMP levels in cultured cells of the renin lineage via forskolin causes an increase in AKR1B7 expression. *In vivo,* deletion of elements of the renin cell's cAMP response pathway- the histone acetyl-transferases p300 and CBP- significantly blunts the expression of AKR1B7 in the murine kidney. Taken together, these experiments demonstrate that cAMP plays a significant role in co-regulating both AKR1B7 and renin in the kidney. Previously, we have also shown that deletion of Recombination Signal Binding Protein for Immunoglobulin Kappa J Region (RBP-J), the final transcriptional mediator of the Notch signaling pathway, resulted in a significant decrease in renin- and AKR1B7-positive cells (36, 59). Whether and how the Notch pathway and cAMP signaling interact to regulate renin and AKR1B7 expression, potentially as part of an overarching genetic program that controlling renin cell identity, remains to be determined.

Perspectives and Significance

AKR1B7 is co-expressed and regulated by the same factors that regulate the renin gene, suggesting the possibility of an overarching program controlling the renin phenotype. Interestingly, when the renin gene is mutated, this program continues to operate and AKR1B7 permits the identification of those cells that were programmed to express renin but cannot do so. Under these circumstances, the renin-less mutated cells do not disappear; they can be identified as AKR1B7 + cells which expand along and around the arterioles of the kidney possibly participating in the concentric obstructive vessel hypertrophy commonly seen in animals with mutations of the renin gene. Thus, AKR1B7 adds a new degree of power when investigating the biology of the renin cell.

Acknowledgments

We gratefully recognize the assistance of Dr. Brian Belyea in helping to prepare this manuscript. We thank LaToya Roker for help with confocal microscopy, and Michelle Ko for assistance with statistical analysis.

Grants

National Institutes of Health grants R37 HL066242 and R01 HL096735 to RAG and R01 DK-091330 to MLS, American Heart Association Pre-Doctoral Grant 13PRE16920043 to EEL

Disclosures

None

IV. RBP-J IN FOXD1+ RENAL STROMAL PROGENITORS IS CRUCIAL FOR THE PROPER DEVELOPMENT AND ASSEMBLY OF THE KIDNEY VASCULATURE AND GLOMERULAR MESANGIAL CELLS

Formatted as a first-authored manuscript and published as:

RBP-J in FOXD1+ Renal Stromal Progenitors is Crucial for the Proper Development and Assembly of the Kidney Vasculature and Glomerular Mesangial Cells. Lin EE, Sequeira-Lopez ML, Gomez RA. Am J Physiol Renal Physiol. 2014 Jan;306(2):F249-58. doi: 10.1152/ajprenal.00313.2013.

Abstract

The mechanisms underlying the establishment, development, and maintenance of the renal vasculature are poorly understood. Here we propose that the transcription factor “recombination signal binding protein for immunoglobulin kappa J region” (RBP-J) plays a key role in the differentiation of the mural cells of the kidney arteries and arterioles, as well as the mesangial cells of the glomerulus. Deletion of RBP-J in renal stromal cells of the forkhead box D1 (FOXD1) lineage, which differentiate into all mural cells of the kidney arterioles along with mesangial cells and pericytes, resulted in significant kidney abnormalities and mortality by day 30 post-partum. In newborn mutant animals we observed a decrease in the total number of arteries and arterioles, along with thinner vessel walls, and depletion of renin cells. Glomeruli displayed striking abnormalities, including a failure of FOXD1-descendent cells to populate the glomerulus, an absence of mesangial cells, and in some cases complete loss of glomerular interior structure and the development of aneurysms. By P30, the kidney malformations were accentuated by extensive secondary fibrosis and glomerulosclerosis. We conclude that RBP-J is essential for proper formation and maintenance of the kidney vasculature and glomeruli.

Introduction

The kidney is a highly vascularized organ, receiving over 20% of the cardiac output in the adult human. However, the developmental cues and mechanisms necessary for proper formation of the complex renal arterial tree are poorly understood. Our lab and others have previously shown that the progenitors for the kidney vasculature are present in the early embryonic kidney, well before vessels can be discerned (13, 35) Prior work using cell-specific lineage tracing has demonstrated that within the embryonic kidney there is a population of stromal mesenchyme cells marked by expression of the transcription factor forkhead box D1 (FOXD1) (20, 31). Cells derived from the *Foxd1*-lineage differentiate to form all the cell types that comprise the mural cell layer of the kidney arteries and arterioles (vascular smooth muscle cells (VSMCs), renin cells and perivascular fibroblasts), along with glomerular mesangial cells, and various cell types of the kidney interstitium including pericytes (29).

In many organisms the Notch signaling pathway is involved in key cell fate and developmental decisions (25, 26). Interestingly, all elements of the Notch pathway share a common downstream transcription factor, “recombination signal binding protein for immunoglobulin kappa J region” (RBP-J) (73). Prior work in our lab has determined that RBP-J, and likely Notch signaling, are essential for establishing and maintaining the identity of renin-expressing cells in adulthood (21). However, it is not currently known whether RBP-J plays a role in the differentiation of FOXD1+ progenitors into the downstream derivative cell types, which includes renin cells along with the previously mentioned cell types. Using the cre-lox system we examined the effects of conditional deletion of RBP-J in the FOXD1+ precursor cell population and found severe vascular

defects in the mural cell layer of arteries and arterioles accompanied by a depletion of renin-expressing cells, and serious glomerular defects characterized by a lack of mesangial cells and development of glomerular aneurysms. Later in life, these developmental alterations were aggravated by striking reactive alterations including glomerulosclerosis, tubular dilations, and fibrosis, suggesting that developmental defects are further complicated by secondary injury and/or repair mechanisms.

Results

Deletion of RBP-J in Foxd1 cells results in defects in the renal arterial smooth muscle layer

To examine the effects of RBP-J deletion on FOXD1-lineage stromal cells and their descendents, we generated animals with conditional deletion of RBP-J in FOXD1-cells ($FOXD1^{cre/+}$; $RBP\text{-}J^{fl/fl}$, hereby termed $FOXD1^{RBPJ-/-}$). Confirmation of RBP-J deletion was conducted using RT-PCR on whole kidney isolated from mutant or control animals (not shown). $FOXD1^{RBPJ-/-}$ mice were born at expected Mendelian ratios (7 out of 24, 25% expected), and on the first day of life (P0) were indistinguishable at a macroscopic level from control animals with the exception of a shorter tail length (Fig. 4.1a), a feature which was retained in older animals at 30 days of postnatal life (Fig. 4.4a). Examination of kidneys harvested from $FOXD1^{RBPJ-/-}$ animals at day of birth however revealed striking renal defects. Newborn $FOXD1^{RBPJ-/-}$ mice had significantly fewer smooth muscle cell (SMC)-coated renal arteries than controls, as shown by immunostaining for alpha-smooth muscle actin (Fig. 4.1b, ACTA2, arrows,), a marker for smooth muscle cells (SMCs). Arterioles appeared to have significantly thinner vessel walls, and the cells comprising the mural cell layer were thinner in appearance. Endothelial cells however, as marked by

staining with platelet and endothelial cell-adhesion molecule (PECAM) showed no morphological alterations, and we did not find evidence for uncoated endothelial vessels lacking a smooth muscle cell coating (not shown). Quantification of vessel numbers showed a nearly six-fold decrease in smooth-muscle coated arteries per area surveyed and a significant reduction in vessel wall thickness, with control animals having an average of 6.1 ± 0.4 (n=5) vessels per area surveyed, while FOXD1$^{RBP\text{-}J\text{-}/\text{-}}$ kidneys had on average 1.1 ± 0.2 (n=5) vessels per area surveyed (Fig. 4.1c, $p<0.05$). In addition, the smooth muscle layer of mutant vessels was thinner, 7.4 ± 0.3 µm (n=5) in mutants versus 9.5 ± 0.5 µm (n=5) in controls ($p<0.005$, Fig. 4.1d). A distribution of the measurements of vessel diameter showed that mutant kidneys had comparable numbers of large-diameter vessels but significantly fewer small-diameter vessels (Fig. 4.1e), indicating that smaller-diameter vessels, mostly afferent arterioles, were the most affected by the mutation.

Because our previous work indicated that RBP-J plays a key role in establishing and maintaining the identity of renin cells, and because renin cells are derived from FOXD1-expressing cells, we investigated the expression of renin in FOXD1$^{RBPJ\text{-}/\text{-}}$ animals by immunostaining. In wild-type animals at day of birth, renin cells can typically be found along afferent arterioles, in addition to larger vessels. However, in FOXD1$^{RBPJ\text{-}/\text{-}}$ animals we found an almost complete absence of immunoreactive renin (Fig. 4.1f), with very few cells positively stained, and renin expression limited to a few juxtaglomerular regions rather than extending along the arterioles as is commonly observed in newborn mammals. Furthermore, we occasionally found that some kidney areas showed tubular dilations and disruption of tubular structure in mutant animals (not shown).

Figure 4.1

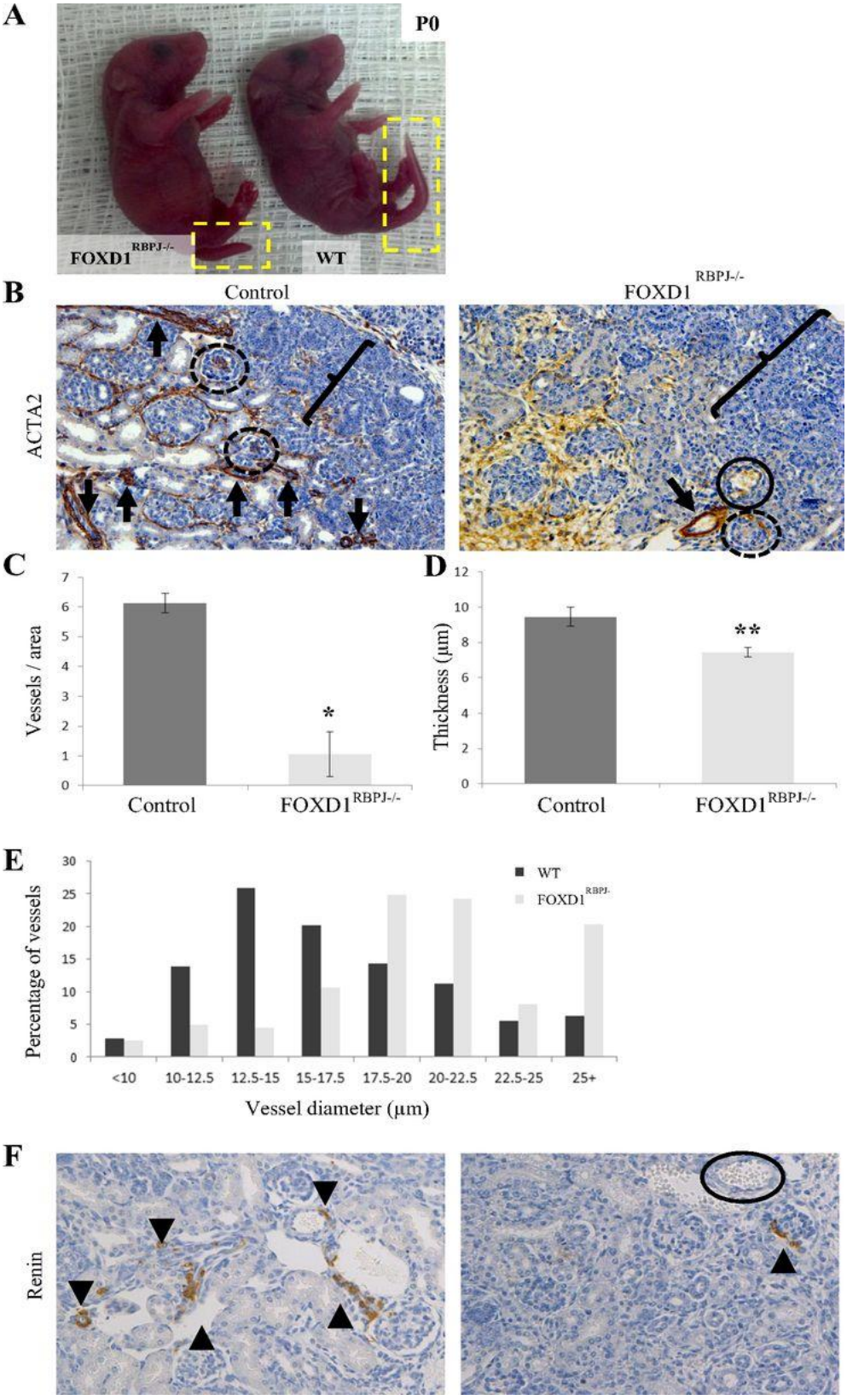
A
P0
FOXD1 RBPJ-/-
WT
B
Control
FOXD1 RBPJ-/-
ACTA2
C
Vessels / area
*
Control
FOXD1 RBPJ-/-
D
Thickness (µm)
**
Control
FOXD1 RBPJ-/-
E
Percentage of vessels
WT
FOXD1 RBPJ-
<10
10-12.5
12.5-15
15-17.5
17.5-20
20-22.5
22.5-25
25+
Vessel diameter (µm)
F
Renin

Figure 4.1: Kidneys from newborn FOXD1$^{RBPJ-/-}$ animals show pronounced vascular and glomerular defects. A) Newborn (P0) FOXD1$^{RBPJ-/-}$ and control pups are indistinguishable other than by tail length (yellow boxes). B) Staining for ACTA2 (brown) in kidney sections. Mutant animals have significantly fewer arteries (arrows), and comparable vessels are thinner in FOXD1$^{RBPJ-/-}$ animals than in controls. Mutant glomeruli (circles) are dilated and have distorted morphology, while some are aneurysmatic and lacking structural cells (solid circles, also 1F). We also note that the nephrogenic zone (brackets) is wider in mutant animals. C) Quantification of arteries shows significant decreases in vessel number per area surveyed in FOXD1$^{RBPJ-/-}$ animals ($p<0.05$). D) Quantification of average vessel thickness shows that FOXD1$^{RBPJ-/-}$ animals have thinner vessels ($p<0.005$). E) In regards to the distribution of arterial diameters, newborn mutant animals show a deficit in the percentage of smaller-diameter vessels, but a higher proportion of larger-diameter vessels. F) Immunostaining for renin (brown, arrowheads) in control animals can be found extending along afferent arterioles and adjacent to glomeruli. Meanwhile, FOXD1$^{RBPJ-/-}$ animals show a significant depletion of renin cells, with almost no renin-positive cells throughout the kidney. The solid circle denotes an aneurysmatic glomeruli, see 1B. (performed by EEL)

Loss of RBP-J in Foxd1 cells results in a loss of mesangial cells and glomerular aneurysms

Further examination of newborn FOXD1$^{RBPJ-/-}$ kidneys also revealed that in mutant animals glomeruli displayed striking morphological abnormalities. Hematoxylin and eosin (H&E) staining (Fig. 2A) showed that glomeruli from FOXD1$^{RBPJ-/-}$ animals (circles) contained an abnormally elevated number of red blood cells, and that in some cases entire glomeruli were replaced by glomerular aneurysms filled with blood (Fig. 4.2A, also Figs. 4.1B and 4.1F, solid circles). Quantification of glomerular alterations showed that more than half of the glomeruli in mutant kidneys appeared abnormal, with nearly a quarter having aneurysms (Fig. 4.2B). The likely cause of the aforementioned glomerular alterations was suggested by the unusual ACTA2 staining, which during development stains mesangial cells, but was diffuse or absent in the glomeruli of mutant kidneys (Fig. 4.1B). To confirm an alteration in the endowment of glomerular mesangium we stained for platelet-derived growth factor receptor β (PDGFR-β), a marker for mesangial cells and a key protein in mesangial differentiation (74). In control kidneys, PDGFR-β-positive mesangial cells populate the interior of the glomerulus. FOXD1$^{RBPJ-/-}$ kidneys however displayed a significant reduction or complete absence of PDGFR-β staining within the glomerulus (Fig. 4.2C), indicating a marked decrease in mesangial cells. As expected and in contrast to the mesangial alterations, PDGFR-β-positive interstitial cells in between the tubules were unaffected and stained positive in control and mutant animals. Alterations to the glomerular mesangium resulted in changes to other cell types that populate the glomerulus. Staining for podocytes using a podocalyxin antibody (PODXL, Fig. 4.2D) demonstrated that podocytes remained in glomeruli (circles), although their localization

and structure was severely affected, with the PODXL-positive cells often confined to a single thick, peripheral ring instead of being spread more uniformly throughout the glomerulus. Remarkably, many podocytes persisted even in cases of severe glomerular aneurysm (solid circle). Glomerular capillaries also showed significant alterations. Staining for Slit3, a marker for glomerular capillaries, shows that the endowment of glomerular capillaries is unaffected, as they can be found even in aneurysmatic glomeruli (Fig. 4.2E). However, in FOXD1$^{RBPJ-/-}$ animals the typical arrangement of multiple capillary loops seen in wild-type animals is lost, with the glomerular capillaries collapsing into fewer loops or a single, giant loop.

Figure 4.2

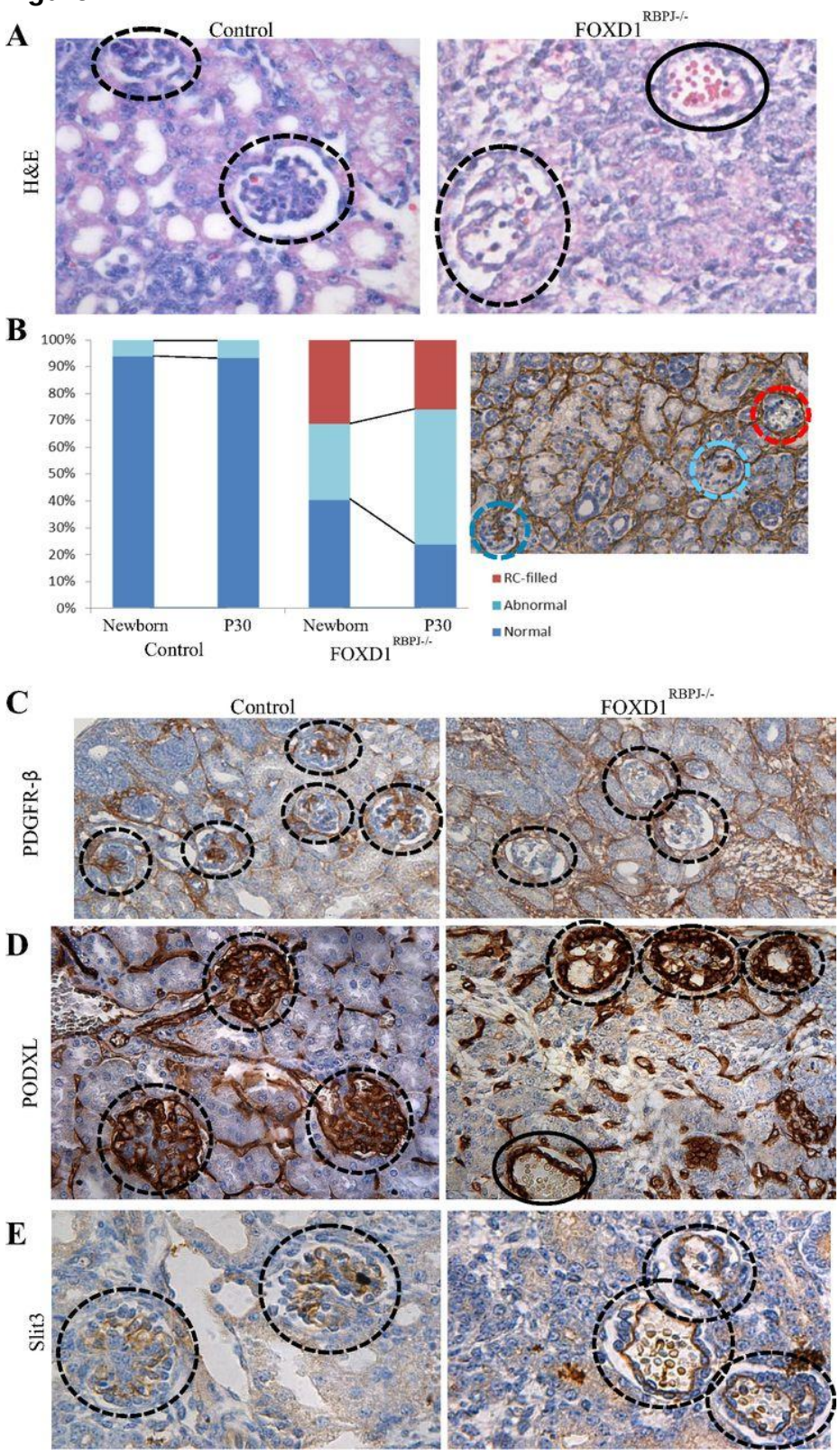
A
Control
FOXD1 RBPJ-/-
H&E
B
100%
90%
80%
70%
60%
50%
40%
30%
20%
10%
0%
Newborn
P30
Newborn
P30
Control
FOXD1 RBPJ-/-
RC-filled
Abnormal
Normal
C
Control
FOXD1 RBPJ-/-
PDGFR-β
D
PODXL
E
Slit3

Figure 4.2: The glomeruli of FOXD1$^{RBPJ-/-}$ kidneys lack mesangial cells and are aneurysmatic. A) High-power view of glomeruli (dashed circles) with H&E staining in control animals shows well-formed glomeruli with few interior red blood cells (RBCs), while a large number of RBCs are found in the interior of glomeruli from FOXD1$^{RBPJ-/-}$ animals. Mutant glomeruli are at different stages of aneurysm formation and glomerular hemorrhage. A glomerulus completely devoid of mesangial cells and filled with RBCs is indicated by the solid circle. B) Analysis of the prevalence of glomerular abnormalities shows that newborn FOXD1$^{RBPJ-/-}$ animals display alterations in almost 2/3rds of their glomeruli, and that an even greater proportion (75%) shows abnormalities by day 30 of life. We also examined the proportion of glomeruli which were devoid of structure and filled with red blood cells. This subtype was completely absent in wild-type kidneys, but comprised 31% of newborn FOXD1$^{RBPJ-/-}$ glomeruli, decreasing slightly to 26% in adults. The right panel is an example of a FOXD1$^{RBPJ-/-}$kidney at P30 stained for ACTA2 with normal (dark blue), abnormal (light blue), and RBC-filled (red) glomeruli. C) Staining for PDGFR-β, a marker for glomerular mesangium (along with vascular smooth muscle cells and pericytes), is absent in the glomeruli in mutants, suggesting a lack of mesangial cells in FOXD1$^{RBPJ-/-}$ animals. D) Staining for podocalyxin (PDXYL) shows that podocytes persist in FOXD1$^{RBPJ-/-}$ glomeruli, even in aneurysmatic glomeruli, although their location is altered. E) Staining for Slit3 labels glomerular endothelial cells. The glomerular capillaries in FOXD1$^{RBPJ-/-}$ kidneys have collapsed into a single capillary loop, in contrast to the multiple capillary loops seen in wild-type animals. (performed by EEL)

RBP-J controls the differentiation of Foxd1 cells into mesangial cells and smooth muscle cells

To examine the fate of FOXD1^{+} cells upon deletion of RBP-J and assess their contribution to the resultant disease processes seen in the vasculature and glomeruli, we traced the lineage of FOXD1^{+} cells by incorporating the R26R (Rosa26) reporter system. We bred our FOXD1^{RBPJ} animals to mice homozygous for the R26R allele, which expresses beta-galactosidase upon cre-mediated recombination. In these animals, termed FOXD1$^{RBPJ-/-;R26R}$, FOXD1- lineage cells can be visualized blue upon reaction with X-gal. As previously reported, in newborn wild-type animals FOXD1-lineage cells comprised the entirety of the mural cell layer of arteries and arterioles, along with undifferentiated kidney stroma, interstitial cells, and mesangial cells (Fig. 4.3). Whereas in control animals afferent and efferent FOXD1-derived arterioles can be clearly seen branching off larger vessels and entering glomeruli (Fig. 4.3, arrows), in mutant animals the arterioles do not branch adequately, are poorly formed, and are markedly more disorganized, making thin connections with nearby glomeruli (see also Supplementary Figure 4.1). FOXD1$^{RBPJ-/-;R26R}$ mice at day of birth also showed an absence of blue FOXD1-lineage cells from the glomerulus (Fig. 4.3, circles). At this age Foxd1-lineage mesangial cells can be typically found in the center of the glomerulus, and their absence indicates a failure of those cells to populate the glomerulus, likely leading to the glomerular aneurysms described above.

Figure 4.3

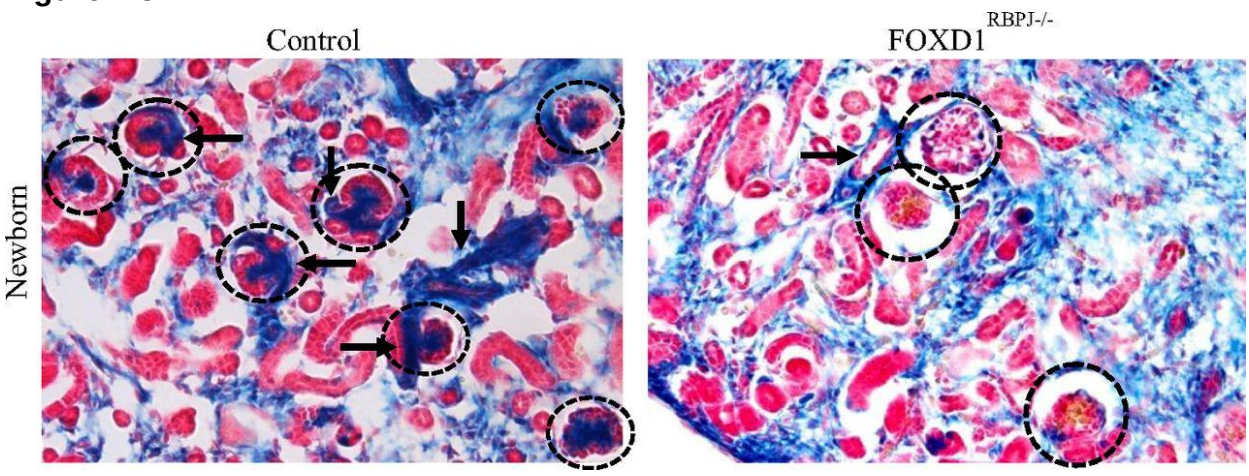

Figure 4.3: Lineage study of FOXD1 cells in newborn animals upon RBP-J deletion. Newborn kidneys were examined for expression of the β-galactosidase reporter after reaction with X-gal. FOXD1-lineage cells are labeled blue and can be found in control mice in undifferentiated stroma, interstitium, the mural cell layer of arteries (arrows), and mesangial cells. Labeled cells in mutants meanwhile show poor vascular wall integrity and branching. FOXD1$^{RBPJ-/-}$ animals also lose expression of the reporter within the interior of the glomerulus (circles), likely corresponding to a loss of mesangial cells. (performed by EEL)

Supplementary Figure 4.1

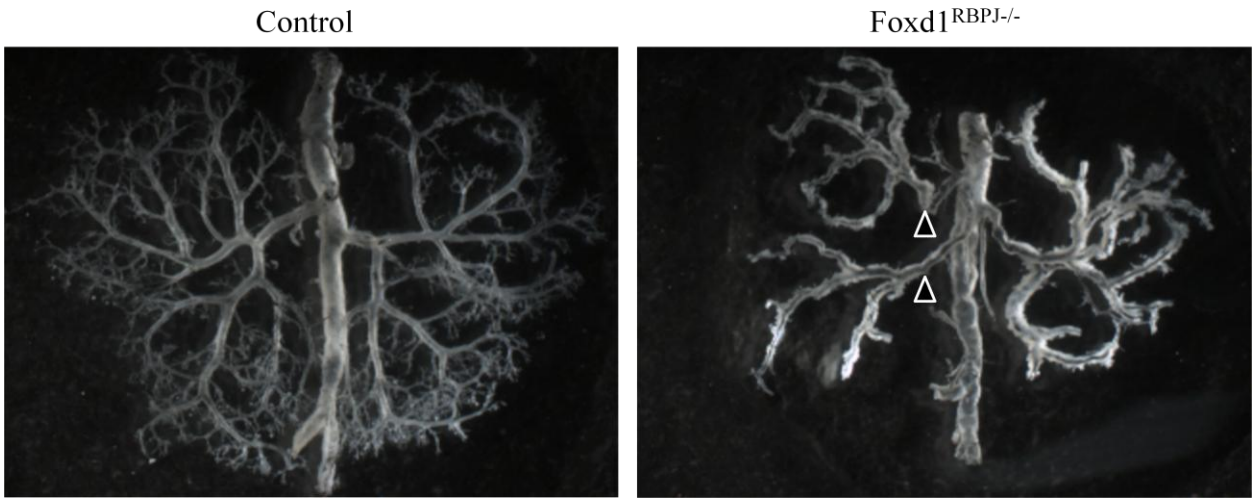

Supplementary Figure 4.1: The renal arterial tree of Foxd1$^{RBP\text{-}J\text{-}/\text{-}}$ mice is severely stunted. The arterial tree of kidneys was dissected using acid maceration and microdissection. Compared to control kidneys (left), mutant kidneys (right) have significantly fewer arteries, with significantly fewer second-order branches and almost no fourth-order branches, reminiscent of animals in which elements of the renin-angiotensin system have been deleted (75, 76). In addition, the surface of the arteries is notably more disorganized than controls. We also noted a duplication of the right renal artery (triangles) that was consistent across animals (n=3). (performed by Masafumi Oka).

Somatic effects of RBP-J deletion in adulthood- arterial fibrosis and glomerulosclerosis

Given the severe developmental alterations seen in the newborn kidney, we wished to examine the progression of kidney alterations in the maturing animal. We observed that a portion of mutant animals died some time after birth, as genotyping of weaned animals (21 days post-partum) showed that, in contrast to newborn animals, P21 animals no longer conformed to expected Mendelian ratios (10 out of 58, 25% expected, $\times^2 = 2.68$, $p < 0.05$). Subsequently, surviving $FOXD1^{RBPJ-/-}$ mice all died by 30 days post-partum. By this age, $FOXD1^{RBPJ-/-}$ animals showed significant secondary defects, as they were on average approximately half the weight of control animals (Fig. 4.4A, $p<0.05$). The kidneys of mutant animals were also smaller than those of controls, being on average half the weight of controls, and were paler in color (Fig. 4.4B, $p<0.05$). However, the ratio of kidney weight to body weight did not differ between control and mutant animals, indicating that RBP-J deletion in the FOXD1-lineage had additional somatic effects (not shown).

Figure 4.4

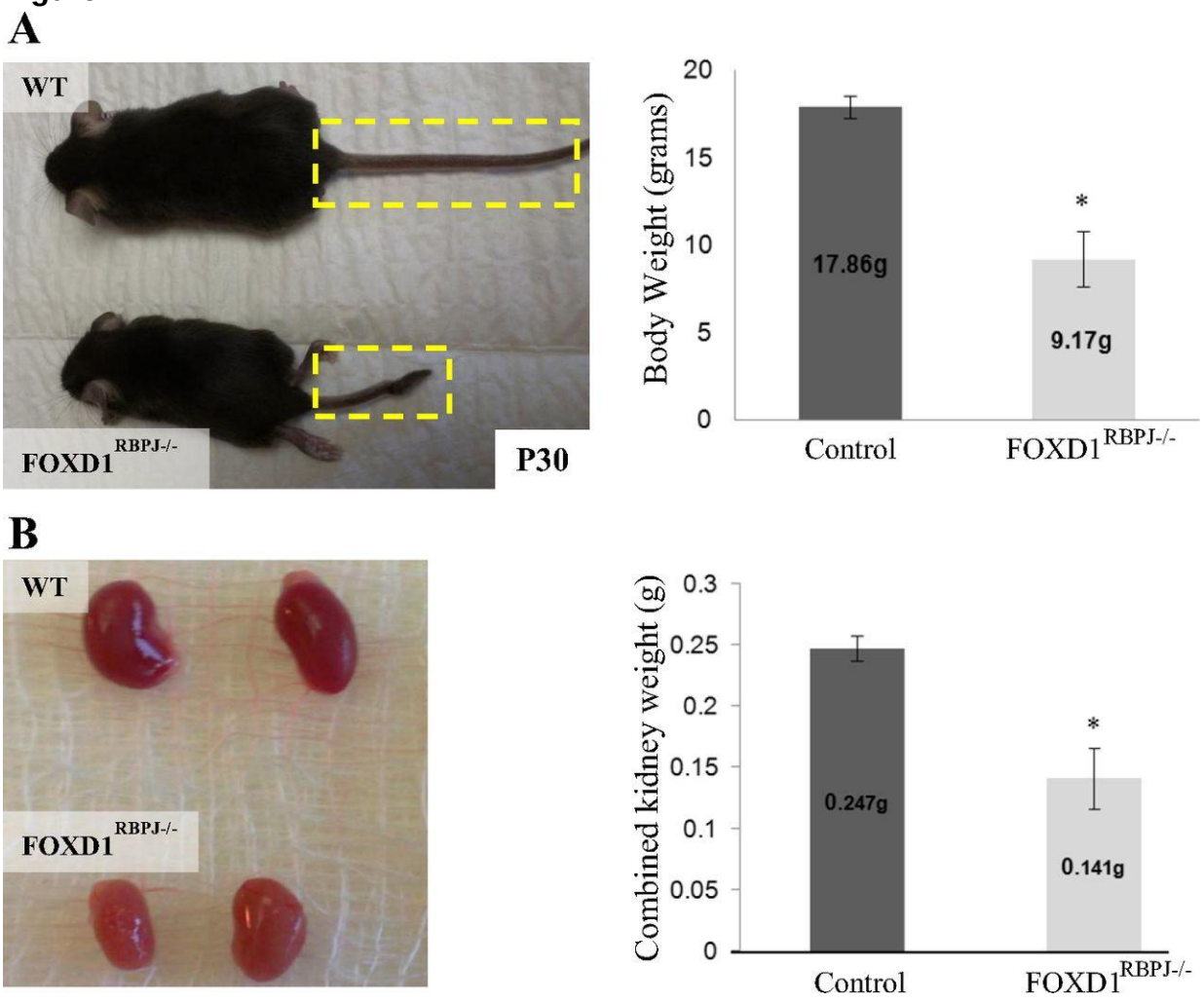

Figure 4.4: FOXD1$^{RBPJ-/-}$ adult animals have growth defects. A) By time of death, around day 30 post-partum (P30), FOXD1$^{RBPJ-/-}$ mice (n=8) are half the size of their control litter-mates (n=6, $p<0.05$). B) FOXD1$^{RBPJ-/-}$ kidneys are significantly smaller than controls ($p<0.05$). (performed by EEL)

Adult mice with deletion of RBP-J in Foxd1 cells display prominent vascular fibrosis

Given the developmental defects seen and subsequent early death of adult FOXD1$^{RBPJ-/-}$ animals we examined FOXD1$^{RBPJ-/-}$ kidneys peri-mortem at around P30, where we found an even more pronounced and complex phenotype compared to newborn animals. In mutant animals staining for ACTA2 (Fig. 4.5A, upper panels) was no longer limited to vessels (arrows), but instead showed extensive expression across multiple regions of the kidney, particularly in interstitial areas surrounding vessels, and within and around glomeruli. Interestingly there was expansion of ACTA2 staining in structures outside known FOXD1-descendents, including tubules and capsular cells, indicating a secondary phenotype in response to vascular damage. As ACTA2 is expressed not only in smooth muscle cells abut also in cells undergoing injury and repair, we conducted staining for another marker of vascular smooth muscle, myosin heavy chain (SM-MHC, Fig. 4.5A lower panels), which showed prominent alterations in the perivascular compartment. As in the newborn FOXD1$^{RBPJ-/-}$ animals, at P30 arteries and arterioles were significantly reduced in number (Fig. 4.5B, $p<0.005$). In contrast to newborn animals however, at P30 there was significant thickening of vessel walls (Fig. 4.5A, arrows), in some occasions to the point of almost occluding the vessel (white arrow). Quantitation of vessel thickness in FOXD1$^{RBPJ-/-}$ animals again showed a deficiency of thin-diameter vessels but an enrichment of the thickest vessels (data not shown). Staining for renin also demonstrated that renin cells were nearly completely absent (data not shown).

The expansion of smooth muscle cell markers suggested an ongoing fibrotic/reparative process in the adult animals. To investigate this possibility we performed Sirius red staining for collagen (Fig. 4.5C). In FOXD1$^{RBPJ-/-}$ kidneys the areas surrounding vessels

(arrow) showed staining for multiple layers of dense collagen fibers which were also birefringent (indicative of thicker collagen fibers), contrasting with control animals where staining is limited to the mural cell layer proper, with collagen fibers less frequently birefringent. Also in support of an active fibrotic process we found that areas surrounding the vessels showed marked increases in fibroblasts (data not shown) and ongoing cellular proliferation, with multiple cells in the perivascular area stained positive for phospho-histone H3 (Fig. 4.5D, arrows). As an indicator of the extent of kidney damage, we also noted signs of tubular atrophy as indicated by tubular dilation and protein casts (data not shown). (performed by EEL)

Figure 4.5

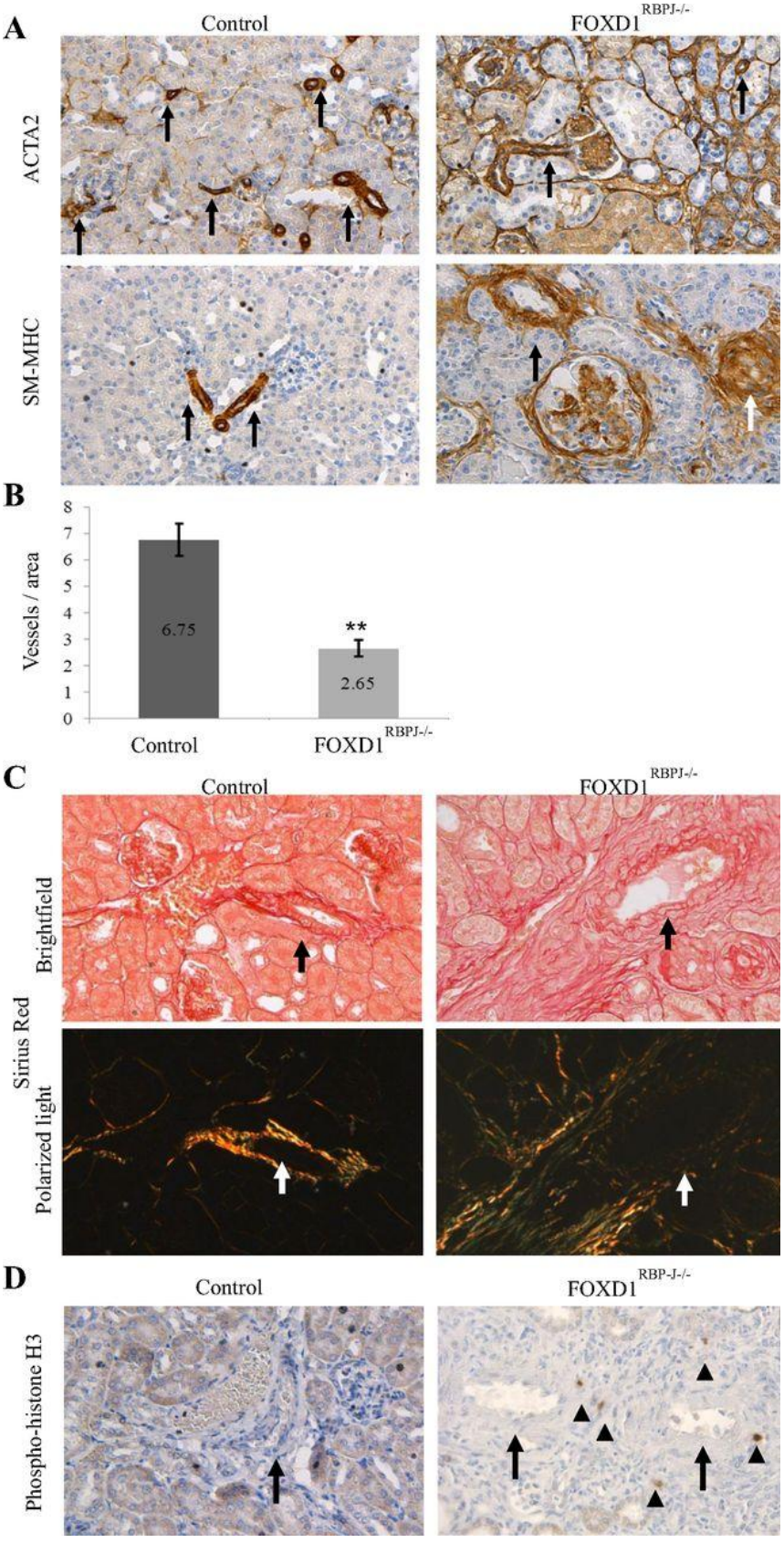
A
Control
FOXD1 RBPJ-/-
ACTA2
SM-MHC
B
Vessels / area
8
7
6
5
4
3
2
1
0
6.75
**
2.65
Control
FOXD1 RBPJ-/-
C
Control
FOXD1 RBPJ-/-
Sirius Red
Brightfield
Polarized light
D
Control
FOXD1 RBP-J-/-
Phospho-histone H3

Figure 4.5: Adult (p30) kidneys of FOXD1$^{RBPJ-/-}$ animals display active vascular remodeling and fibrosis A) Immunostaining for ACTA2 (top) and SM-MHC (bottom) in kidney sections, with blood vessels marked with arrows. In wild-type animals, ACTA2 and SM-MHC expression is limited to the vascular smooth muscle cells. Expression of ACTA2 expands significantly in mutant animals, and can be seen in peritubular and perivascular areas, within tubules, and also in the interior and around glomeruli. SM-MHC in mutants meanwhile stains more specifically for vascular smooth muscle cells, but also shows expansion in peri-vascular areas and within glomeruli, occasionally to the point of almost occluding a vessel (white arrow). B) Quantification of arterioles as assessed by SM-MHC staining shows significantly fewer vessels in FOXD1$^{RBPJ-/-}$ animals ($p<0.005$). C) Sirius red staining for collagen stains collagen fibers red under visible light collagen (upper panels), while when viewing under polarized light birefringence is an indication of thicker collagen fibers (lower panels). In wild type animals, only the areas comprising the vascular smooth muscle cell layer (arrows) stain red and are also birefringent (arrows). FOXD1$^{RBPJ-/-}$ animals show significant expansion of collagen in perivascular areas, with large regions of birefringence around the vessel. D) Staining for phospho-histone H3, a marker for actively dividing cells, in FOXD1$^{RBPJ-/-}$ kidneys shows multiple proliferating cells around vessel areas (upper right panel, arrows), while areas surrounding wild-type vessels are devoid of proliferating cells. (performed by EEL)

Foxd1 cells contribute to an ongoing injury process in Foxd1$^{RBPJ-/-}$ animals

Lineage tracing of Foxd1 cells again using the FOXD1$^{RBPJ-/-;R26R}$ reporter mouse showed significant expansion of FOXD1-lineage cells in peri-vascular areas, especially around larger vessels, in comparison to controls (Fig. 4.6). These cells stain positive for ACTA2 (data not shown) and are likely indicative of vascular damage and fibrosis. We also found an expansion in the number of FOXD1-lineage interstitial cells in the areas between tubules, suggesting an expansion of the pericyte compartment (Figure 6, asterisks), which was confirmed using quantification of cellular proliferation markers (not shown).

Also at P30, glomeruli showed thickening characteristic of glomerulosclerosis, and stained positive for smooth muscle markers which are typically absent by this age in control animals (Fig. 4.5A). Interestingly, mutant animals displayed a decrease in glomerular number (Fig. 4.7A, $p<0.005$), accompanied by significant increases of glomerular size in mutant animals compared to controls ($p<0.0005$); no such differences were found at newborn age (not shown). Glomerular morphology in FOXD1$^{RBPJ-/-}$ adult kidneys was distorted and sometimes aneurysmatic (Fig. 4.7B, also 4.5A), but at a higher occurency compared to newborn animals (Fig. 4.2B), all indicative of a continuous injurious process. As in the newborn animals, glomeruli in mutant kidneys at P30 showed a significant decrease in PDGFR-β staining, indicating a lack of mesangial cells (Fig. 4.7B).

Figure 4.6

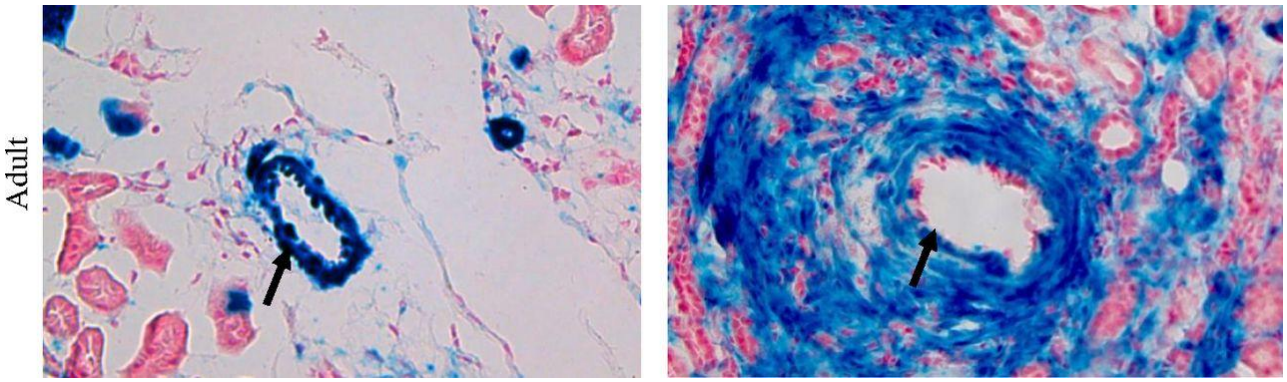

Figure 4.6: Lineage study of FOXD1 cells in adult animals upon RBP-J deletion. Examination of FOXD1-lineage cells in adult animals in perivascular areas indicates significant proliferation of FOXD1-lineage cells in areas surrounding blood vessels (arrows), in addition to an increase in interstitial cells. (performed by EEL)

Figure 4.7

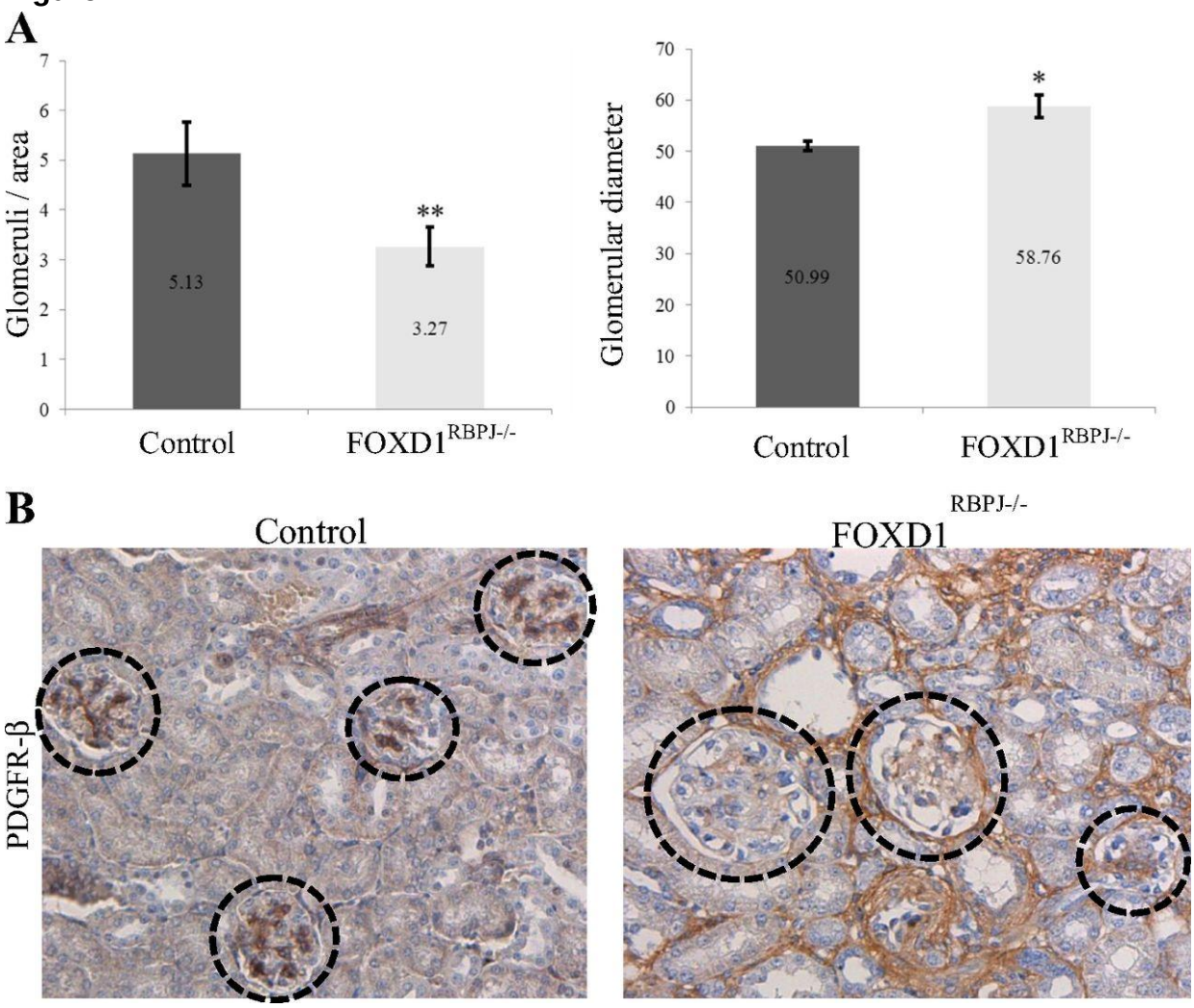

Figure 4.7: FOXD1$^{RBPJ-/-}$ adult mice have larger and fewer glomeruli, and lack mesangial cells. A) Quantification of glomerular size and number indicates on average fewer ($p<0.005$) but larger ($p<0.05$) glomeruli per region in FOXD1$^{RBPJ-/-}$ adult animals, indicating an incomplete glomerular complement accompanied by glomerular hypertrophy. B) A decrease in immunostaining for PDGFR-β in mutant glomeruli demonstrates that mesangial cells are absent in the glomeruli of FOXD1$^{RBPJ-/-}$ adults, as in newborn mutant animals. (performed by EEL)

Discussion

This study demonstrates that RBP-J, the final transcriptional effector of Notch signaling, is crucial for kidney vascular development, and indispensable for establishing the identity of the cells of the renal arterial mural cell layer and the glomerular mesangium. Lack of RBP-J in the FOXD1-positive precursor cell population results in kidneys with a significant decrease in the number of vessels. Remaining vessels show striking abnormalities, including a thinner smooth muscle cell layer, loss of renin cells, and eventually in the adult animal perivascular fibrosis and associated perivascular hypertrophy. In addition, we found that differentiation of mesangial cells within the glomerulus is also dependent upon RBP-J. In summary, our results indicate that differentiation of stromal FOXD1+ progenitors is severely disrupted by RBP-J deletion, resulting in abnormal development of the kidney vasculature and glomeruli.

While the role of Notch signaling and RBP-J with regards to endothelial cell differentiation and proliferation has been suggested by several investigators (28, 77, 78), less understood is the role that canonical Notch signaling, and thus RBP-J, plays in the recruitment of the smooth muscle cell coating as the endothelial layer is being established. Although it is known that downstream effectors of the Notch pathway directly bind to and regulate specific smooth muscle genes (79, 80), reports on the effects of Notch signaling on vascular smooth muscle have been contradictory. Studies variously suggest that Notch signaling can repress (79, 81, 82) or activate (83, 84), the smooth muscle cell program. The discrepancies in the data are likely due to a context-dependent effect of Notch signaling and interaction with other signaling pathways such as SRF/Myocardin (85) or TGF-β (86). Our data strongly suggests a requirement for RBP-J for the proper

development of the mural cell layer of the renal arteries. At day of birth, mice that lacked RBP-J in FOXD1-lineage cells displayed vessels that had a significantly thinner smooth muscle cell layer, indicating that RBP-J is necessary for proper recruitment and/or differentiation of the mural cell layer during intrauterine life. It would be interesting to define how early in the embryo RBP-J effect(s) in the renal vasculature become established. Similarly, whether this effect proceeds through canonical Notch signaling, and if so by which receptors and ligands, remains to be determined.

Interestingly, although the role of Notch signaling in endothelial cells regarding vascular branching is well established, we found that disruption of the Notch pathway in VSMCs through deletion of RBP-J also affects vascular patterning. Mutant mice lacking RBP-J in the vascular smooth muscle precursors exhibit a significant decrease in total vessel number (without a concomitant increase in uncoated vessels), as well as poor arteriolar branching. Also in support of a possible role of RBP-J in smooth muscle cells in vascular patterning, we note that FOXD1$^{RBPJ-/-}$ animals displayed a reduced complement of smaller-diameter vessels, corresponding to arterioles. Although there is evidence that suggests the identity of endothelial cells and vascular smooth muscle cells is established independently, as seen in the persistence of normal endothelial cell marker expression in instances of VSMC perturbation (87) or the EC-autonomous role of S1P1 signaling (88), there is increasing evidence for several possible mechanisms for VSMCs to affect vascular patterning. For example, direct signaling from VSMCs through nitric oxide production may play a vasoprotective role for endothelial cells and promote their survival (89). In addition, SMCs have proven to be key mediators of vascular remodeling after injury, as the perturbation of key VSMC genes can alter the response of the vasculature to injury (90).

Alternatively, the interaction of VSMCs with other cell types, such as monocytes (91), may induce the expression of key vascular growth factors. Our data supports a model in which signaling between the two cell types and their respective vascular layers may be necessary for proper vessel patterning.

In addition to the developmental defects mentioned above, we observed significant ongoing perivascular remodeling as the animals aged. At thirty days of postnatal life, around time of death, we found a marked expansion of proliferating alpha smooth muscle actin expressing cells surrounding defective arterioles, accompanied by increased interstitial collagen accumulation as indicated by Sirius red staining. The reason(s) for this additional reactive phenotype is not entirely clear. It is known that perivascular fibroblasts and pericytes descend from FOXD1-expressing progenitors. Thus absence of RBP-J in either or both these cell types may have led to a change in cell fate and expansion of the myofibroblast population, thus explaining the subsequent ongoing fibrosis seen in our animals. Alternatively, it is possible that the perivascular fibrosis is due to renal hypoperfusion resulting from abnormal vascular architecture and a lack of renin cells, and is thus a secondary, reparative phenotype resulting from the primary defect, the deletion of RBP-J. We have previously shown that mice with deletion of the renin gene or reduction in renal renin expression show a similar phenotype, with significant hypertrophy in areas surrounding renal vessels and regions of marked fibrosis, possibly due to tissue ischemia resulting from hypotension and renal hypoperfusion (7, 8, 56). It remains to be determined whether lack of RBP-J in the renal vascular and perivascular cells leads to a dysregulation of the pathways that control tissue oxygenation of the perivascular compartment.

The striking lack of renin cells in FOXD1$^{RBPJ-/-}$ animals also strongly supports our earlier studies demonstrating the integral role of RBP-J in the identity of the renin cells (21). However, we noted a more severe decrease in renin expression, as renin cells were nearly completely absent in FOXD1$^{RBPJ-/-}$ kidneys. Our data also showed an earlier depletion in renin cells, at day of birth in FOXD1$^{RBPJ-/-}$ animals, while deletion of RBP-J in renin cells did not cause an appreciable alteration in renin expression until adulthood (21). It is likely that deletion of RBP-J in the earlier progenitor cell, the FOXD1^{+} stromal cell, results in a more profound phenotype.

Deletion of RBP-J in FOXD1 cells also caused severe glomerular defects. Mutant glomeruli exhibited a range of phenotypes, either lacking mesangial cells, or lacking all of the interior cells including mesangium, podocytes and the glomerular tuft. This phenotype mimics the mesangial defects found in mice lacking platelet-derived growth factor-beta (PDGF-β) (92) or its receptor (93). It is unknown at this time, however, whether a lack of RBP-J causes a defect in the development of the entire glomerular tuft, or whether the primary defect is on mesangial cells, which are derived from the FOXD1-lineage stromal cells, and then the other cell types are subsequently lost due to lack of physical support and integrity. Interestingly, it has been shown that mice expressing a hypomorphic allele of Notch 2 exhibit improper differentiation and development of the glomerular capillaries and mesangial cells (94), which in combination with our data demonstrates an important role for Notch signaling in glomerular development. Later in life, glomeruli show signs of hypertrophy and glomerulosclerosis, as the kidney attempts to repair and compensate for the function lost due to the renal damage.

The cause(s) of the early mortality seen in FOXD1$^{RBPJ-/-}$ animals is currently unknown. The timing of the animals' death, corresponding with the maximum degree of observed kidney injury (glomerular aneurysms and sclerosis, vascular degeneration and scarring), implies that kidney failure plays a significant role. This conclusion is supported by limited urinalysis of FOXD1$^{RBPJ-/-}$ mice, which showed proteinuria and dilute urine (data not shown). However, it is known that Foxd1-lineage cells can be found in multiple other tissues, including the brain, retina, along with the lungs and the smooth muscle cells lining the aorta (unpublished data). Although we do not observe abnormalities in those tissues, it is possible that more subtle alterations to those organs could over time result in early death.

In summary, RBP-J regulates the fate of stromal FOXD1+ vascular progenitors and glomerular mesangium. Figure 4.8 illustrates the consequences of RBP-J deletion on this early progenitor. At day of birth, kidneys from FOXD1$^{RBPJ-/-}$ animals have fewer and thinner vessels, lack mesangial and renin cells, and have abnormal glomeruli with aberrant structure and glomerular aneurysms. By day 30 of life, these animals display an additional, possibly secondary and reactive phenotype in the kidney including perivascular fibrosis, glomerulosclerosis, tubular degeneration and early death.

Figure 4.8

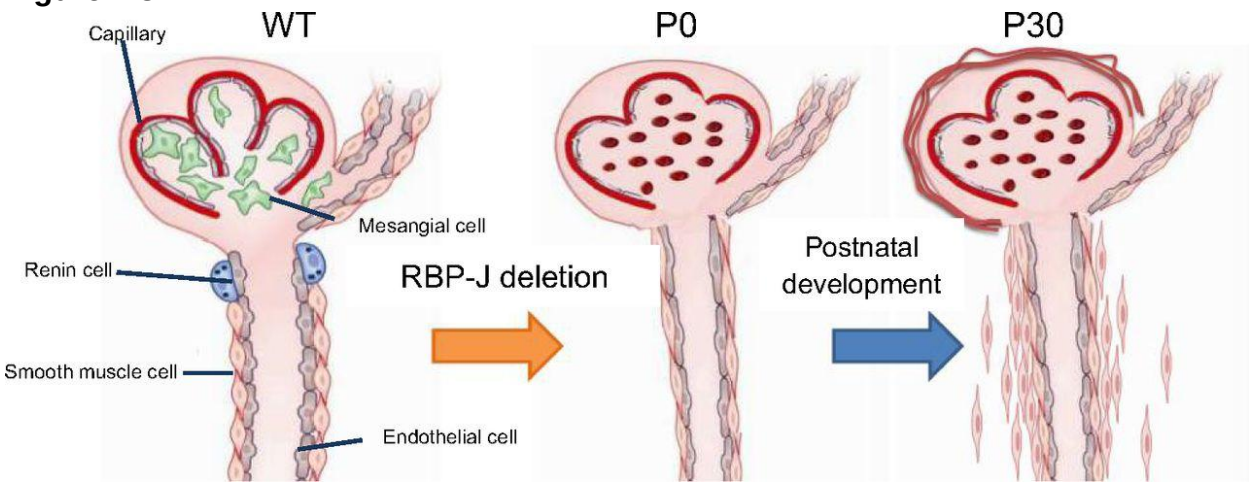

Figure 4.8: Deletion of RBP-J in the FOXD1-positive stromal precursors results in severe vascular and glomerular abnormalities. This figure summarizes our findings on the effects on the kidney upon RBP-J deletion in FOXD1-lineage cells at newborn (P0) and adult (P30) ages. FOXD1$^{RBPJ-/-}$ newborns have fewer arteries and arterioles with poor branching, accompanied by a decrease in vessel wall thickness. These animals also lack renin cells and glomerular mesangial cells. In adulthood, FOXD1$^{RBPJ-/-}$ adults also exhibit mural cell proliferation and fibrosis, accompanied by glomerulosclerosis and tubular degeneration.

Acknowledgments

We would like to thank Dr. Ellen S. Pentz for helping to revise the manuscript, PCR primer design, and for her excellent discussions and guidance. We gratefully acknowledge the work of Masafumi Oka in the dissection of the renal arterial trees. We would also like to thank Takele Yazew, Kimberly Hilsen and Cristina Monteagudo for excellent technical assistance. We acknowledge funding from National Institutes of Health Grants RO1 DK-091330 (to Sequeira-Lopez MLS) and R37 HL066242 and RO1 HL096735, the Center of Excellence in Pediatric Nephrology P50 DK096373 (to Gomez RA), and the American Heart Association Pre-doctoral Fellowship 13PRE16920043 (to Lin EE).

CHAPTER V: DISCUSSION

In this thesis we have identified the precursor cell for the mural cells of the renal arteries and the glomerular mesangium- the Foxd1-expressing renal stromal cells (Figure 5.1). In addition we have examined three key molecules involved in Foxd1 cell differentiation and function: Foxd1 itself, AKR1B7, and RBP-J. Here we speculate further on the potential roles of those proteins.

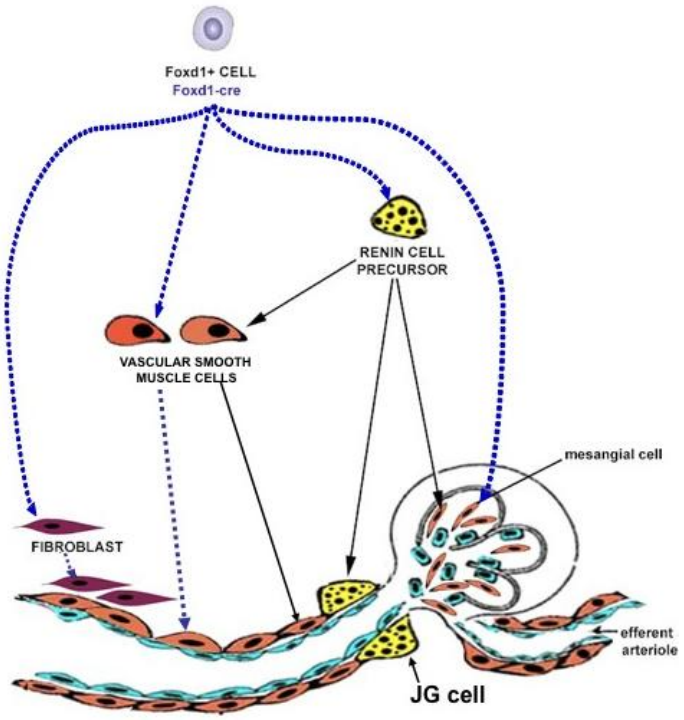

Fig. 5.1 Proposed model for the formation of the renal arteriole from Foxd1+ progenitor cells. Black solid arrows indicate current knowledge. Blue dashed arrows indicate the hypotheses we propose to test. The renin cell precursor gives rise to a subset of vascular SMCs.

What are the targets of Foxd1 in the kidney?

We have shown that Foxd1 itself plays a vital role in kidney development, particularly in the control of vascular patterning- deletion of Foxd1 resulted in ectopic arteries entering the kidney from various sites in the periphery, a reversal of their normal pattern. However, one important task is to identify the downstream molecules and pathways that are perturbed upon Foxd1 deletion and result in the vascular misguidance. The fact that deletion of Foxd1 cells (Foxd1-DTA) resulted in a near-phenocopy of the deletion of the Foxd1 gene strongly suggests that the proximal cause of the vascular phenotype is cell autonomous and that the signaling molecule(s) and pathway(s) perturbed upon Foxd1 deletion are intrinsic to the Foxd1 cell and not another cell type. However, the downstream targets of regulation by Foxd1, including the direct binding targets of the

Foxd1 transcription factor, are poorly studied, in particular those that control vascular patterning.

We have attempted multiple approaches to this problem. One method is to conduct ChIP-seq analysis to identify the gene promoters bound by Foxd1. We generated several antibodies against Foxd1, and we show immunostaining using them in the appendix of Supplementary Figure 2.1, indicating that the antibodies work for that purpose. To qualify the antibodies for ChIP we probed for Foxd1 binding against published targets of Foxd1 binding (PLGF (95), decorin (40), and $p27^{kip1}$ (96)). However, none of these assays displayed binding greater than background (data not shown). It is unknown at this time whether this is due to our antibodies being inadequate for ChIP analysis, or because Foxd1 does not actually bind the targets chosen in mice- the work done in identifying those targets was conducted *in vitro* and/or in other organisms. Work in this area is ongoing- either to identify other putative targets of Foxd1, or to directly test the Foxd1 antibodies for ChIP-seq capability.

Using *in silico* analysis several labs have identified a putative recognition sequence for Foxd1 (40, 97, 98). Although all the published sequences vary slightly, they all share the same core “GTAAACA” motif. Examining promoter regions for that sequence could identify potential targets of Foxd1. We have searched the promoters for several important SMC and renin cell genes- ACTA2, calponin, myosin heavy chain, renin and AKR1B7- for the core Foxd1 binding motif. None of those appear to have a Foxd1 binding site, which could be consistent with a lack of active Foxd1 expression in those cell types. Alternately, regulation of those genes by Foxd1 could be indirect and be mediated by other transcription factors such as SRF (99, 100).

Another approach to this problem would be to compare the gene expression profile of animals with deletion of the Foxd1 gene to those where Foxd1 is intact using RNA microarray analysis or RNA-seq. Previously, members of our lab conducted microarray analysis of whole kidney from Foxd1-null animals (unpublished data) and identified the most dysregulated genes in the kidney. We utilized this data to identify several that were at least two-fold increased or decreased have been shown to regulate angiogenesis (44): Slit3 (101), EphB4 (102, 103), ephrin B2 (104, 105), semaphorin 3a (105, 106), ephrin A6 (107), and ephrin 3a (108). Immunostaining revealed that the staining pattern for those proteins was not altered upon deletion of Foxd1, and in fact that none of those proteins were actively expressed in SMCs or mesangial cells. These findings highlight an important drawback to the way the experiment was conducted- the microarray analysis was done with whole kidney, as opposed to isolated Foxd1(-lineage) cells. Our lab and others have shown multiple secondary defects following Foxd1 deletion in cells outside the Foxd1-lineage (19), and thus the microarray data is subject to confounding variables by contributions from extra-lineage cells. This experiment is now planned to be done using specific isolation of GFP-positive Foxd1 lineage cells from $Foxd1^{cre/cre}$; mT/mG mice.

Are Foxd1 cells the bona-fide progenitors for arterial mural cells and mesangium?

The original purpose of the Foxd1-DTA experiment was to completely ablate the Foxd1 stromal cell and thus determine whether the Foxd1 cell is the required and essential progenitor for the mural cells and mesangium. However, lineage labeling clearly demonstrated that deletion of Foxd1 cells was mosaic in our Foxd1-DTA mice. Despite

the purported lethality of the DTA construct even at low levels of expression (34), a not-insignificant subset of Foxd1 cells survived the manipulation, as seen in the persistence of populations of mural cells and mesangial cells labeled with a Foxd1 lineage marker (Figure 2.8G). Particularly since our data suggests a possible extra-lineage contribution to the cell types that normally derive from Foxd1 cells (Figure 2.8H), it is worthwhile examining methods that could result in more complete Foxd1 cell ablation. One possibility would be to use the tamoxifen inducible Foxd1 cre mouse (B6;129S4-*Foxd1*$^{tm2(GFP/cre/ERT2)Amc}$/J, a gift from the McMahon laboratory), in hopes it would be a more efficient deleter than the standard Foxd1-cre. However, unpublished data generated in our lab using other cre recombinases (endothelial-SCL-Cre-ER(T), (109)), as well as work done in other labs (110, 111), has demonstrated that cre-mediated ablation of cells by DTA is mosaic and incomplete. It would also be possible to pursue other methods of cell ablation using other ribosomal inactivators such as saporin (112, 113), or employing other methods of deletion (for a review see (114)) in hopes that they would exhibit increased lethality in comparison to DTA.

One possible extra-Foxd1-lineage candidate that could serve as a progenitor for the smooth muscle cells and mesangium are the Cited1/Six2-lineage cap mesenchyme. Our lab and others (115) have reported that a small subset of proximal tubules report Foxd1 promoter activity using the Foxd1 R26R/mTmG reporter system. It is possible that these cells possess or retain the ability to differentiate into the downstream cell types of Foxd1 cells through their expression of Foxd1. To test this hypothesis, it may be possible to double immunostain for markers of Foxd1 lineage cells (α-SMA, PDGFR-

ß, et al.) and markers of the cap mesenchyme lineage, which may still be expressed after transdifferentiation.

What is the role of AKR1B7 in the kidney?

I speculate on several potential roles for AKR1B7 in chapter 3, including detoxification of the toxic byproducts of hormone synthesis, or prostaglandin synthesis to regulate renin release. AKR1B7 could also play a role in regulating the plasticity of the renin cell phenotype. AKR1B7 has been implicated as a regulatory factor in the differentiation of adipocytes *in vitro* (116). Mouse 3T3 cell cultures with the ability to differentiate into adipocytes showed a marked inhibition of this behavior when treated with siRNA or antisense RNA for AKR1B7. Thus, AKR1B7 could potentially also be involved in the phenotype transition of renin cells to smooth muscle cells, or vice versa. Interestingly, Pastel et al. also propose a role for AKR1B7 in obesogenesis related to its ability to synthesize prostaglandins (117). As it has been proposed that inhibition of the renin-angiotensin system can be protective against obesity (118), this suggests a link between renin cells, AKR1B7, and obesity.

A particular quirk about AKR1B7 may provide insight into a classic question about the renin cell. Despite renin being clearly and visibly stored in secretory granules, exocytic fusion of the vesicle with the exterior of the cell appears to be an extremely rare event, as determined using electron microscopy, and the mechanism of renin secretion is still debated (66, 119). So how does renin get out of the renin cell? Perhaps it would be informative to consider AKR1B7- in mice AKR1B7 is secreted in large amounts into the lumen of the vas deferens (the protein was first identified as “Mouse Vas Deferens Protein”, MVDP). Manin et al. show that this occurs through apocrine secretion (120),

where entire portions of the cell bud off to release the secretory materials (as an example, the mammary glands use this method to produce milk). It is certainly a stretch to compare AKR1B7 secretion into the vas deferens, which appears to occur only in the mouse (120), to renin secretion in the kidney, but given the tight co-regulation of the two genes perhaps the secretion processes are related.

How does RBP-J regulate the fate of the renal vasculature?

The final part of my thesis discusses the role of RBP-J in the differentiation of Foxd1-lineage stromal cells. Deletion of RBP-J in Foxd1 cells resulted in a striking loss of smooth muscle, renin and mesangial cells, in addition to defects in vascular branching. One important question is whether RBP-J acts through the Notch pathway to control the differentiation of Foxd1 cells, or if RBP-J is acting in a non-Notch-canonical manner. Singular deletion of Jagged 1, Notch 1, Notch 2, or Notch 3 was insufficient to cause any major disruption to the arterial mural cells or mesangium (Appendix A). It is possible that combinatorial deletion of one or more receptors and/or ligands will be necessary to evoke a phenotype, as multiple studies have demonstrated some degree of redundancy and/or compensation in the Notch pathway (121-123). Another possibility is to approach the problem at other points in the Notch pathway, such as the gamma secretase complex (124), which is responsible for cleavage of the NICD from the Notch extracellular domain. Inhibition could be done pharmacologically (125, 126) or through deletion of components of the complex such as presenilin (127, 128) or nicastrin (129), however, the enzyme has other roles in the cell and inhibition could cause unwanted side effects.

Xu et al. (130) report that mice with deletion of the transcription factor Tbx18 exhibit a decrease in smooth muscle cells and mesangial cells, accompanied by glomerular aneurysms, which replicates the phenotype of the RBP-J deletion in Foxd1 cells. Interestingly, it has been previously suggested that Tbx18 cooperates with the Notch pathway to control anterior/posterior patterning of the somites (131, 132). Whether Tbx18 interacts with the Notch pathway in the kidney remains to be determined. Microarray expression studies could demonstrate an epistatic relationship between the two genes, while co-IP experiments could identify a direct binding relationship between the two proteins.

Implications for human health

Over 26 million Americans currently suffer from renal disease, and nearly half a million are on dialysis due to kidney failure (133, 134). On a personal note, the author's country of origin, Taiwan, has some of the highest rates of end-stage renal disease in the world (135)[6]. Although chronic kidney disease commonly does not manifest until later in life, proper renal development in early life is crucial for normal adult kidney function, and abnormalities during ontogeny can lead to an increased susceptibility to kidney injury and disease in adulthood (136, 137). However, surprisingly little is known about the mechanisms that underlie prenatal and early childhood kidney disease, and the resulting implications over the course of a patient's life, and it is our hope that our findings will inform future studies in this area.

The phenotypes of the Foxd1-knockout, Foxd1-DTA, and Foxd1-RBPJ mice all fall within the broad spectrum of diseases encompassed by CAKUT, Congenital

[6] And my paternal grandfather passed away from complications following renal failure

Abnormalities of the Kidney and Urinary Tract (for a review see (138)). For example, the Foxd1-null mice exhibit characteristics of renal hypoplasia, multiple ectopic renal arteries, and horseshoe kidney, which are included within CAKUT. As another example, the Foxd1$^{RBPJ-/-}$ mice display renal hypodysplasia and glomerular aneurysms. The genetic architecture underlying CAKUT is complex and largely unknown (139, 140), and diagnosis, particularly pre-natally and peri-natally, is complicated and difficult. The genes identified in this thesis may be targets for therapy, or provide the background for the development of diagnostic tools such as gene testing or biomarkers (141, 142).

The Foxd1 protein is also expressed in humans, but its role in the kidney has not been examined. Work on human Foxd1 has thus far has been done *in vitro* and has largely focused on the role of Foxd1 as a proto-oncogene (96, 143). Interestingly, elevated Foxd1 expression was found in the cells from Clear cell sarcoma of the kidney (144), suggesting a role for Foxd1 in the human kidney. However these tumoral cells also expressed Cited1, a marker for cells which originate from the cap mesenchyme, so the appropriateness of Foxd1 as a specific lineage marker for stromal cells in the human kidney cannot be determined (particularly in light of what is probably an altered transcriptional profile following the induction of cancer). These works also strongly suggest that Foxd1 promotes cell proliferation, which would be in line with our data showing that kidneys in mice are hypoplastic following deletion of Foxd1.

Determining the exact role for AKR1B7 in renin cells could prove important to studies of human kidney function. The AKR1B7 protein is specific to mouse, but homologues are expressed in humans, notably AKR1B1 which shares an 82% sequence homology (145). Indeed, low levels of aldo-keto reductase have been reported in the human

kidney (146), raising the possibility that a member of the AKR super-family plays a role in human renal function. In addition, similar to AKR1B7 in renin-null mice, a homologue of AKR1B7 could identify renin-less renin cells in patients where renin expression is perturbed, such as humans suffering from tubular dysgenesis (147) or carrying a mutation of the renin gene. As our data shows that these cells contribute prominently in the resulting vascular pathology, examination of those cells in humans could provide insight into the phenotype.

Careful modulation of Notch signaling and RBP-J (CBF1 in humans) has been shown to be crucial for the maintenance of kidney architecture and function. Activation of the Notch pathway has been shown in hypertensive nephrosclerosis (148) and renal fibrosis (149, 150), while Notch signaling blockade has been shown to facilitate the formation of fibrosis/glomerulosclerosis and cysts (151, 152). In general, disruption of the Notch pathway, particularly mutations in the receptors and ligands, has been shown to play a crucial role in several developmental syndromes that result in negative renal consequences in childhood and adult life (153-155). Little study has been done regarding the role of Notch in the vascular compartment of the kidney. We note that CADASIL ("cerebral autosomal-dominant arteriopathy with subcortical infarcts and leukoencephalopathy), a disease caused by mutations of the *Notch 3* gene, results in degeneration of the smooth muscle cell layer in arteries, similar to that seen in Foxd1$^{RBPJ-/-}$ animals. It would be interesting to see if patients with CADASIL have abnormalities in their renal structure and function, and to determine if there are any resultant effects on renal function.

Closing Remarks

It is abundantly clear that Foxd1, RBP-J, and AKR1B7 are only a small part of the bigger picture of renal vascular formation and patterning. Thinking broadly, I[7] believe that the work done in my thesis touches on several important questions regarding vascular development.

One thing that always struck me when looking at microdissected renal vascular trees is how regular the vessel branching is. One question I would like to see addressed is to what degree the development of the renal vasculature is stereotyped. And what about the tubular nephrons as well? It was shown that lung development in mice, for all of its complex branching, is highly stereotyped, and that the fractal patterning could result from the input of only a few signaling molecules (156). Could the same be true for the kidney? This also led to another realization- I (and others) would posit that lung and kidney development are quite morphologically similar[8]. The branching morphogenesis characteristic of tubular development can be seen as analogous to the bronchi and bronchioles, the glomeruli to alveoli, and of course both organs possess a highly complex and critical vascular network. I would also mention that both lungs and kidneys express Foxd1 in their respective stromal cells, and that in both organs those cells differentiate into vascular pericytes! The two organs arise from different germ layers, but perhaps there are evolutionary links in how the organs develop. These questions would be best addressed using whole-organ imaging, where there have been many recent advances using novel clearing methods (157, 158). Currently, most whole-organ data

[7] Switching to first person here. The wild speculation that follows is completely the author's and probably something other lab members would want to avoid being affiliated with

[8] I would add that I've misidentified one as the other in whole embryo sections, and that this apparently isn't an uncommon error.

has been done with digital reconstruction of serial sections, which is slow, lossy, and labor-intensive.

As was discussed primarily in Chapter 2, there is usually a single site of entry for the vasculature into the kidney. I find it particularly remarkable that this setup is preserved in the kidney and for many other organs, but particularly so for the kidney as one of the primary drivers of vasculogenesis is hypoxia, and the environment of the kidney is especially hypoxic during development. Despite this, it is only following deletion of Foxd1 that there are multiple sites of vascular entry into the kidney, similar to humans with ectopic renal vessels, so I hypothesize that: A) the kidney capsule is not a sufficient physical barrier to vascular entry, and B) that some sort of repulsive cue is absent from the kidney capsule upon deletion of Foxd1 (as opposed to say, an attractant cue being expressed ectopically). This makes me first comment upon the need to study the cellular composition and proteins expressed in the kidney capsule. This structure is often ignored and was routinely discarded when processing the kidney, but clearly there is more to it than simple connective tissue. Second, I am also struck by the sharp demarcation (in wild-type animals), between the avascular (and aglomerular) kidney periphery and the rest of the kidney parenchyma. I've always found particularly compelling the classic work of Briscoe et al., which demonstrated that two transcription factors can directly inhibit each other in order to generate sharp boundaries, in this case for neuron guidance, from a chemical gradient (159). Perhaps a similar mechanism exists in the kidney periphery, in the very Foxd1-lineage cells that line the capsule. In addition, looking upstream, both the Foxd1 stromal precursors and the cap mesenchyme differentiate from the metanephric mesenchyme. How is this distinction

established? Do other transcription factors interact with Foxd1 and regulate its activity? It is clear that something is very strictly regulating Foxd1 expression temporally and spatially- I am still particularly struck by Supplementary Figure 2.1, which shows steady restriction of Foxd1 to “islands” of expression before completely disappearing. Is there any particular significance to the areas where Foxd1 expression persists later into renal development (“islands”) versus the rest of the kidney parenchyma? What is responsible for regulating Foxd1 expression?

Finally, I would like to see investigated in greater depth the contribution of the smooth muscle cell layer to vascular patterning. The conventional paradigm is that it is the differentiation, interaction (notably through the Notch pathway, for a review see (160)), and migration of endothelial cells that determines the vascular pattern. At the very least the endothelial cells are established before the smooth muscle layer- a full two days before in the kidney. However, the work done here and in other labs (161) strongly implicates a role for the smooth muscle cells in regulating vascular patterning. Do the smooth muscle cells provide signals for vascular guidance? Or is this simply a matter of smooth muscle cell-coated vessels preferentially surviving over non-muscularized arteries? Even better, are there any competition mechanics involved between nascent vessels?

So many questions, so little time. Fortunately or unfortunately, I’m (probably) not going to be the one who has to figure these things out. Much luck to whoever that ends up being.

(But no, seriously, look into the apocrine thing. I have a good feeling about it).

CHAPTER VI: MATERIALS AND METHODS

6.1 Mice and Genotyping

All mice were maintained in compliance with NIH guidelines and the Animal Care and Use Committee at the University of Virginia. Mice were either obtained from Jackson Laboratories or the referenced sources.

To understand the expression and regulation of AKR1B7 and renin, we studied mice with manipulations known to affect renin expression. Mice studied included wild-type c57B6 mice (Jackson Labs), and several genetically modified mouse strains including deletion of *aldosterone synthase* ($AS^{-/-}$), which displays a prominent increase in the number of renin cells along the arterioles (52), deletion of the micro-RNA processing enzyme Dicer in renin cells (*Dicer*$^{flox/del}$ *; Ren1d*$^{cre/+}$), which results in a severe decrease in renin cells (7), deletion of the renin gene (*Ren1c-KO*) (56), homozygous deletion of histone acetyl transferases CBP and P300 in renin cells (*CBP*$^{fl/fl}$ *x P300*$^{fl/fl}$ *x Ren1d*$^{cre/+}$), which shows a marked diminution of renin expression (48), ablation of renin cells with diphtheria toxin (*Ren1d-DTA*) (8), and expression of YFP driven by the Ren1c promoter (*Ren1c-YFP*), which reports activity of the renin promoter (49). A minimum of three animals per group were examined. Physiological challenge to induce increased renin expression was done using seven day treatment with captopril and administering a low-sodium diet as previously described (21).

To study the role of RBP-J in FOXD1-lineage cells, FOXD1$^{cre/+}$; RBP-J$^{fl/+}$ animals were crossed to RBP-J$^{fl/fl}$ animals to produce FOXD1$^{cre/+}$; RBP-J$^{fl/fl}$ animals (termed FOXD1$^{RBPJ-/-}$), at an expected Mendelian ratio of 25%. Control animals either lacked cre-recombinase (FOXD1$^{+/+}$; RBP-J$^{fl/fl}$), or had conditional deletion of only one RBP-J

allele (FOXD1$^{cre/+}$; RBP-J$^{+/fl}$). For lineage study, we crossed in the Rosa26 (R26R) allele by breeding FOXD1$^{cre/+}$; RBP-J$^{fl/+}$ animals with RBP-J$^{fl/fl}$; R26R$^{+/+}$ to produce FOXD1$^{cre/+}$; RBP-J$^{fl/fl}$; R26R$^{+/-}$animals (termed FOXD1$^{RBP\text{-}JcKO;R26R}$). RBP-J^{fl} mice were a kind gift of Dr. Tasuku Honjo, and FOXD1^{cre} animals were generated by the McMahon laboratory (10). R26R animals were obtained from Jackson Laboratories.

Genotyping was done using DNA isolated from tails, and sent to Transnetyx (Cordova, TN). Genotyping primers are provided when known in Supplementary Table 1.

6.2 Histologic Analysis and Immunostaining

Mice were anesthetized with tribromoethanol. Organs were removed, weighed, and either fixed in 2% paraformaldehyde (PFA) for 30 minutes for frozen sections or in Bouin's fixative overnight for paraffin sections.

Immunostaining was performed on 5 µm thick paraffin sections as previously described (16, 48). Briefly, slides were deparaffinized and rehydrated using a succession of xylenes and alcohols. Slides were exposed to 0.3% H_2O_2 for 30 minutes to extinguish endogenous peroxides. Antigen retrieval was carried out using a sodium citrate solution where noted in the table. Slides were blocked with 3% BSA in PBS, and then exposed to antibody either 2 hours RT or overnight at 4°C. Cells were incubated with the appropriate secondary antibodies using the appropriate Vectastain ABC kit (Vector Laboratories, Burlingame, CA). Sections were exposed to di-amino-benzidine for two minutes, and then counterstained with hematoxylin followed by blueing with Lithium Chloride.

To evaluate β-gal expression, mouse organs fixed in 2% PFA were cryoprotected in 30% sucrose in PBS then frozen in OCT (Miles, Elkhart, IL). Cryosections (7 µm) were cut using a Leica Cryocut 1800 cryostat, post-fixed in 0.2% PFA in 0.1 M PIPES (pH 6.9) at

4°C for 10 min, washed in PBS plus 2 mM MgCl2, incubated in detergent rinse (0.1 M phosphate buffer [pH 7.4], containing 2 mM MgCl2, 0.01% sodium deoxycholate, and 0.02% tergitol NP-40) for 10 min on ice, and placed in staining solution [detergent rinse, 5 mM $K_3Fe(CN)_6$, 5 mM $K_4Fe(CN)_6$ $3H_2O$, and 1 mg/ml 5-bromo-4-chloro-3-indolyl β-D-galactopyranoside (X-gal; Fisher Biotech) overnight in the dark at 37°C. The slides were post-fixed in 4% PFA in PBS at 4°C for 1 hr, dehydrated in graded alcohols to xylenes, and mounted with xylenes based mounting medium (Cytoseal XYL; Richard-Allen Scientific, Kalamazoo, MI). When β-gal staining was followed by immunohistochemistry,

slides were postfixed in Bouins for 5 min after the X-gal staining, rinsed in PBS, and then subjected to immunostaining (see above).

To evaluate GFP or RFP expression, organs were processed as previously described (17).

For examination of hemorrhages, Bouins fixed paraffin sections were stained with hematoxylin and eosin (6).

Quantification of renin positive areas, total kidney areas and α-SMA positive vascular areas was performed on 50X magnification images from 4 kidney sections per animal (2 controls and 4 *Foxd1-/-)* using a Leica MM AF powered by MetaMorph (Leica Microsystems, Version 1.5).

6.3 Cell Culture

To examine expression and regulation of AKR1B7 *in vitro,* we isolated and cultured CFP-expressing arterial smooth muscle cells of the renin lineage, which also carried a YFP-expressing renin promoter (CFP/YFP cells), as previously described (49). Cells were exposed to either 10 mM forskolin to stimulate cAMP production or DMSO vehicle

as previously described (49) every 24 hours until harvesting after 2 days, with an additional treatment 1 hour before harvest.

6.3 RT-PCR

RNA was isolated using the RNeasy Mini Kit (Qiagen), with 2 micrograms of RNA reverse transcribed to cDNA as previously described (162).

6.4 Single cell isolation from whole kidney

Kidneys were dissected from mice anesthetized with tribromoethanol. Kidneys were decapsulated and minced into a fine mash (<1mm^2 pieces) using a razor blade. Kidney homogenate was dissolved into a single cell suspension using an enzymatic solution of 0.1% collagenase A (Roche), 0.25% Trypsin (Sigma), and 0.02% DNAse (Life Technologies). Cells were filtered through successive cell strainers with pore diameters of 100 and then 40 microns (Millipore). Following RBC lysis, DAPI was added if necessary and cells were sorted into GFP+ and RFP+ populations using an Influx cell sorter (Becton, Dickinson and Company).

6.5 Renal arterial trees dissection

Kidneys attached to the aorta were dissected from embryos at E17.5 days of gestation and newborn mice an incubated in hydrochloric acid (6M at 42^{o}C) for 30 minutes. After incubation, the kidneys were washed several times with acidified water (pH 2.5). The arterial renal vasculature (arterial “tree”) was then carefully dissected from the aorta under direct stereoscopic visualization, using a pair of 20x1$^1/_2$ ” blunt needles attached to 1ml insulin syringes at an angle of 120^o

6.6 Morphometric measurements

The total kidney (or lung) to BW ratio is a computed value of the total weight of both kidneys (or lungs) in grams divided by the BW in grams.

1400 x 1200 μm fields of comparable kidney sections were examined, and all blood vessels and glomeruli within the area were counted. Vessel thickness was calculated as the difference between inner and outer vessel diameter as marked by staining for appropriate VSMC markers. Glomerular diameter was calculated as the average of the glomerulus at its widest point and on an axis perpendicular to that point. For newborn kidneys all fields within the kidney were counted, while for adults at least 5 fields per kidney were randomly selected and examined. Glomeruli were scored as “normal” or “abnormal” based on general morphology and staining/lack of staining for appropriate markers, while glomeruli filled with at least 50% red blood cells were classified as “RC-filled”.

6.7 Statistical analysis

qPCR experiments were performed in triplicate, and qPCR measurements were conducted three times per replicate. Results are presented as mean ± SEM. Statistical significance between 2 groups was determined by Student’s *t* test. A P value < 0.05 was considered significant.

CHAPTER VII: REFERENCES References

1. Srinivas S, Goldberg MR, Watanabe T, D'Agati V, al-Awqati Q, Costantini F. Expression of green fluorescent protein in the ureteric bud of transgenic mice: A new tool for the analysis of ureteric bud morphogenesis. *Dev Genet.* 1999; 24(3-4): 241-251.

2. Watanabe T, Costantini F. Real-time analysis of ureteric bud branching morphogenesis in vitro. *Dev Biol.* 2004 Jul 1; 271(1): 98-108.

3. Srinivas S, Watanabe T, Lin CS, William CM, Tanabe Y, Jessell TM, Costantini F. Cre reporter strains produced by targeted insertion of EYFP and ECFP into the ROSA26 locus. *BMC Dev Biol.* 2001; 1(1471-213): 4.

4. Kobayashi A, Valerius MT, Mugford JW, Carroll TJ, Self M, Oliver G, McMahon AP. Six2 defines and regulates a multipotent self-renewing nephron progenitor population throughout mammalian kidney development. *Cell Stem Cell.* 2008 08/07; 3(1875-9777; 2): 169-181.

5. Boyle S, Misfeldt A, Chandler KJ, Deal KK, Southard-Smith EM, Mortlock DP, Baldwin HS, de Caestecker M. Fate mapping using Cited1-CreERT2 mice demonstrates that the cap mesenchyme contains self-renewing progenitor cells and gives rise exclusively to nephronic epithelia. *Dev Biol.* 2008 Jan 1; 313(1): 234-245. PMCID: PMC2699557.

6. R.Ariel Gomez, Sequeira-Lopez ML. Vascular development of the kidney. In: Robert J.Tomanek, editor. Assembly of the vasculature and its regulation. Boston: Birkhauser; 2002. p. 193-210.

7. Sequeira-Lopez ML, Weatherford ET, Borges GR, Monteagudo MC, Pentz ES, Harfe BD, Carretero O, Sigmund CD, Gomez RA. The microRNA-processing enzyme dicer maintains juxtaglomerular cells. *J Am Soc Nephrol.* 2010 03; 21(1533-3450; 1046-6673; 3): 460-467.

8. Pentz ES, Moyano MA, Thornhill BA, Sequeira Lopez ML, Gomez RA. Ablation of renin-expressing juxtaglomerular cells results in a distinct kidney phenotype. *Am J Physiol Regul Integr Comp Physiol.* 2004 03; 286(0363-6119; 3): R474-R483.

9. Gomez RA, Norwood VF. Developmental consequences of the renin-angiotensin system. *Am J Kidney Dis.* 1995 09; 26(0272-6386; 3): 409-431.

10. Owens GK. Control of hypertrophic versus hyperplastic growth of vascular smooth muscle cells. *Am J Physiol.* 1989 12; 257(0002-9513; 6): H1755-H1765.

11. Carey AV, Carey RM, Gomez RA. Expression of alpha-smooth muscle actin in the developing kidney vasculature. *Hypertension.* 1992 02; 19(0194-911; 2): II168-II175.

12. Reddi V, Zaglul A, Pentz ES, Gomez RA. Renin-expressing cells are associated with branching of the developing kidney vasculature. *J Am Soc Nephrol.* 1998 01; 9(1046-6673; 1): 63-71.

13. Sequeira Lopez ML, Pentz ES, Robert B, Abrahamson DR, Gomez RA. Embryonic origin and lineage of juxtaglomerular cells. *Am J Physiol Renal Physiol.* 2001 08; 281(0363-6127; 2): F345-F356.

14. Robert B, St John PL, Abrahamson DR. Direct visualization of renal vascular morphogenesis in Flk1 heterozygous mutant mice. *Am J Physiol.* 1998 07; 275(0002-9513; 1): F164-F172.

15. Gomez RA, Chevalier RL, Everett AD, Elwood JP, Peach MJ, Lynch KR, Carey RM. Recruitment of renin gene-expressing cells in adult rat kidneys. *Am J Physiol.* 1990 10; 259(0002-9513; 4): F660-F665.

16. Sequeira Lopez ML, Pentz ES, Nomasa T, Smithies O, Gomez RA. Renin cells are precursors for multiple cell types that switch to the renin phenotype when homeostasis is threatened. *Dev Cell.* 2004 05; 6(1534-5807; 5): 719-728.

17. Kim HS, Maeda N, Oh GT, Fernandez LG, Gomez RA, Smithies O. Homeostasis in mice with genetically decreased angiotensinogen is primarily by an increased number of renin-producing cells. *J Biol Chem.* 1999 05/14; 274(0021-9258; 20): 14210-14217.

18. Brunskill EW, Sequeira-Lopez ML, Pentz ES, Lin E, Yu J, Aronow BJ, Potter SS, Gomez RA. Genes that confer the identity of the renin cell. *J Am Soc Nephrol.* 2011 12; 22(1533-3450; 1046-6673; 12): 2213-2225.

19. Hatini V, Tao W, Lai E. Expression of winged helix genes, BF-1 and BF-2, define adjacent domains within the developing forebrain and retina. *J Neurobiol.* 1994 Oct; 25(10): 1293-1309.

20. Hatini V, Huh SO, Herzlinger D, Soares VC, Lai E. Essential role of stromal mesenchyme in kidney morphogenesis revealed by targeted disruption of winged helix transcription factor BF-2. *Genes Dev.* 1996 06/15; 10(0890-9369; 12): 1467-1478.

21. Castellanos Rivera RM, Monteagudo MC, Pentz ES, Glenn ST, Gross KW, Carretero O, Sequeira-Lopez ML, Gomez RA. Transcriptional regulator RBP-J regulates the number and plasticity of renin cells. *Physiol Genomics.* 2011 09/08; 43(1531-2267; 1094-8341; 17): 1021-1028.

22. Schroeter EH, Kisslinger JA, Kopan R. Notch-1 signalling requires ligand-induced proteolytic release of intracellular domain. *Nature.* 1998 05/28; 393(0028-0836; 0028-0836; 6683): 382-386.

23. Kawaichi M, Oka C, Shibayama S, Koromilas AE, Matsunami N, Hamaguchi Y, Honjo T. Genomic organization of mouse J kappa recombination signal binding protein (RBP-J kappa) gene. *J Biol Chem.* 1992 02/25; 267(0021-9258; 0021-9258; 6): 4016-4022.

24. Tamura K, Taniguchi Y, Minoguchi S, Sakai T, Tun T, Furukawa T, Honjo T. Physical interaction between a novel domain of the receptor notch and the transcription factor RBP-J kappa/su(H). *Curr Biol.* 1995 12/01; 5(0960-9822; 0960-9822; 12): 1416-1423.

25. Honjo T. The shortest path from the surface to the nucleus: RBP-J kappa/su(H) transcription factor. *Genes Cells.* 1996 01; 1(1356-9597; 1356-9597; 1): 1-9.

26. Artavanis-Tsakonas S, Matsuno K, Fortini ME. Notch signaling. *Science.* 1995 04/14; 268(0036-8075; 0036-8075; 5208): 225-232.

27. de la Pompa JL, Wakeham A, Correia KM, Samper E, Brown S, Aguilera RJ, Nakano T, Honjo T, Mak TW, Rossant J, Conlon RA. Conservation of the notch signalling pathway in mammalian neurogenesis. *Development.* 1997 03; 124(0950-1991; 0950-1991; 6): 1139-1148.

28. Krebs LT, Xue Y, Norton CR, Shutter JR, Maguire M, Sundberg JP, Gallahan D, Closson V, Kitajewski J, Callahan R, Smith GH, Stark KL, Gridley T. Notch signaling is essential for vascular morphogenesis in mice. *Genes Dev.* 2000 06/01; 14(0890-9369; 11): 1343-1352.

29. Sequeira Lopez ML, Gomez RA. Development of the renal arterioles. *J Am Soc Nephrol.* 2011 12; 22(1533-3450; 1046-6673; 12): 2156-2165.

30. Schmidt-Ott KM, Chen X, Paragas N, Levinson RS, Mendelsohn CL, Barasch J. C-kit delineates a distinct domain of progenitors in the developing kidney. *Dev Biol.* 2006 11/01; 299(0012-1606; 0012-1606; 1): 238-249.

31. Humphreys BD, Lin SL, Kobayashi A, Hudson TE, Nowlin BT, Bonventre JV, Valerius MT, McMahon AP, Duffield JS. Fate tracing reveals the pericyte and not epithelial origin of myofibroblasts in kidney fibrosis. *Am J Pathol.* 2010 01; 176(1525-2191; 0002-9440; 1): 85-97.

32. Soriano P. Generalized lacZ expression with the ROSA26 cre reporter strain. *Nat Genet.* 1999 01; 21(1061-4036; 1): 70-71.

33. Muzumdar MD, Tasic B, Miyamichi K, Li L, Luo L. A global double-fluorescent cre reporter mouse. *Genesis.* 2007 09; 45(1526-954; 1526-954; 9): 593-605.

34. Wu S, Wu Y, Capecchi MR. Motoneurons and oligodendrocytes are sequentially generated from neural stem cells but do not appear to share common lineage-restricted progenitors in vivo. *Development.* 2006 02; 133(0950-1991; 0950-1991; 4): 581-590.

35. Hyink DP, Tucker DC, St John PL, Leardkamolkarn V, Accavitti MA, Abrass CK, Abrahamson DR. Endogenous origin of glomerular endothelial and mesangial cells in grafts of embryonic kidneys. *Am J Physiol.* 1996 05; 270(0002-9513; 5): F886-F899.

36. Lin EE, Sequeira-Lopez ML, Gomez RA. RBP-J in FOXD1+ renal stromal progenitors is crucial for the proper development and assembly of the kidney vasculature and glomerular mesangial cells. *Am J Physiol Renal Physiol.* 2014 01; 306(1522-1466; 1522-1466; 2): F249-F258.

37. Sims-Lucas S, Schaefer C, Bushnell D, Ho J, Logar A, Prochownik E, Gittes G, Bates CM. Endothelial progenitors exist within the kidney and lung mesenchyme. *PLoS One.* 2013; 8(1932-6203; 1932-6203; 6): e65993.

38. Levinson RS, Batourina E, Choi C, Vorontchikhina M, Kitajewski J, Mendelsohn CL. Foxd1-dependent signals control cellularity in the renal capsule, a structure required for normal renal development. *Development.* 2005 02; 132(0950-1991; 3): 529-539.

39. Das A, Tanigawa S, Karner CM, Xin M, Lum L, Chen C, Olson EN, Perantoni AO, Carroll TJ. Stromal-epithelial crosstalk regulates kidney progenitor cell differentiation. *Nat Cell Biol.* 2013 09; 15(1476-4679; 1465-7392; 9): 1035-1044.

40. Fetting JL, Guay JA, Karolak MJ, Iozzo RV, Adams DC, Maridas DE, Brown AC, Oxburgh L. FOXD1 promotes nephron progenitor differentiation by repressing decorin in the embryonic kidney. *Development.* 2014 01; 141(1477-9129; 0950-1991; 1): 17-27.

41. Liu J, Krautzberger AM, Sui SH, Hofmann OM, Chen Y, Baetscher M, Grgic I, Kumar S, Humphreys BD, Hide WA, McMahon AP. Cell-specific translational profiling in acute kidney injury. *J Clin Invest.* 2014 03/03; 124(1558-8238; 0021-9738; 3): 1242-1254.

42. Hum S, Rymer C, Schaefer C, Bushnell D, Sims-Lucas S. Ablation of the renal stroma defines its critical role in nephron progenitor and vasculature patterning. *PLoS One.* 2014; 9(1932-6203; 1932-6203; 2): e88400.

43. Carreres MI, Escalante A, Murillo B, Chauvin G, Gaspar P, Vegar C, Herrera E. Transcription factor Foxd1 is required for the specification of the temporal retina in mammals. *J Neurosci.* 2011 04/13; 31(1529-2401; 0270-6474; 15): 5673-5681.

44. Adams RH, Eichmann A. Axon guidance molecules in vascular patterning. *Cold Spring Harb Perspect Biol.* 2010 05; 2(1943-0264; 5): a001875.

45. Pailhoux E, Martinez A, Jean-Faucher C, Veyssiere G, Jean C. Lack of expression of the mRNA encoding a major protein of the mouse vas deferens after neonatal exposure to oestrogens. *J Mol Endocrinol.* 1991 Aug; 7(1): 63-69.

46. Aigueperse C, Martinez A, Lefrancois-Martinez AM, Veyssiere G, Jean CI. Cyclic AMP regulates expression of the gene coding for a mouse vas deferens protein related to the aldo-keto reductase superfamily in human and murine adrenocortical cells. *J Endocrinol.* 1999 01; 160(0022-0795; 0022-0795; 1): 147-154.

47. Pentz ES, Cordaillat M, Carretero OA, Tucker AE, Sequeira Lopez ML, Gomez RA. Histone acetyl transferases CBP and p300 are necessary for maintenance of renin cell identity and transformation of smooth muscle cells to the renin phenotype. *Am J Physiol Heart Circ Physiol.* 2012 06/15; 302(1522-1539; 0363-6135; 12): H2545-H2552.

48. Gomez RA, Pentz ES, Jin X, Cordaillat M, Sequeira Lopez ML. CBP and p300 are essential for renin cell identity and morphological integrity of the kidney. *Am J Physiol Heart Circ Physiol.* 2009 05; 296(0363-6135; 5): H1255-H1262.

49. Pentz ES, Sequeira Lopez ML, Cordaillat M, Gomez RA. Identity of the renin cell is mediated by cAMP and chromatin remodeling: An in vitro model for studying cell recruitment and plasticity. *Am J Physiol Heart Circ Physiol.* 2008 02; 294(0363-6135; 2): H699-H707.

50. Robillard JE, Weismann DN, Gomez RA, Ayres NA, Lawton WJ, VanOrden DE. Renal and adrenal responses to converting-enzyme inhibition in fetal and newborn life. *Am J Physiol.* 1983 02; 244(0002-9513; 2): R249-R256.

51. Gomez RA, Robillard JE. Developmental aspects of the renal responses to hemorrhage during converting-enzyme inhibition in fetal lambs. *Circ Res.* 1984 03; 54(0009-7330; 3): 301-312.

52. Lee G, Makhanova N, Caron K, Lopez ML, Gomez RA, Smithies O, Kim HS. Homeostatic responses in the adrenal cortex to the absence of aldosterone in mice. *Endocrinology.* 2005 06; 146(0013-7227; 6): 2650-2656.

53. Makhanova N, Sequeira-Lopez ML, Gomez RA, Kim HS, Smithies O. Disturbed homeostasis in sodium-restricted mice heterozygous and homozygous for aldosterone synthase gene disruption. *Hypertension.* 2006 12; 48(1524-4563; 6): 1151-1159.

54. Fransen JA. Lysosomal characteristics of human renin-containing granules. *Lab Invest.* 1987 Jan; 56(1): 124.

55. Taugner R, Metz R. Development and fate of the secretory granules of juxtaglomerular epithelioid cells. *Cell Tissue Res.* 1986; 246(3): 595-606.

56. Takahashi N, Lopez ML, Cowhig JE,Jr., Taylor MA, Hatada T, Riggs E, Lee G, Gomez RA, Kim HS, Smithies O. Ren1c homozygous null mice are hypotensive and polyuric, but heterozygotes are indistinguishable from wild-type. *J Am Soc Nephrol.* 2005 01; 16(1046-6673; 1): 125-132.

57. Seamon KB, Daly JW. Forskolin: A unique diterpene activator of cyclic AMP-generating systems. *J Cyclic Nucleotide Res.* 1981; 7(0095-1544; 0095-1544; 4): 201-224.

58. Thompson HA, Burson JM, Lang JA, Gross KW, Sigmund CD. Tissue-specific expression of novel messenger ribonucleic acids cloned from a renin-expressing kidney tumor cell line (As4.1). *Endocrinology.* 1995 07; 136(0013-7227; 7): 3037-3045.

59. Castellanos-Rivera RM, Pentz ES, Lin E, Gross KW, Medrano S, Yu J, Sequeira-Lopez ML, Gomez RA. Recombination signal binding protein for ig-kappaJ region regulates juxtaglomerular cell phenotype by activating the myo-endocrine program and suppressing ectopic gene expression. *J Am Soc Nephrol.* 2014 06/05(1533-3450; 1046-6673).

60. Medrano S, MC M, Sequeira-Lopez MLS, Pentz E.S., Gomez R.A. Two microRNAs -miR-330 and miR-125b-5p- mark the juxtaglomerular cell and balance its smooth muscle phenotype. *Am J Physiol Renal Physiol.* 2011; Oct 12. [Epub ahead of print].

61. Machura K, Iankilevitch E, Neubauer B, Theuring F, Kurtz A. The aldo-keto reductase AKR1B7 coexpresses with renin without influencing renin production and secretion. *Am J Physiol Renal Physiol.* 2013 Mar 1; 304(5): F578-84.

62. Martinez A, Aigueperse C, Val P, Dussault M, Tournaire C, Berger M, Veyssiere G, Jean C, Lefrancois MA. Physiological functions and hormonal regulation of mouse vas deferens protein (AKR1B7) in steroidogenic tissues. *Chem Biol Interact.* 2001 01/30; 130-132(0009-2797; 0009-2797; 1-3): 903-917.

63. Lefrancois-Martinez AM, Bertherat J, Val P, Tournaire C, Gallo-Payet N, Hyndman D, Veyssiere G, Bertagna X, Jean C, Martinez A. Decreased expression of cyclic adenosine monophosphate-regulated aldose reductase (AKR1B1) is associated with malignancy in human sporadic adrenocortical tumors. *J Clin Endocrinol Metab.* 2004 06; 89(0021-972; 0021-972; 6): 3010-3019.

64. Chevalier RL, Carey RM, Kaiser DL. Endogenous prostaglandins modulate autoregulation of renal blood flow in young rats. *Am J Physiol.* 1987 07; 253(0002-9513; 1): F66-F75.

65. Vander AJ. Direct effects of prostaglandin on renal function and renin release in anesthetized dog. *Am J Physiol.* 1968 Feb; 214(2): 218-221.

66. Schweda F, Kurtz A. Cellular mechanism of renin release. *Acta Physiol Scand.* 2004 08; 181(0001-6772; 4): 383-390.

67. Kabututu Z, Manin M, Pointud JC, Maruyama T, Nagata N, Lambert S, Lefrancois-Martinez AM, Martinez A, Urade Y. Prostaglandin F2alpha synthase activities of aldo-keto reductase 1B1, 1B3 and 1B7. *J Biochem.* 2009 02; 145(1756-2651; 0021-924; 2): 161-168.

68. Lambert-Langlais S, Pointud JC, Lefrancois-Martinez AM, Volat F, Manin M, Coudore F, Val P, Sahut-Barnola I, Ragazzon B, Louiset E, Delarue C, Lefebvre H, Urade Y, Martinez A. Aldo keto reductase 1B7 and prostaglandin F2alpha are regulators of adrenal endocrine functions. *PLoS ONE.* 2009; 4(1932-6203; 10): e7309.

69. Yu Y, Lucitt MB, Stubbe J, Cheng Y, Friis UG, Hansen PB, Jensen BL, Smyth EM, FitzGerald GA. Prostaglandin F2alpha elevates blood pressure and promotes atherosclerosis. *Proc Natl Acad Sci U S A.* 2009 May 12; 106(19): 7985-7990. PMCID: PMC2673134.

70. Whorton AR, Lazar JD, Smigel MD, Oates JA. Prostaglandins and renin release: III. effects of PGE1, E2 F2 alpha and D2 on renin release from rabbit renal cortical slices. *Prostaglandins.* 1981 Sep; 22(3): 455-468.

71. Sequeira Lopez ML, Gomez RA. Novel mechanisms for the control of renin synthesis and release. *Curr Hypertens Rep.* 2010 02; 12(1534-3111; 1522-6417; 1): 26-32.

72. Chen L, Faulhaber-Walter R, Wen Y, Huang Y, Mizel D, Chen M, Sequeira Lopez ML, Weinstein LS, Gomez RA, Briggs JP, Schnermann J. Renal failure in mice with gsalpha deletion in juxtaglomerular cells. *Am J Nephrol.* 2010; 32(1421-9670; 0250-8095; 1): 83-94.

73. Kato H, Sakai T, Tamura K, Minoguchi S, Shirayoshi Y, Hamada Y, Tsujimoto Y, Honjo T. Functional conservation of mouse notch receptor family members. *FEBS Lett.* 1996 10/21; 395(0014-5793; 0014-5793; 2-3): 221-224.

74. Shultz PJ, DiCorleto PE, Silver BJ, Abboud HE. Mesangial cells express PDGF mRNAs and proliferate in response to PDGF. *Am J Physiol.* 1988 10; 255(0002-9513; 0002-9513; 4): F674-F684.

75. Davisson RL, Kim HS, Krege JH, Lager DJ, Smithies O, Sigmund CD. Complementation of reduced survival, hypotension, and renal abnormalities in angiotensinogen-deficient mice by the human renin and human angiotensinogen genes. *J Clin Invest.* 1997 03/15; 99(0021-9738; 6): 1258-1264.

76. Matsusaka T, Fogo A, Ichikawa I. Targeting the genes of angiotensin receptors. *Semin Nephrol.* 1997 09; 17(0270-9295; 5): 396-403.

77. Dou GR, Wang YC, Hu XB, Hou LH, Wang CM, Xu JF, Wang YS, Liang YM, Yao LB, Yang AG, Han H. RBP-J, the transcription factor downstream of notch receptors, is essential for the maintenance of vascular homeostasis in adult mice. *FASEB J.* 2008 05; 22(1530-6860; 0892-6638; 5): 1606-1617.

78. Gridley T. Notch signaling in vascular development and physiology. *Development.* 2007 08; 134(0950-1991; 15): 2709-2718.

79. Morrow D, Scheller A, Birney YA, Sweeney C, Guha S, Cummins PM, Murphy R, Walls D, Redmond EM, Cahill PA. Notch-mediated CBF-1/RBP-J{kappa}-dependent regulation of human vascular smooth muscle cell phenotype in vitro. *Am J Physiol Cell Physiol.* 2005 11; 289(0363-6143; 0363-6143; 5): C1188-C1196.

80. Noseda M, Fu Y, Niessen K, Wong F, Chang L, McLean G, Karsan A. Smooth muscle alpha-actin is a direct target of notch/CSL. *Circ Res.* 2006 06/23; 98(1524-4571; 0009-7330; 12): 1468-1470.

81. Tang Y, Urs S, Liaw L. Hairy-related transcription factors inhibit notch-induced smooth muscle alpha-actin expression by interfering with notch intracellular domain/CBF-1 complex interaction with the CBF-1-binding site. *Circ Res.* 2008 03/28; 102(1524-4571; 0009-7330; 6): 661-668.

82. Proweller A, Pear WS, Parmacek MS. Notch signaling represses myocardin-induced smooth muscle cell differentiation. *J Biol Chem.* 2005 03/11; 280(0021-9258; 0021-9258; 10): 8994-9004.

83. Grieskamp T, Rudat C, Ludtke TH, Norden J, Kispert A. Notch signaling regulates smooth muscle differentiation of epicardium-derived cells. *Circ Res.* 2011 04/01; 108(1524-4571; 0009-7330; 7): 813-823.

84. Liu H, Zhang W, Kennard S, Caldwell RB, Lilly B. Notch3 is critical for proper angiogenesis and mural cell investment. *Circ Res.* 2010 10/01; 107(1524-4571; 0009-7330; 7): 860-870.

85. Du KL, Ip HS, Li J, Chen M, Dandre F, Yu W, Lu MM, Owens GK, Parmacek MS. Myocardin is a critical serum response factor cofactor in the transcriptional program regulating smooth muscle cell differentiation. *Mol Cell Biol.* 2003 04; 23(0270-7306; 7): 2425-2437.

86. Kennard S, Liu H, Lilly B. Transforming growth factor-beta (TGF- 1) down-regulates Notch3 in fibroblasts to promote smooth muscle gene expression. *J Biol Chem.* 2008 01/18; 283(0021-9258; 0021-9258; 3): 1324-1333.

87. Domenga V, Fardoux P, Lacombe P, Monet M, Maciazek J, Krebs LT, Klonjkowski B, Berrou E, Mericskay M, Li Z, Tournier-Lasserve E, Gridley T, Joutel A. Notch3 is

required for arterial identity and maturation of vascular smooth muscle cells. *Genes Dev.* 2004 11/15; 18(0890-9369; 22): 2730-2735.

88. Ben SA, Malkinson G, Krief S, Shwartz Y, Ely Y, Ferrara N, Yaniv K, Zelzer E. S1P1 inhibits sprouting angiogenesis during vascular development. *Development.* 2012 10; 139(1477-9129; 0950-1991; 20): 3859-3869.

89. de FT, de Miguel LS, Garcia-Duran M, Gonzalez-Fernandez F, Rodriguez-Feo JA, Monton M, Guerra J, Farre J, Casado S, Lopez-Farre A. NO from smooth muscle cells decreases NOS expression in endothelial cells: Role of TNF-alpha. *Am J Physiol.* 1999 10; 277(0002-9513; 0002-9513; 4): H1317-H1325.

90. Regan CP, Manabe I, Owens GK. Development of a smooth muscle-targeted cre recombinase mouse reveals novel insights regarding smooth muscle myosin heavy chain promoter regulation. *Circ Res.* 2000 09/01; 87(1524-4571; 5): 363-369.

91. Hojo Y, Ikeda U, Maeda Y, Takahashi M, Takizawa T, Okada M, Funayama H, Shimada K. Interaction between human monocytes and vascular smooth muscle cells induces vascular endothelial growth factor expression. *Atherosclerosis.* 2000 05; 150(0021-9150; 0021-9150; 1): 63-70.

92. Leveen P, Pekny M, Gebre-Medhin S, Swolin B, Larsson E, Betsholtz C. Mice deficient for PDGF B show renal, cardiovascular, and hematological abnormalities. *Genes Dev.* 1994 08/15; 8(0890-9369; 0890-9369; 16): 1875-1887.

93. Soriano P. Abnormal kidney development and hematological disorders in PDGF beta-receptor mutant mice. *Genes Dev.* 1994 08/15; 8(0890-9369; 0890-9369; 16): 1888-1896.

94. McCright B, Gao X, Shen L, Lozier J, Lan Y, Maguire M, Herzlinger D, Weinmaster G, Jiang R, Gridley T. Defects in development of the kidney, heart and eye vasculature in mice homozygous for a hypomorphic Notch2 mutation. *Development.* 2001 02; 128(0950-1991; 4): 491-502.

95. Zhang H, Palmer R, Gao X, Kreidberg J, Gerald W, Hsiao L, Jensen RV, Gullans SR, Haber DA. Transcriptional activation of placental growth factor by the forkhead/winged helix transcription factor FoxD1. *Curr Biol.* 2003 Sep 16; 13(18): 1625-1629.

96. Zhao YF, Zhao JY, Yue H, Hu KS, Shen H, Guo ZG, Su XJ. FOXD1 promotes breast cancer proliferation and chemotherapeutic drug resistance by targeting p27. *Biochem Biophys Res Commun.* 2015 Jan 2; 456(1): 232-237.

97. Pierrou S, Hellqvist M, Samuelsson L, Enerback S, Carlsson P. Cloning and characterization of seven human forkhead proteins: Binding site specificity and DNA bending. *EMBO J.* 1994 Oct 17; 13(20): 5002-5012. PMCID: PMC395442.

98. Balwierz PJ, Pachkov M, Arnold P, Gruber AJ, Zavolan M, van Nimwegen E. ISMARA: Automated modeling of genomic signals as a democracy of regulatory motifs. *Genome Research.* 2014 February 10.

99. Madsen CS, Regan CP, Owens GK. Interaction of CArG elements and a GC-rich repressor element in transcriptional regulation of the smooth muscle myosin heavy chain gene in vascular smooth muscle cells. *J Biol Chem.* 1997 11/21; 272(0021-9258; 47): 29842-29851.

100. Hautmann MB, Thompson MM, Swartz EA, Olson EN, Owens GK. Angiotensin II-induced stimulation of smooth muscle alpha-actin expression by serum response factor and the homeodomain transcription factor MHox. *Circ Res.* 1997 10; 81(0009-7330; 4): 600-610.

101. Paul JD, Coulombe KL, Toth PT, Zhang Y, Marsboom G, Bindokas VP, Smith DW, Murry CE, Rehman J. SLIT3-ROBO4 activation promotes vascular network formation in human engineered tissue and angiogenesis in vivo. *J Mol Cell Cardiol.* 2013 Nov; 64: 124-131. PMCID: PMC3885335.

102. Bai J, Wang YJ, Liu L, Zhao YL. Ephrin B2 and EphB4 selectively mark arterial and venous vessels in cerebral arteriovenous malformation. *J Int Med Res.* 2014 Apr; 42(2): 405-415.

103. Yang C, Guo Y, Jadlowiec CC, Li X, Lv W, Model LS, Collins MJ, Kondo Y, Muto A, Shu C, Dardik A. Vascular endothelial growth factor-A inhibits EphB4 and stimulates delta-like ligand 4 expression in adult endothelial cells. *J Surg Res.* 2013 Jul; 183(1): 478-486. PMCID: PMC3661748.

104. Wang HU, Chen ZF, Anderson DJ. Molecular distinction and angiogenic interaction between embryonic arteries and veins revealed by ephrin-B2 and its receptor eph-B4. *Cell.* 1998 May 29; 93(5): 741-753.

105. Gerety SS, Wang HU, Chen ZF, Anderson DJ. Symmetrical mutant phenotypes of the receptor EphB4 and its specific transmembrane ligand ephrin-B2 in cardiovascular development. *Mol Cell.* 1999 Sep; 4(3): 403-414.

106. Serini G, Valdembri D, Zanivan S, Morterra G, Burkhardt C, Caccavari F, Zammataro L, Primo L, Tamagnone L, Logan M, Tessier-Lavigne M, Taniguchi M, Puschel AW, Bussolino F. Class 3 semaphorins control vascular morphogenesis by inhibiting integrin function. *Nature.* 2003 Jul 24; 424(6947): 391-397.

107. Kozulin P, Natoli R, O'Brien KM, Madigan MC, Provis JM. Differential expression of anti-angiogenic factors and guidance genes in the developing macula. *Mol Vis.* 2009; 15: 45-59. PMCID: PMC2622716.

108. van Gils JM, Ramkhelawon B, Fernandes L, Stewart MC, Guo L, Seibert T, Menezes GB, Cara DC, Chow C, Kinane TB, Fisher EA, Balcells M, Alvarez-Leite J, Lacy-Hulbert A, Moore KJ. Endothelial expression of guidance cues in vessel wall homeostasis dysregulation under proatherosclerotic conditions. *Arterioscler Thromb Vasc Biol.* 2013 May; 33(5): 911-919. PMCID: PMC3647028.

109. Gothert JR, Gustin SE, van Eekelen JA, Schmidt U, Hall MA, Jane SM, Green AR, Gottgens B, Izon DJ, Begley CG. Genetically tagging endothelial cells in vivo: Bone marrow-derived cells do not contribute to tumor endothelium. *Blood.* 2004 09/15; 104(0006-4971; 0006-4971; 6): 1769-1777.

110. Sicking EM, Fuss A, Uhlig S, Jirak P, Dijkman H, Wetzels J, Engel DR, Urzynicok T, Heidenreich S, Kriz W, Kurts C, Ostendorf T, Floege J, Smeets B, Moeller MJ. Subtotal ablation of parietal epithelial cells induces crescent formation. *J Am Soc Nephrol.* 2012 Apr; 23(4): 629-640. PMCID: PMC3312496.

111. Golden JP, Demaro JA,3rd, Knoten A, Hoshi M, Pehek E, Johnson EM,Jr, Gereau RW,4th, Jain S. Dopamine-dependent compensation maintains motor behavior in mice with developmental ablation of dopaminergic neurons. *J Neurosci.* 2013 Oct 23; 33(43): 17095-17107. PMCID: PMC3807031.

112. Thorpe PE, Brown AN, Bremner JA,Jr, Foxwell BM, Stirpe F. An immunotoxin composed of monoclonal anti-thy 1.1 antibody and a ribosome-inactivating protein from saponaria officinalis: Potent antitumor effects in vitro and in vivo. *J Natl Cancer Inst.* 1985 Jul; 75(1): 151-159.

113. Goz D, Studholme K, Lappi DA, Rollag MD, Provencio I, Morin LP. Targeted destruction of photosensitive retinal ganglion cells with a saporin conjugate alters the effects of light on mouse circadian rhythms. *PLoS One.* 2008 Sep 5; 3(9): e3153. PMCID: PMC2519834.

114. Lewandoski M. Conditional control of gene expression in the mouse. *Nat Rev Genet.* 2001 Oct; 2(10): 743-755.

115. Kobayashi A, Mugford JW, Krautzberger AM, Naiman N, Liao J, McMahon AP. Identification of a multipotent self-renewing stromal progenitor population during mammalian kidney organogenesis. *Stem Cell Reports.* 2014 Oct 14; 3(4): 650-662. PMCID: PMC4223698.

116. Tirard J, Gout J, Lefrancois-Martinez AM, Martinez A, Begeot M, Naville D. A novel inhibitory protein in adipose tissue, the aldo-keto reductase AKR1B7: Its role in adipogenesis. *Endocrinology.* 2007 05; 148(0013-7227; 0013-7227; 5): 1996-2005.

117. Pastel E, Pointud JC, Loubeau G, Dani C, Slim K, Martin G, Volat F, Sahut-Barnola I, Val P, Martinez A, Lefrancois-Martinez AM. Aldose reductases influence

prostaglandin F2alpha levels and adipocyte differentiation in male mouse and human species. *Endocrinology.* 2015 May; 156(5): 1671-1684.

118. Kalupahana NS, Moustaid-Moussa N. The renin-angiotensin system: A link between obesity, inflammation and insulin resistance. *Obes Rev.* 2012 Feb; 13(2): 136-149.

119. Peti-Peterdi J, Fintha A, Fuson AL, Tousson A, Chow RH. Real-time imaging of renin release in vitro. *Am J Physiol Renal Physiol.* 2004 Aug; 287(2): F329-35.

120. Manin M, Lecher P, Martinez A, Tournadre S, Jean C. Exportation of mouse vas deferens protein, a protein without a signal peptide, from mouse vas deferens epithelium: A model of apocrine secretion. *Biol Reprod.* 1995 01; 52(0006-3363; 0006-3363; 1): 50-62.

121. Kokubo H, Miyagawa-Tomita S, Nakazawa M, Saga Y, Johnson RL. Mouse hesr1 and hesr2 genes are redundantly required to mediate notch signaling in the developing cardiovascular system. *Dev Biol.* 2005 Feb 15; 278(2): 301-309.

122. Nobta M, Tsukazaki T, Shibata Y, Xin C, Moriishi T, Sakano S, Shindo H, Yamaguchi A. Critical regulation of bone morphogenetic protein-induced osteoblastic differentiation by Delta1/Jagged1-activated Notch1 signaling. *J Biol Chem.* 2005 Apr 22; 280(16): 15842-15848.

123. Sieger D, Tautz D, Gajewski M. The role of suppressor of hairless in notch mediated signalling during zebrafish somitogenesis. *Mech Dev.* 2003 Sep; 120(9): 1083-1094.

124. De SB, Annaert W, Cupers P, Saftig P, Craessaerts K, Mumm JS, Schroeter EH, Schrijvers V, Wolfe MS, Ray WJ, Goate A, Kopan R. A presenilin-1-dependent gamma-secretase-like protease mediates release of notch intracellular domain. *Nature.* 1999 04/08; 398(0028-0836; 0028-0836; 6727): 518-522.

125. Olsauskas-Kuprys R, Zlobin A, Osipo C. Gamma secretase inhibitors of notch signaling. *Onco Targets Ther.* 2013 Jul 23; 6: 943-955. PMCID: PMC3726525.

126. Imbimbo BP. Therapeutic potential of gamma-secretase inhibitors and modulators. *Curr Top Med Chem.* 2008; 8(1): 54-61.

127. Tamboli IY, Prager K, Thal DR, Thelen KM, Dewachter I, Pietrzik CU, St George-Hyslop P, Sisodia SS, De Strooper B, Heneka MT, Filippov MA, Muller U, van Leuven F, Lutjohann D, Walter J. Loss of gamma-secretase function impairs endocytosis of lipoprotein particles and membrane cholesterol homeostasis. *J Neurosci.* 2008 Nov 12; 28(46): 12097-12106.

128. Dewachter I, Reverse D, Caluwaerts N, Ris L, Kuiperi C, Van den Haute C, Spittaels K, Umans L, Serneels L, Thiry E, Moechars D, Mercken M, Godaux E, Van Leuven F. Neuronal deficiency of presenilin 1 inhibits amyloid plaque formation and corrects hippocampal long-term potentiation but not a cognitive defect of amyloid precursor protein [V717I] transgenic mice. *J Neurosci.* 2002 May 1; 22(9): 3445-3453.

129. Klinakis A, Lobry C, bdel-Wahab O, Oh P, Haeno H, Buonamici S, van DW,I, Cathelin S, Trimarchi T, Araldi E, Liu C, Ibrahim S, Beran M, Zavadil J, Efstratiadis A, Taghon T, Michor F, Levine RL, Aifantis I. A novel tumour-suppressor function for the notch pathway in myeloid leukaemia. *Nature.* 2011 05/12; 473(1476-4687; 0028-0836; 7346): 230-233.

130. Xu J, Nie X, Cai X, Cai CL, Xu PX. Tbx18 is essential for normal development of vasculature network and glomerular mesangium in the mammalian kidney. *Dev Biol.* 2014 Jul 1; 391(1): 17-31. PMCID: PMC4038151.

131. Farin HF, Mansouri A, Petry M, Kispert A. T-box protein Tbx18 interacts with the paired box protein Pax3 in the development of the paraxial mesoderm. *J Biol Chem.* 2008 Sep 12; 283(37): 25372-25380.

132. Bussen M, Petry M, Schuster-Gossler K, Leitges M, Gossler A, Kispert A. The T-box transcription factor Tbx18 maintains the separation of anterior and posterior somite compartments. *Genes Dev.* 2004 May 15; 18(10): 1209-1221. PMCID: PMC415645.

133. U.S. renal data system, USRDS 2014 annual data report: Atlas of end-stage renal disease in the united states. National Institutes of Health, National Institute of Diabetes and Digestive and Kidney Disease, Bethesda, MD; 2014.

134. Coresh J, Selvin E, Stevens LA, Manzi J, Kusek JW, Eggers P, Van Lente F, Levey AS. Prevalence of chronic kidney disease in the united states. *JAMA.* 2007 Nov 7; 298(17): 2038-2047.

135. Hwang SJ, Tsai JC, Chen HC. Epidemiology, impact and preventive care of chronic kidney disease in taiwan. *Nephrology (Carlton).* 2010 Jun; 15 Suppl 2: 3-9.

136. Moritz KM, Singh RR, Probyn ME, Denton KM. Developmental programming of a reduced nephron endowment: More than just a baby's birth weight. *Am J Physiol Renal Physiol.* 2009 Jan; 296(1): F1-9.

137. Sanna-Cherchi S, Ravani P, Corbani V, Parodi S, Haupt R, Piaggio G, Innocenti ML, Somenzi D, Trivelli A, Caridi G, Izzi C, Scolari F, Mattioli G, Allegri L, Ghiggeri GM. Renal outcome in patients with congenital anomalies of the kidney and urinary tract. *Kidney Int.* 2009 Sep; 76(5): 528-533.

138. dos Santos Junior AC, de Miranda DM, Simoes e Silva AC. Congenital anomalies of the kidney and urinary tract: An embryogenetic review. *Birth Defects Res C Embryo Today.* 2014 Dec; 102(4): 374-381.

139. Fassett RG, Venuthurupalli SK, Gobe GC, Coombes JS, Cooper MA, Hoy WE. Biomarkers in chronic kidney disease: A review. *Kidney Int.* 2011 Oct; 80(8): 806-821.

140. - de Geus HRH, - Betjes MG, - Bakker J. - Biomarkers for the prediction of acute kidney injury: A narrative review on current status and future challenges. - *Clinical Kidney Journal.* (- 2): - 102.

141. Jetton JG, Askenazi DJ. Acute kidney injury in the neonate. *Clin Perinatol.* 2014 Sep; 41(3): 487-502.

142. Mussap M, Noto A, Fanos V, Van Den Anker JN. Emerging biomarkers and metabolomics for assessing toxic nephropathy and acute kidney injury (AKI) in neonatology. *Biomed Res Int.* 2014; 2014: 602526. PMCID: PMC4071811.

143. Nakayama S, Soejima K, Yasuda H, Yoda S, Satomi R, Ikemura S, Terai H, Sato T, Yamaguchi N, Hamamoto J, Arai D, Ishioka K, Ohgino K, Naoki K, Betsuyaku T. FOXD1 expression is associated with poor prognosis in non-small cell lung cancer. *Anticancer Res.* 2015 Jan; 35(1): 261-268.

144. Karlsson J, Holmquist Mengelbier L, Ciornei CD, Naranjo A, O'Sullivan MJ, Gisselsson D. Clear cell sarcoma of the kidney demonstrates an embryonic signature indicative of a primitive nephrogenic origin. *Genes Chromosomes Cancer.* 2014 May; 53(5): 381-391. PMCID: PMC4334316.

145. Pailhoux E, Veyssiere G, Fabre S, Tournaire C, Jean C. The genomic organization and DNA sequence of the mouse vas deferens androgen-regulated protein gene. *J Steroid Biochem Mol Biol.* 1992 07; 42(0960-0760; 0960-0760; 6): 561-568.

146. Lau ET, Cao D, Lin C, Chung SK, Chung SS. Tissue-specific expression of two aldose reductase-like genes in mice: Abundant expression of mouse vas deferens protein and fibroblast growth factor-regulated protein in the adrenal gland. *Biochem J.* 1995 Dec 1; 312 (Pt 2)(Pt 2): 609-615. PMCID: PMC1136305.

147. Gubler MC, Antignac C. Renin-angiotensin system in kidney development: Renal tubular dysgenesis. *Kidney Int.* 2010 Mar; 77(5): 400-406.

148. Lavoz C, Droguett A, Burgos ME, Carpio DJ, Ortiz A, Egido J, Mezzano S, Ruiz-Ortega M. Translational study of the notch pathway in hypertensive nephropathy. *Nefrologia.* 2014 May 21; 34(3): 369-376.

149. Lavoz C, Rodrigues-Diez R, Benito-Martin A, Rayego-Mateos S, Rodrigues-Diez RR, Alique M, Ortiz A, Mezzano S, Egido J, Ruiz-Ortega M. Angiotensin II contributes to

renal fibrosis independently of notch pathway activation. *PLoS One.* 2012; 7(7): e40490. PMCID: PMC3392235.

150. Sirin Y, Susztak K. Notch in the kidney: Development and disease. *J Pathol.* 2012 01; 226(1096-9896; 0022-3417; 2): 394-403.

151. Sanchez-Nino MD, Ortiz A. Notch3 and kidney injury: Never two without three. *J Pathol.* 2012 Nov; 228(3): 266-273.

152. Barak H, Surendran K, Boyle SC. The role of notch signaling in kidney development and disease. *Adv Exp Med Biol.* 2012; 727: 99-113.

153. Martin BM, Ivanova MH, Sarukhanov A, Kim A, Power P, Pugash D, Popescu OE, Lachman RS, Krakow D, Patel MS. Prenatal and postnatal findings in serpentine fibula polycystic kidney syndrome and a review of the NOTCH2 spectrum disorders. *Am J Med Genet A.* 2014 Oct; 164A(10): 2490-2495.

154. Kamath BM, Spinner NB, Rosenblum ND. Renal involvement and the role of notch signalling in alagille syndrome. *Nat Rev Nephrol.* 2013 Jul; 9(7): 409-418.

155. Penton AL, Leonard LD, Spinner NB. Notch signaling in human development and disease. *Semin Cell Dev Biol.* 2012 Jun; 23(4): 450-457. PMCID: PMC3638987.

156. Metzger RJ, Klein OD, Martin GR, Krasnow MA. The branching programme of mouse lung development. *Nature.* 2008 Jun 5; 453(7196): 745-750. PMCID: PMC2892995.

157. Yang B, Treweek JB, Kulkarni RP, Deverman BE, Chen CK, Lubeck E, Shah S, Cai L, Gradinaru V. Single-cell phenotyping within transparent intact tissue through whole-body clearing. *Cell.* 2014 Aug 14; 158(4): 945-958. PMCID: PMC4153367.

158. Chung K, Deisseroth K. CLARITY for mapping the nervous system. *Nat Methods.* 2013 Jun; 10(6): 508-513.

159. Briscoe J, Pierani A, Jessell TM, Ericson J. A homeodomain protein code specifies progenitor cell identity and neuronal fate in the ventral neural tube. *Cell.* 2000 May 12; 101(4): 435-445.

160. Hofmann JJ, Iruela-Arispe ML. Notch signaling in blood vessels: Who is talking to whom about what? *Circ Res.* 2007 Jun 8; 100(11): 1556-1568.

161. Hurtado R, Zewdu R, Mtui J, Liang C, Aho R, Kurylo C, Selleri L, Herzlinger D. Pbx1 dependent control of VMC differentiation kinetics underlies gross renal vascular patterning. *Development.* 2015 Jul 2.

162. Sequeira Lopez ML, Chernavvsky DR, Nomasa T, Wall L, Yanagisawa M, Gomez RA. The embryo makes red blood cell progenitors in every tissue simultaneously with blood vessel morphogenesis. *Am J Physiol Regul Integr Comp Physiol.* 2003 04; 284(0363-6119; 4): R1126-R1137.

APPENDIX 1: The role of Notch pathway receptors and ligands in the differentiation of Foxd1-lineage cells

We have previously shown that RBP-J, the shared transcriptional mediator for the various Notch receptors and ligands, is required for proper differentiation of Foxd1+ stromal precursor cells into downstream cell types- arterial mural cells and mesangial cells. However, RBP-J has been shown to have roles outside canonical Notch signaling, particularly as a repressor. To explore the role of the Notch pathway in the differentiation of Foxd1 cells, and to determine which particular Notch receptors and ligands are expressed in Foxd1 cells and their derivatives, we conducted PCR analysis of FACS-isolated Foxd1 cells in newborn and adult life. Attempted amplification of transcripts for the Notch receptors (1-4) and ligands (Delta-like 1, 3, 4, and Jagged 1 and 2) in isolated Foxd1 cells revealed the expression of Notch 1-3 and Jagged 1 in newborn animals, and continued expression of Notch 3 in adult life. Previous work in our lab showed that global deletion of Notch3 had no discernable kidney vascular phenotype (unpublished data, not shown). To investigate the function of the remaining receptors (Notch 1 and 2) and ligand (Jagged 1), we used the cre-lox system to individually delete those proteins in Foxd1 cells (Figure 3). Deletion of Notch 1 (FOXD1-cre ; Notch1 $^{fl/del}$) did not result in any changes to SMC or mesangial cell endowment or patterning. Deletion of Notch 2 in Foxd1-lineage cells (FOXD1-cre ; Notch 2 $^{fl/del}$) resulted in a mild phenotype of small numbers of arteries and glomeruli lying directly underneath the renal capsule, reminiscent of the phenotype upon deletion of Foxd1, but not nearly to the same degree. Deletion of Jagged 1 in Foxd1-lineage cells (Foxd1-cre ; Jagged1 $^{fl/fl}$) did not result in any changes to SMC or mesangial cell endowment or

patterning. Thus we find that Notch 1-3 and Jagged 1 are individually dispensable within Foxd1 cells.

Interestingly, deletion of Notch 2 in a subset of Foxd1 cells, the renin cells (Ren1d-cre ; Notch 2 $^{del/fl}$), resulted in areas of focal renal fibrosis and tubular dilation, as shown using alpha actin staining (Figure 4, top). These effects were exacerbated with age, and resulted in kidney damage accompanied by elevated blood urea nitrogen (control: 29±1.31 mg/dL (n=11) vs Ren1d-cre ; Notch 2 $^{del/fl}$ 35±1.27 mg/dL (n=15; $p<0.01$)) and hydronephrosis. In addition, renin was seen extending from the glomerulus in a recapitulation of the embryonic phenotype (Figure 4, bottom). However, plasma renin levels were not significantly different. No effect was found regarding the endowment of mural cells or mesangial cells. We conclude that Notch 2 in renin cells plays a role in maintenance of normal kidney morphology.

Appendix A, Figure 1

Protein	Result
Receptors	
Notch 1	Faint expression
Notch 2	Expression mostly during newborn life
Notch 3	Expression in newborn and adult life
Notch 4	Negative
Ligands	
Jagged 1	Faint expression in newborns
Jagged 2	Negative
Dll1	Negative
Dll3	Negative
Dll4	Negative

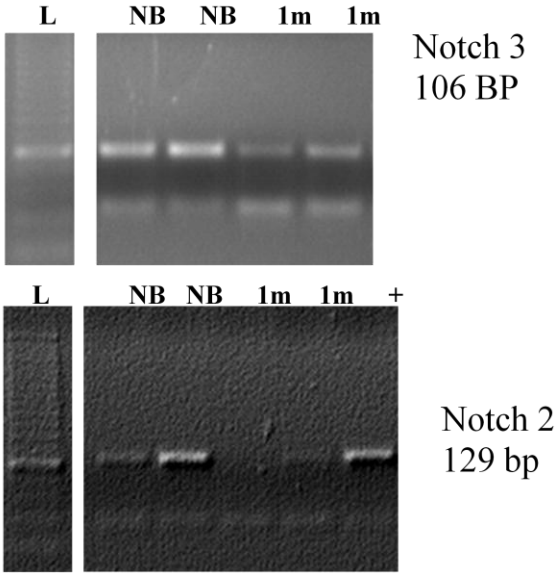

Figure A1: Foxd1-lineage cells express various ligands and receptors of the Notch pathway. mRNA was isolated from FACS-isolated Foxd1-lineage cells, and probed for expression of Notch pathway ligands and receptors using RT-PCR. Left panel: chart of the expression of elements of the Notch pathway. Right panel: sample PCR gels. (Performed by EEL)

Appendix A, Figure 2

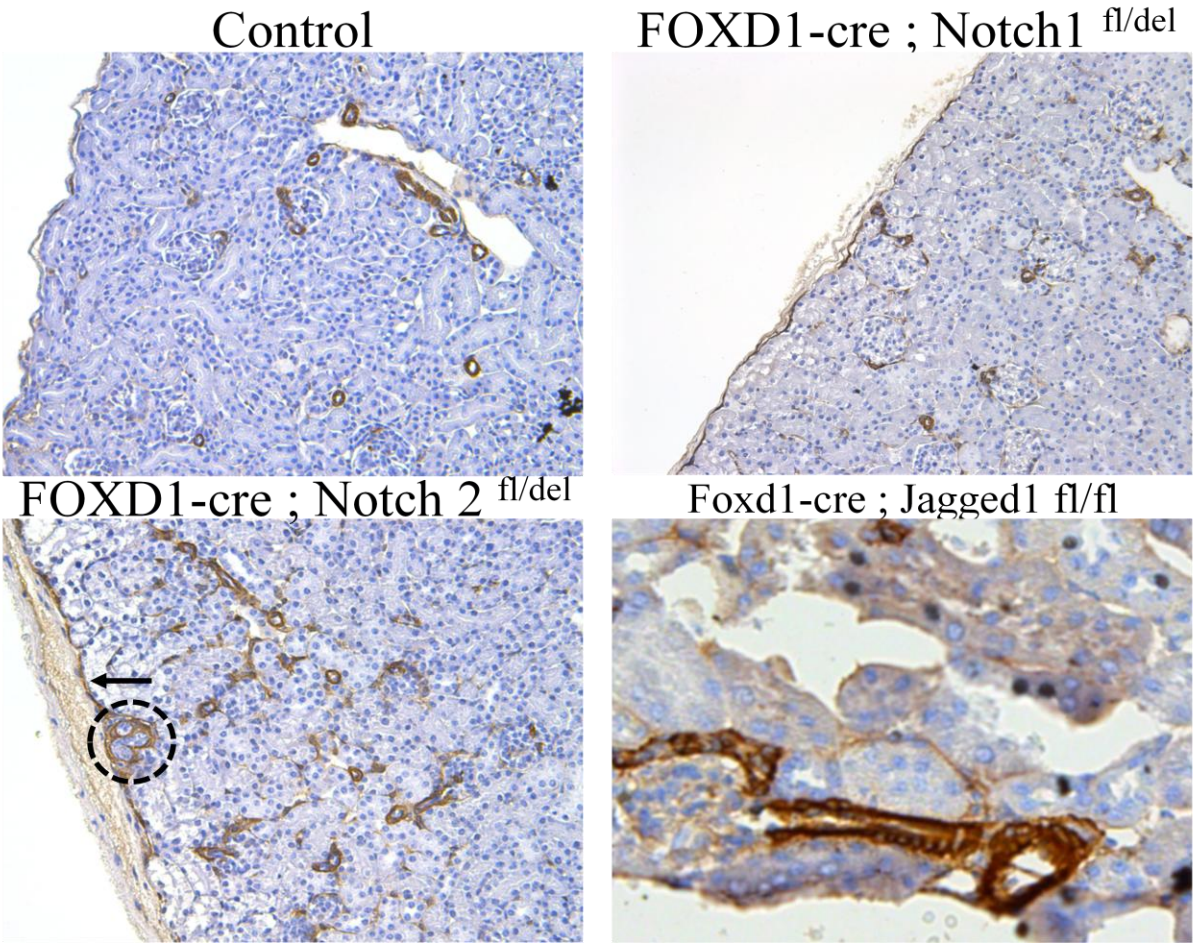

Figure A2: Individually, Notch 1, Notch 2, and Jagged 1 are largely dispensible for Foxd1 cell differentiation. The cre-lox system was used to delete Notch 1, Notch 2, and Jagged 1 in Foxd1 cells. Staining with alpha actin showed that deletion of Notch 1 resulted in no phenotype within the kidney vasculature. Deletion of Notch 2 resulted in a small number of subcapsular glomeruli (circle) and arteries (arrow). Kidney section of an animal with deletion of Jagged 1 in renin cells (high power view), shows a healthy artery with properly formed smooth muscle cells. (Performed by Ellen Pentz)

Appendix A, Figure 3

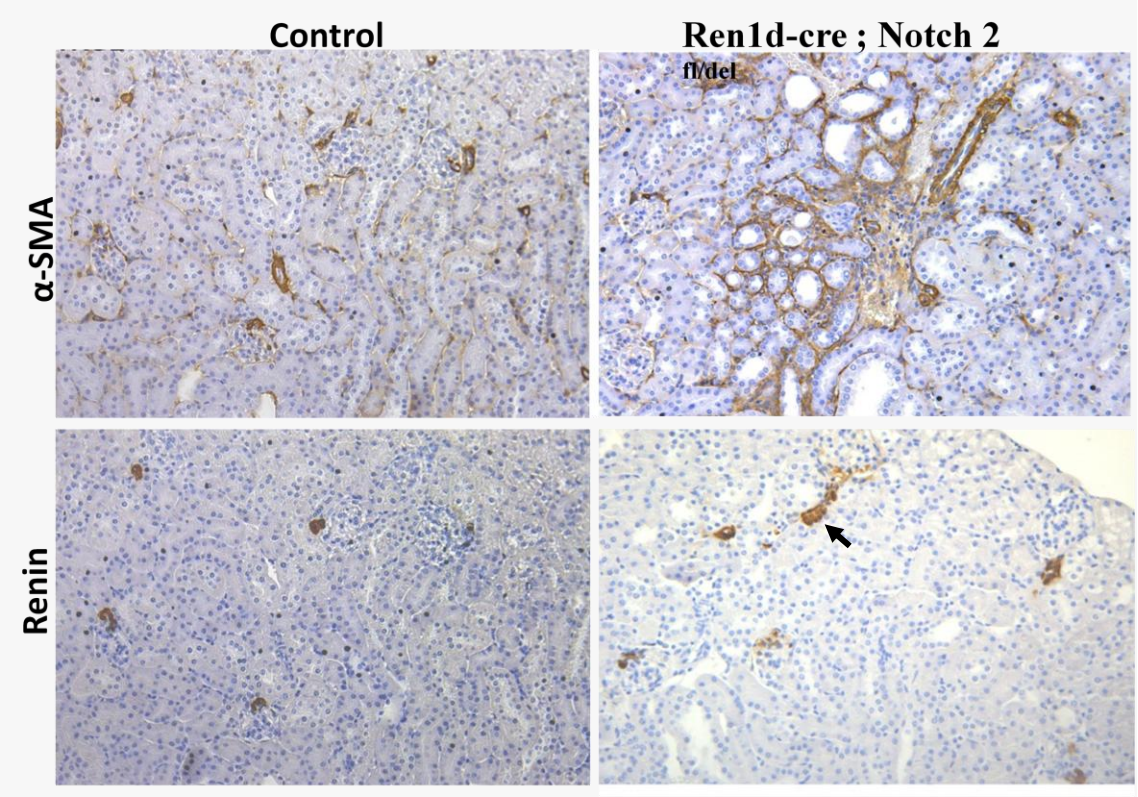

Figure A3: Deletion of Notch 2 in renin cells results in focal renal fibrosis and extension of renin expression along kidney arterioles. Staining with α-SMA (top panels) shows focal areas of active fibrosis in the renal parenchyma of animals with deletion of Notch 2 in renin cells. No alteration to vascular patterning is detected. Staining with renin (bottom panels) shows extension of renin staining distal from the glomerulus, in a replication of the embryonic pattern.

APPENDIX 2: Antibodies

Antigen	Host Species	Dilution	Antigen Retrieval?	Source
α-SMA	mouse mAb	1:10,000	no	Sigma
AKR1B7	goat	1:200	yes	Santa Cruz
LYVE	rabbit	1:1000	yes	Abcam
PDGFR-ß	rabbit	1:200	yes	Cell Signaling Technologies
PECAM	goat	1:400	yes	Santa Cruz
phospho-histone H3	rabbit	1:200	yes	Cell Signaling Technologies
Podocalyxin	goat	1:200	yes	R&D Systems
Renin	rabbit	1:500	no	Gomez Lab
Slit3	rabbit	1:100	yes	Abcam
SM-MHC	rabbit	1:1000	no	Sigma
TUJ1	Mouse mAb	1:500	Yes	Gift from Dr. A. Frankfurter

APPENDIX 3: PCR primers

	Gene	Forward	Reverse
qPCR	AKR1B7	CAGATTGAGAGCCACCCTTA	TGGGAATCTCCATTACTACG
	GAPDH	AACTTTGGCATTGTGGAAGGGCTC	ACCAGTGGATGCAGGGATGATGTT
	Tie2	TGTCAATCAGGCCTGGAAATAC	GAGGAGGGAGAATGTCACTAAGG
	β-globin	CACAACCCCAGAAACAGACA	CTGACAGATGCTCTCTTGGG
Genotyping	Foxd1-cre	ATAAGCAATCCCCAGAAA	AGGCGTTTTCTG AGC ATA CC
	RBP-J (del)	GGCTAAAATGTTTGCCACCAGA	GACCAGTGGCTCTCAACTCC
	RDTAR	CGACCTGCAGGTCCTCG	CTCGAGTTTGTCCAATTATGTCAC

APPENDIX 4: Abbreviations

α-SMA/ACTA2	alpha smooth-muscle actin
AKR1B7	Aldo-keto reductase family 1, subfamily B member 7
ATP	Adenosine Triphosphate
BSA	Bovine Serum Albumin
cAMP	cyclic adenosine mono-phosphate
ChIP	chromatin immunoprecipitation
ChIP-seq	ChIP sequencing
DAPI	4',6-diamidino-2-phenylindole
DMEM	Dulbecco's modified Eagle's medium
DMSO	Di-methyl sulfoxide
DTA	Diphtheria toxin chain A
FACS	fluoresence-activated cell sorting
FBS	Fetal Bovine Serum
fl	floxed allele
Foxd1	Forkhead box family D member 1
GAPDH	Glyceraldehyde 3-phosphate dehydrogenase
JG	Juxtaglomerular
JGA	(Cells of the) Juxtaglomerular apparatus
KO	Knock-out
LYVE	Lymphatic vessel endothelial receptor 1
PBS	Phosphate buffered saline
PCR	Polymerase chain reaction
PDGFR-ß	Platelet-derived growth factor receptor beta
PECAM	Platelet and endothelial cell adhesion molecule
PLGF	Placental growth factor

RBP-J	Recombinant signal binding protein for immunoglobulin kappa J region
SMC	Smooth muscle cell
WT	Wild-type